ALTERATIONS OF THE LUNG ENVIRONMENT DURING A PNEUMONIA VIRUS OF MICE (PVM) INFECTION: STUDYING THE EFFECTS OF ALLERGEN INHALATION DURING AN UNDERLYING PVM INFECTION

A Thesis Submitted to the College of
Graduate and Postdoctoral Studies
In Partial Fulfillment of the Requirements
For the Degree of Master of Science
In the Department of Biochemistry, Microbiology and Immunology
University of Saskatchewan
Saskatoon, Canada

Written By:

AMANDA CAITLIN PHYLLIS GALAS-WILSON

PERMISSION TO USE

In presenting this thesis in partial fulfillment of the requirements for a postgraduate degree from the University of Saskatchewan, I agree that the Libraries of this University may make it freely available for inspection. I further agree that permission for copying of this thesis in any manner, in whole or in part, for scholarly purposes may be granted by the professor who supervised my thesis work or, in their absence, by the Head of the Department or the Dean of the College in which my thesis work was done. It is understood that any copying or publication or use of this thesis or parts thereof for financial gain shall not be allowed without my written permission. It is also understood that due recognition shall be given to me and to the University of Saskatchewan in any scholarly use which may be made of any material in my thesis.

Request for permission to copy or make other use of material in this thesis in whole or part should be addressed to:

Head of the Department of Biochemistry, Microbiology and Immunology
2D01, Health Sciences Building
107 Wiggins Road
University of Saskatchewan
Saskatoon, Saskatchewan, S7N 5E5
Canada

Or:

Dean
College of Graduate and Postdoctoral Studies
University of Saskatchewan
116 Thorvaldson Building, 110 Science Place
Saskatoon, Saskatchewan S7N 5C9
Canada

ABSTRACT

Respiratory syncytial virus (RSV) and other respiratory viruses are known for their implications in asthma exacerbation and development; many population-wide epidemiological studies indicate this correlation. Among children less than two years old, 99% have experienced an RSV infection, and about 36% of those children have also had a second infection. Due to this high frequency of RSV infections, infants also have a high chance of exposure to benign particulates before, during, and after a viral infection has peaked. There are many mouse models used to deduce immunological pathways leading to asthma development and exacerbation. I developed a model in mice where a natural route of allergen entry was utilized with another timeline of viral infection and allergen exposure. In this model, allergen exposure occurs during viral infection and after clearance; this realistically replicates a situation in children who are constantly exposed to benign allergens irrespective of their viral clearance status.

My model shows that if initial exposure occurs during a pneumonia virus of mice (PVM) infection, a secondary immune response towards cockroach allergen (CRA) is modified and becomes more inflammatory than if CRA exposure happens without any viral infection. Utilizing this model, we observed an increase in mucin mRNA (Gob5 and Muc5AC), as well as induction of IFN-γ, IL-4, and IL-10 mRNA and their corresponding cytokine proteins. Furthermore, we observed an increase in the influx of macrophages and dendritic cells in the lungs, indicating the presence of an inflammatory response towards CRA. Neutrophil and eosinophil influx within the bronchoalveolar lavage fluid and the lung tissue changed when mice were exposed to CRA during acute viral infection. This influx occurred despite the second exposure taking place after viral clearance and suggested a Th-2 skewed inflammatory response. IDO (indoleamine-2,3-dioxygenase)-1 expression was also enhanced towards CRA when the first exposure occurred during an underlying PVM infection. Thus, the overall response was stronger towards CRA than what CRA induced without an underlying PVM infection. This stronger response may correlate to the enhanced IDO-1 expression previously observed. Therefore, our data indicate that exposure to benign allergens during a respiratory infection can modify the response due to infection and produce a Th-2 type inflammatory response without additional eosinophil influx.

ACKNOWLEDGEMENTS

I would like to thank Dr. Sylvia van den Hurk for giving me the opportunity to work in her lab. I have learned a lot during my almost three years here, and none of it could have been learnt if she had not accepted my application back then. I would also like to thank my committee members Dr. Linda Chelico, and Dr. Calliopi Havele, for their guidance and advice throughout this project.

I want to thank my past and current lab members, including Elisa Martinez, Dr. Ravendra Garg, Dr. Indranil Sarkar, and Laura Latimer for all of their technical and emotional support. I would also like to thank Animal Care for all of their attentiveness towards tending my mice before and during my trials and collecting all of the samples with me at the end of each trial. A big thank-you to VIDO as a whole for accepting me into their family for the past three years; without their welcoming presence, coming here every day would have been much more difficult. A massive thank-you to all of my friends (past and current) for the emotional support that helped me get through the difficulties and continue placing one step in front of the other. Thank-you to my continuous pillars of support: mom (Ula Galas), dad (Barry Wilson) and my sister and her husband (Justyna and Justin Daenckaert) for all of the Skype calls and Facebook messages supporting my decisions and helping me stay on my feet. I am also thankful for my grandparents (Teresa and Jerzy Galas) and parents for their emotional and financial support during my degree. I would not have been able to survive as well as I did without their continued help.

I would also like to acknowledge how much Lindy Hop dancing has affected my outlook on life during my degree. Without dancing, I am not sure if I could've maintained a strong and positive mentality. I also wouldn't have met my amazing boyfriend, Christopher Mahadeo, who has been a pillar of support since he came into my life. Being able to go from great dancing friends and to continue dancing as we started dating has been the best experience in my life. I cannot wait to see what the next stage of my journey will be alongside him. I'd also like to thank Kevin Newman, for the support he was able to give at the beginning of this journey. Without knowing him, I wouldn't have done my masters here, and I am quite happy where I am right now.

DEDICATION

I want to dedicate this document to my loving family.

Without their continued emotional and financial support, this journey would have been much more arduous and trying.

TABLE OF CONTENTS

PERMISSION TO USE i

ABSTRACT ii

ACKNOWLEDGEMENT iii

DEDICATION iv

TABLE OF CONTENTS v

LIST OF TABLES viii

LIST OF FIGURES ix

LIST OF ABBREVIATIONS x

1 INTRODUCTION AND LITERATURE REVIEW 1

1.1 Human Respiratory Syncytial Virus (RSV) Within the Human Population 1

1.1.1 RSV disease burden and epidemiology 1

1.1.2 Animal models of RSV 1

1.1.3 RSV pathology 3

1.2 Pneumonia Virus of Mice (PVM) in Mice as an RSV Model 8

1.2.1 Disease 8

1.2.2 Innate immunity 8

1.2.3 Adaptive immunity 11

1.3 Indoleamine 2,3-dioxygenase (IDO)-1: An Enzyme and a Signalling Molecule 15

1.3.1 Activation of IDO 15

1.3.2 Enzymatic activity 18

1.3.3 Signalling activity 19

1.4 Asthma: Disease or Syndrome 19
1.4.1 Asthma development and epidemiology 19
1.4.2 Implications of the Immune System 20
1.4.3 Effects of cockroach allergen on allergy development 22
1.4.4 Clinical symptoms 25
1.4.5 Viral induction of asthma development or exacerbation 26
1.4.6 Management of asthma 28

2 HYPOTHESIS AND OBJECTIVES 30

3 MATERIALS AND METHODS 31
3.1 Cell line and virus propagation 31
3.2 Cockroach allergen preparation 32
3.3 Mouse pathogenesis model 49
3.4 Sample preservations 32
3.4.1 Lung tissue 32
3.4.2 Bronchoalveolar lavage (BAL) fluid 33
3.4.3 Blood samples 34
3.5 Virus titration assay 34
3.6 qPCR RNA procedure for analysis of mRNA expression 35
3.6.1 Isolation of mRNA from homogenate lung tissue 35
3.6.2 Transcription to cDNA for qPCR 35
3.6.3 qPCR and data analysis 35
3.7 FLOW cytometry procedure 38
3.8 Multiplex ELISA procedure for analysis of cytokine and chemokine profiles 41
3.9 Total IgE titration 41

3.10 Statistical analysis 41

4 RESULTS 42

4.1 Developing an asthma model 42

4.1.1 The first model 42

4.1.2 Modification of this model 45

4.2 Cockroach allergen and PVM infection inflict different long-lasting alterations to the lung environment 49

4.2.1 Gene expression within the lung tissue 55

4.2.2 Cytokine and chemokine protein analysis 58

4.2.3 Lung tissue and BAL fluid cell efflux and influx 60

4.3 The lung environment is altered when an allergen is introduced during an acute viral infection 62

4.3.1 Gene Expression Within the Lung Tissue 62

4.3.2 Cytokine and chemokine protein analysis 64

4.3.3 Total IgE concentrations 68

4.3.4 Lung tissue and BAL fluid cell efflux and influx 69

5 DISCUSSION AND CONCLUSION 73

5.1 RSV infection and allergen exposure 73

5.2 Understanding the implications of allergen exposure during early-childhood 75

5.3 General conclusion and future directions 76

LIST OF TABLES

Table 3.1 qPCR primer list 37
Table 3.2 FLOW Cytometry cell marker list 40

LIST OF FIGURES

Figure 3.1 Gating for FLOW cytometry 39

Figure 4.1 First asthmatic model 43
Figure 4.2 Cytokine and IDO-1 mRNA 44
Figure 4.3 Modified asthmatic model 46
Figure 4.4 Cytokine and IDO-1 mRNA, and cellular influx in BAL fluid and lung tissue 47
Figure 4.5 Schematic representation of mouse model 50
Figure 4.6 Lung tissue mRNA, and cellular influx in BAL fluid and lung tissue 52
Figure 4.7 PVM-15 virus titration peak and clearance 54
Figure 4.8 mRNA data of the lung tissue environment 57
Figure 4.9 Protein profile of the BAL fluid 59
Figure 4.10 Cellular influx and efflux of neutrophils and eosinophils 61
Figure 4.11 mRNA profile of the lung tissue within the three groups 63
Figure 4.12 Protein profile of the BAL fluid and the lung tissue of the groups 66
Figure 4.13 Total IgE titers in LFC and BAL fluid samples 68
Figure 4.14 BAL fluid and lung tissue cellular influx and efflux 71

LIST OF ABBREVIATIONS

AAFA = Asthma and Allergy Foundation of America

ATCC = American Type Culture Center

Arg = Arginase

BAL = Bronchoalveolar Lavage

BHK = Baby Hamster Kidney

BSA = Bovine Serum Albumin

CCA = Chimpanzee Corya Agent

CCL = C-C Chemokine ligand motif

CD = Cluster of Differentiation

cDNA = complementary DNA

CRA = German Cockroach Allergen

CTLA = cytotoxic T-lymphocyte-associated protein

CXCL = C-X-C chemokine motif ligand

DC = Dendritic Cell

DNA = Deoxyribonucleic Acid

DMEM = Dubelcco's Modified Eagle Medium

ECP = Eosinophilic Cation Protein

ELISA = Enzyme-Linked Immunosorbent Assay

FACS = Fluorescence-Activated Cell Sorting

FBS = Fetal Bovine Serum

FEV1 = Forced Expiratory Volume in 1 second

Foxp3 = Forkhead Box P3

GAPDH = Glyceraldehyde 3-Phosphate Dehydrogenase

GINA = Global Initiative for Asthma

3-HAA = 3-Hydroxyanthranilic Acid

HDM = House Dust Mite

IDO = Indoleamine – 2,3 – Deoxygenase

IFA = Incomplete Freud's Adjuvant

IFN = Interferon

Ig = Immunoglobulin

IL = Interleukin

IN = intranasal

IP = Interferon gamma-Inducing Protein

ITIM = Immunoreceptor Tyrosin-based Inhibitory Motif

JAK = Janus Kinase

KO = knock-out

Kyn = Kynurenine

LFC = Lung Fragment Culture

LPS = lipopolysaccharide

LRT(I) = Lower Respiratory Tract (Infections)

MEM = Minimum Essential Medium

MIP = Macrophage Inflammatory Protein

MOI = Multiplicity of Infection

mRNA = Messenger RNA

NF-κB = Nuclear factor-kappa B

NK = Natural Killer

Par = Protease-activated Receptor

PD = Programmed Cell Death Protein

PD-L = Programmed Death-Ligand

p.i. = post infection

PBS = Phosphate-buffered saline

PCR = Polymerase Chain Reaction

pfu = Plaque-forming Units

PVM = Pneumonia Virus of Mice

qPCR = Quantitative Real-Time PCR

QUIN = Quinolinic Acid

SOCS = Suppressor of Cytokine Signalling

STAT = Signal Transducer and Activator of Transcription

RNA = Ribonucleaic Acid

RSV = Respiratory Syncytial Virus

Th-1 = T helper cell type 1

Th-2 = T helper cell type 2

Th-17 = T helper cell type 17

TLR = Toll-like Receptor

TNF = Tumor Necrosis Factor

TNFR = Tumor Necrosis Factor Receptor

T-reg = Regulatory T-Cell

Tryp = tryptophan

URT(I) = Upper Respiratory Tract (Infection)

WHO = World Health Organization

1 INTRODUCTION AND LITERATURE REVIEW

1.1 Human Respiratory Syncytial Virus (RSV) Within the Human Population

1.1.1 RSV disease burden and epidemiology

RSV (*Human Orthopneumovirus*) is a member of the *Pneumoviridae* family (1). It is a single-stranded negative-sense RNA virus that infects the epithelial cells of the upper airway. Once there, RSV may also travel to the lower respiratory tract (2). It usually causes a common cold within immunocompetent individuals; within immunocompromised persons, such as infants and the elderly, RSV infection can develop into bronchiolitis and eventually lead to hospitalization and death (1, 3). RSV is transmitted through large droplets and fomites and is stable for hours in the environment (4), and close contact (person to person or person to fomites) is necessary for transmission (4).

There is no vaccine against this disease, but there is an antibody called Palivizumab that is used preventatively for infants classified as high-risk according to the World Health Organization (WHO) (5). Once infected, the administration of ribavirin and supplemental oxygen have been used as therapies (6).

Severe bronchiolitis due to RSV can produce wheezing symptoms in 40-50% of hospitalized infants, (7) and can exacerbate asthmatic symptoms (5, 8). Due to these factors, severe RSV bronchiolitis is now considered a risk factor for asthma development if contracted during infancy (5, 8, 9). Therefore, extensive research is necessary to understand the pathogenesis of RSV infection, and how it may lead to severe bronchiolitis and subsequent asthma development.

1.1.2 Animal models of RSV

The viruses within the *Pneumoviridae* family are quite species-specific, meaning that animal models of human RSV are somewhat inaccurate. A classic mouse model is the Balb/c

strain, though the viral titer needed for infection is quite high (5×10^5 pfu/mouse). Even so, the mice can clear the infection with some clinical symptoms observed (10). This clearance, with little to no symptoms, is also seen in RSV infection of Balb/c neonates, which does not replicate a human neonatal RSV infection (10).

A cotton rat model that replicates human RSV infections more accurately still has its drawbacks since cotton rats seem to be better able to combat RSV infection. Cotton rats also have slightly different cellular markers and subsequent functions when compared to the human immune system (similar to the significant drawbacks of the mouse model). Also, there is a smaller array of reagents for measuring cotton rat immunological responses.

Other animal models of RSV include sheep, rabbits, and guinea pigs (10), but they all have their advantages and disadvantages. Despite being more easily manageable, the smaller animals do not always accurately replicate a response to RSV infection similar to the general human population. Again, this can be partially due to vital immunogenetic differences between the smaller host animals and humans (11). Apart from the mouse model, there are fewer research tools developed for the other smaller animal models. The most significant disadvantage is, of course, that these viruses are species-specific. As such, a human study was performed on adults inoculated with RSV, and the disease symptoms were not representative of human neonatal disease (11). This difference in RSV infection between the two age groups suggests that age also plays a critical factor within these models.

Other models using the animal RSV viruses with their corresponding hosts are used to overcome the somewhat inaccurate results from RSV animal models. There are two well-known models of this kind: the bovine respiratory syncytial virus (bRSV) cattle model and the pneumonia virus of mice (PVM) mouse model. The bRSV virus causes a natural respiratory infection in cattle. The respiratory tract infection within younger calves causes severe bronchitis, while older cattle have a less severe form of the infection. These differences replicate different infection severities between human adults and infants with RSV (6). Likewise, if bRSV is processed using the same protocol as the formalin-inactivated-RSV/alum vaccine, young calves show similar enhanced disease seen in the infants who were administered the RSV vaccine (12). These critical similarities imply that the bRSV cattle model may be best for understanding RSV infections within infants. The downside to this model is that large animals are more cumbersome, challenging to handle, and expensive due to their size and housekeeping needs (6).

Another useful model is the RSV chimpanzee model. RSV was first isolated from chimpanzees with an upper respiratory tract infection (URTI), that was called chimpanzee coryza agent (CCA). Soon after, CCA was identified as a human-born virus (6). Most studies using this RSV chimpanzee model have documented coughing, sneezing, and rhinorrhea. One study documented a lower respiratory tract infection (LRTI) with bronchopneumonia in a 14-month-old chimpanzee (6). Therefore, this model can replicate the URTI caused by human RSV, which shares the same set of symptoms documented in most healthy adults (5). The use of this model for RSV-induced LRTIs within infants may not be as accurate, assuming that most studies with chimpanzees are utilizing adults instead of infants. The case of LRTI within a young chimpanzee suggests that younger hosts may have an RSV infection that replicates what is seen in human infants. The use of chimpanzees for RSV studies has been vital, although the high cost, and unique housekeeping needs limit their use for general RSV vaccine trials (6).

1.1.3 RSV pathology

RSV enters the upper airways of its host and replicates in the nasopharynx before traversing lower and infecting the epithelial layer of the lungs (6). Here, innate immunity is triggered, and an immune response develops that leads to clearance of the virus (13). Epidemiological studies of RSV have specified differences in disease severity between adults and infants, and these infants seem to be biased towards developing a Th-2 response (13). There is evidence that while the virus is still cleared, the cytokines attributed to the Th-2 response may cause long-lasting modifications to the lung tissue (14) and can lead to wheezing (15).

Many biomarkers have been examined to discern which infants are predisposed to developing severe disease and discover correlations between disease and wheezing (1, 14-17). In the Moreno-Solis *et al.* study, infants with bronchiolitis who needed oxygen supplementation due to the severity of their disease were distinguished from those with less severe bronchiolitis by increased IL-6 and MIP-1β within the nasopharyngeal aspirate (16). Generally, infants with RSV bronchiolitis showed increased IL-4 and IFN-γ protein expression as a mixed response with more IFN-γ than IL-4 protein produced. In addition, IL-6, IL-8, IL-10, MIP-1α, MIP-1β, and TNF-α proteins were all found in the nasopharyngeal aspirates. Infants with RSV bronchiolitis also showed increased IL-8, MIP-1α, and MIP-1β in the plasma (16). These plasma chemokines are indicative of the systemic need for neutrophil recruitment and other leukocytes to the lungs.

Both Shinohara *et al.* and Okamoto *et al.* performed studies focusing on eosinophilia and wheezing in infants with respiratory diseases (15, 17). Both studies compared nasal secretions and blood samples and correlated them with environmental factors such as family history and pre-existing allergies. While each study focused on different aspects and severity of the disease, both groups suggested that eosinophilia was commonly observed in both URTIs and LRTIs. They also indicated that factors of eosinophilia during LRTIs were correlated to allergy factors; eosinophilia in URTIs did not show this same correlation.

Shinohara *et al.* used a cohort of 35 children (mixed sexes) diagnosed with rhinorrhea aged 6-33 months (15). In this study, eosinophilia did not correlate with any environmental factors such as pre-existing allergies, family history, age, nor sex. Results from the blood samples taken at the end of the study identified no correlation between nasal eosinophilia, factors such as total IgE, and neither percent, nor quantity, of eosinophils seen at the start of the study. However, there was a correlation between wheezing and eosinophilia seen at the beginning of the study and wheezing 2 months after entry of the participants. By 12 months after entry, the patients no longer exhibited any correlation between factors measured at the beginning of the study and wheezing at 12 months (15). From this study, it can be determined that a respiratory tract infection localized to the URT does not seem to result in long-lasting wheezing. Also, eosinophilia within the nasal secretions during the infection did not correlate with either family history or laboratory findings. These lack of correlations suggests that eosinophilia is a typical response towards a URTI, and not indicative of long-lasting wheezing nor changes within the lung environment that may make a systemic impact on the children. Even so, a follow-up study measuring the forced expiration of volume in 1 second (FEV1) of the lungs, nasal secretions, and blood samples during and between later respiratory illnesses may be beneficial in understanding if there are any long-lasting, but more silent, changes within their lungs.

In contrast, Okamoto *et al.* compared and contrasted the primary eosinophil protein eosinophilic cation protein (ECP) within infants less than 2 years old who were hospitalized for LRTs, including RSV infections (17). These infants were separated based on sex, pre-existing allergies or a serum IgE titer of over 200 U/mL, whether their infection was caused by RSV, whether they had wheezing, and whether they were predisposed to allergies due to family history. All samples were taken at the time of hospitalization, declared the infectious phase. It was shown that a significant increase in ECP within the nasal secretions, but not the plasma,

correlated with wheezing within the infants. When ECP was compared between children with RSV infections and those with other LRTIs, ECP was also significantly increased in those with the RSV infection. Again, this was seen in the nasal secretions, but not replicated within the plasma. Even so, there was no correlation between nasal or plasma ECP in the infants regardless of predispositions to asthma and allergies. Some samples were also taken one day before discharge, and once respiratory symptoms had resolved, which was designated the recovery phase. Neither nasal secretions nor plasma ECP levels showed significant differences between the infectious and recovery phases. However, there were correlations between the infectious and recovery phases and neutrophil and eosinophil counts when compared to ECP levels. There was also a correlation between ECP levels at the recovery phase and pre-existing allergy factors (17). All of these correlations suggest that while the presence of ECP seems to be a general response towards LRTIs, RSV induces eosinophilia and increases ECP concentrations in comparison to other viruses. The ECP is always localized to the nasal secretions, and these levels do not significantly decrease one day after symptoms resolve. The levels of ECP during the recovery phase did correlate to pre-existing allergy factors. Since traditional allergies are known to be eosinophilic responses towards food or air-born particles, this is reasonable to expect. In addition, it is not surprising that there are no noticeable differences in ECP levels between the infectious and recovery phases since mouse models have indicated that it takes weeks after symptoms have diminished for the lung environment to return to basal levels (18).

While these two studies on infants identified eosinophilic infiltration during RSV infection, Bertrand *et al.* looked at the cytokine and chemokine profiles from both nasopharyngeal aspirates and bronchoalveolar lavage (BAL) fluid of 14 infants (aged 0-9 months) with severe RSV-induced bronchiolitis and 5 control infants (aged 1-6 months) (19). In follow-ups occurring for 3 years after the study, it was concluded that wheezing, asthma, or the need for corticosteroid therapies were more likely to occur within the infants who had RSV-bronchiolitis during this study. According to the study, BAL fluid sampled for select proteins described significant increases in IL-4, IL-10, IL-1β, IL-6, TNF-β, IL-12p40, CCL2, CCL3, and CXCL8 (IL-8) within the infants who had severe RSV-induced bronchiolitis relative to the control group of infants. Additionally, CCL-11 (eotaxin) and IL-12p70 levels were decreased in these same infants with RSV bronchiolitis. Neither IFN-γ nor IL-17 protein levels were found to change between the two cohorts. The nasopharyngeal aspirates were used for qPCR analysis and

contained significantly decreased IL-1β, IL-6, and CCL2 mRNA levels. During the last follow-up, infants who developed asthma were found to have increased CCL11, IL-5, TNF-β, IL-12p40, and IL-12p70 within their BAL fluid during the previous RSV bronchiolitis. Also, those infants whose parents were atopic (one or both parents diagnosed with rhinitis or atopic asthma), had significantly higher levels of IL-33 mRNA expression (19). Although no cell populations were identified in this study, the overall decrease of eotaxin and increase of CCL2, CCL3, and IL-8 suggests suppression of eosinophils, and recruitment of leukocytes, such as neutrophils. Even so, there was a predominant Th-2 and pro-inflammatory response in these infants with bronchiolitis. Thus, the lung environment was Th-2 dominant with suspected neutrophilia and suppressed eosinophilia. Interestingly, those infants who developed asthma within the 3-year follow-up had a slight, but significant, increase in proteins that would suggest eosinophilia. Therefore, infants that may have a slightly mixed neutrophilia and eosinophilia response may be more prone to developing asthma as opposed to just neutrophilia, as seen here, or eosinophilia, as seen previously (15, 17).

In an FVB/n mouse model from Sun *et al.* production of CXCL1, CCL2, MIP-1α (CCL3) protein and expression of IP-10 (CXCL10), and MIP-2 (CXCL2) mRNA were induced within 24 hrs of infection (8). In addition to those chemokines, IL-1β, IL-6, IL-12, and IFN-α protein production were also induced at 24 hrs (8). These protein increases led to a pro-inflammatory response with general leukocyte and neutrophil recruitment, which was necessary for viral clearance. The adaptive immune response mounted by day 8 and was specific for RSV virions (8). Researchers observed increases in IFN-γ, IL-13, IL-4, Muc5AC, and Gob5 mRNA expression, and an increase in IL-12 protein production. This study also showed a nominal increase of neutrophils at days 9 and 14, but no eosinophils were detected. Sun *et al.* were studying the effects of IL-10 on early and late RSV infection; therefore mice were transgenic to express human IL-10 (hIL-10), but mouse IL-10 (mIL-10) expression was not modified. As such, Sun *et al.* identified the complex nature of IL-10 functioning as both an immunosuppressive and proinflammatory cytokine. IL-10 was identified as suppressing the pro-inflammatory Th-2 responses because anti-IL-10 serum, administered at the time of infection, resulted in significantly increased IL-13, IL-4, IL-5, Muc5AC, and Gob5 mRNA levels (8). Therefore, 24 hrs after RSV infection, there was a pro-inflammatory response that was more neutrophilic. This response led to a mixed Th-1/Th-2 response by day 8 with high mucus mRNA production.

Neutrophilia was still detectable at days 9 and 14 showing this long-lasting effect soon after viral clearance generally occurs. Other results within the same study discovered that overexpression of hIL-10, both before infection and during peak viral infection, still increased Muc5AC and Gob5 mRNA levels. This contradiction could be due to IL-10 being overexpressed instead of a gradual increase over the course of infection as mediated by endogenous IL-10 mRNA levels.

Mukherjee *et al.* performed an RSV study explicitly looking at IL-17A during infection (20). First, infants with and without RSV infection (hospitalized with mechanical ventilation) had tracheal aspirates taken to determine IL-17 protein concentrations. These samples showed a significant increase in IL-17 concentrations when infants had RSV infections compared to those that did not have an RSV infection. They then used Balb/c mice and RSV strain A (line 19) to show that IL-17 was induced by RSV infection with $CD4^+$ T-cells producing the most IL-17A within the lungs compared to both NK cells and γδ T-cells. Day 8 was shown to be the peak of IL-17A production and was used to determine effects of anti-IL-17A antibodies or in IL-17A KO mice with RSV infection. Both suppression and KO of IL-17A showed a significant decrease in Muc5AC and Gob5 mRNA levels. In addition, this RSV infection caused both neutrophilia and eosinophilia, but suppression of IL-17A decreased neutrophilia and seemed to ablate eosinophilia within the BAL fluid. This suppression did not interfere with either macrophage or lymphocyte influx.

Additionally, the suppression of IL-17A decreased KC mRNA levels, which would explain the decrease in neutrophilia within the BAL fluid. No other chemokines measured were affected by the anti-IL-17A antibodies. They also showed that this RSV infection stimulated a mixed Th-1/Th-2 response with similar levels of IL-4 and IFN-γ mRNA expression, but a slightly higher IFN-γ than IL-4 protein production. IL-17A suppression did not interfere with these cytokines.

Additionally, IL-5 (essential for eosinophils) and IL-13 (Th-2 cytokine known to induce mucus production within goblet cells) were also induced by RSV, but not through IL-17A induction. They then looked at $CD8^+$ T-cells and found that there was a higher percentage of these effector cells expressing IL-17RA, the receptor for IL-17A. Suppression of IL-17A not only increased the number of $CD8^+$ T-cells specific for the RSV by staining the RSV-specific immunodominant T-cell receptor, but also increased the overall quantity of $CD4^+$ and $CD8^+$ T-cells. These $CD8^+$ T-cells were more likely to express IFN-γ, the transcription factors t-bet and

eomesodermin (eomes), and the apoptosis-inducing factor granzyme B.

Therefore, RSV pathology is incredibly complex, with many different factors playing a role in the immune-mediated infection. Genetic backgrounds within humans could influence these factors, and these manipulations could lead to the development of the different asthmatic phenotypes we are witnessing today.

1.2 Pneumonia Virus of Mice (PVM) in Mice as an RSV Model

1.2.1 Disease

Pneumonia virus of mice (PVM) is a pneumovirus that causes an immune-mediated disease in mice that is similar to the neonatal RSV infection (21). The mice show significant weight loss, a lack of grooming, and limited mobility while they are combating the disease (22). It was also found that all PVM proteins have homologues within RSV (21), which display homologous functions. Susceptibility to infection is based on the strain of mouse used, which corresponds to the immune response mounted by each strain (21). Overall, the Balb/c mouse is more susceptible to PVM infection than the C57Bl/6 mouse (21, 23). There are also two different strains of PVM virus (21). The first strain is PVM-15. A lethal dose of this virus is 3000 pfu/mouse, and this strain induces a neutrophilic infection within mouse lung tissue (21). The second strain of PVM (PVM-J3666) is highly infectious in comparison and induces an eosinophilic response within susceptible strains of mice. Despite their differences in cellular influx, both viral strains are commonly-used models for RSV infection (21, 24).

1.2.2 Innate immunity

According to Dyer *et al.* (25), PVM activates TLR7 (a receptor that recognizes single-stranded RNA) since mice lacking this receptor did not recruit neutrophils and NK cells; the induction of interferons and viral clearance was also delayed. Additionally, macrophages are necessary for the clearance of virus particles, but their depletion resulted in a larger influx of NK cells and a corresponding increase of IFN-γ, which still led to viral clearance. The implication of macrophages and NK cells along with IFN-γ induction suggests the development of a Th-1 biased adaptive immune response.

Domachowske *et al.* compared PVM-15 and PVM-J3666 within C57Bl/6 mice and found

differences in the immunology response between the two viruses (26). The group used 200 pfu of each virus, which is a known lethal dose of PVM-J3666 and a sub-lethal dose of PVM-15. Mice inoculated with PVM-J3666 all succumbed to the infection by day 7 p.i.; PVM-15 infected mice became quite ill with ruffled fur and lack of grooming between days 4-6 p.i., but recovered from their infections and were virus-free by day 10. Histological samples from the PVM-15 infected mice on day 4 p.i. showed almost no airway inflammation or structural changes. There was one mouse in this group that developed slightly more severe symptoms and had more structural changes and some leukocyte infiltration within its lungs. Contrastingly, the mice inoculated with PVM-J3666 had severe structural changes and increased neutrophil numbers within their lungs on day 4 p.i.

Furthermore, analysis of the leukocytes within the lung infiltrates on days 1, 2, 3, and 4 p.i. revealed little change in total cell numbers within the PVM-15 group; the lungs of these mice contained a balance of both granulocytes (neutrophils and eosinophils) and lymphocytes on day 1 p.i. This balance shifted to a large influx of granulocytes coupled with a small efflux of the lymphocytes. By day 1, the mice inoculated with PVM-J3666 had a larger proportion of granulocytes compared to lymphocytes with a similar total cell number when compared to the PVM-15 group. The total cell numbers drastically increased and became completely comprised of granulocytes, while no lymphocytes were seen within these lungs. MIP-1α (macrophage, neutrophil, eosinophil, and lymphocyte chemoattractant) and MCP-1 (monocyte, memory T-cell, and dendritic cell chemoattractant) production in the PVM-J3666 infected mice were detected by day 2 p.i. and continued to increase in concentration on both days 3 and 4 p.i. However, no protein was detected on these same days within the PVM-15 infected mice. PVM-J3666 infected lungs responded to the virus with high induction of proinflammatory mRNAs including IFN-β and MCP-1 even though there was no induction of either IFN-α or IFN-γ on day 3 p.i. according to microarray analysis. PVM-15 infection did not induce any of these same mRNAs except for RANTES (an eosinophil chemoattractant) (26). Therefore, the general conclusion of this study was that PVM-15 had a non-pathogenic phenotype within C57Bl/6 mice.

An earlier study also performed by Domachowske *et al.* in 2000 observed the pathology of PVM-J3666 within Balb/c mice (27). At an inoculation of 300 pfu per mouse, the Balb/c mice all succumbed to their illness by day 6 p.i. The BAL fluid consisted of about 12% eosinophils and 60% neutrophils on day 3 p.i. but it shifted to become less than 5% eosinophils and about

80% neutrophils by day 5 p.i. On day 3 p.i., the lung tissue, through microscopic analysis and H&E staining, had a predominant eosinophilic influx with some neutrophilic influx. Therefore, the early and innate response towards PVM-J366 within BALB/c mice is predominantly neutrophilic with some eosinophilic influx within the BAL fluid. These eosinophils start leaving the BAL fluid as the infection continues. At the same early time-point, the lung tissue has a predominant eosinophilic influx and lower neutrophilic influx. Eotaxin and RANTES protein concentrations (eosinophil chemokines) did not differ during this infection, and IL-5 was not detected. MIP-1α protein was detected within the mice at day 3 p.i., and the concentrations peaked at day 4 p.i., followed by a decrease at day 5 p.i. (27). Therefore, Domachowske *et al.* concluded that although eotaxin and RANTES were not contributing to this infection, MIP-1α may be the eosinophil chemoattractant necessary for the 12% eosinophil influx at day 3 p.i., and its decrease may account for the efflux seen on days 4 and 5 p.i.

However, in 2004, a study performed by Krempl *et al.* re-evaluated the virulence of PVM-15 within Balb/c mice (23). In addition to the Domachowske paper in 2000 (26), a 1995 paper by Randhawa *et al.* (28) and one done in 1967 by Harter *et al.* (29) concluded that PVM-15 was not as infective in Albino Swiss mice as compared to the PVM-J3666 strain. Krempl *et al.* used a PVM-15 strain from ATCC, which is one of the strains originally isolated by Horsfall and Hahn in 1939 (30). They compared this strain with the PVM-J3666 strain in Balb/c mice and concluded that mice infected with either viral strains succumbed to their illnesses around the same day; these symptoms were dose-dependent in both strains. Genome sequencing revealed mutations within the PVM-15 strain used by Domachowske *et al.* and Randhawa *et al.* that were not seen within the PVM-15 strain used in the Krempl *et al.* study (23, 28). Additionally, a second study by Krempl *et al.* deduced the dose-dependent lethality of PVM-15 within Balb/c mice: 10^1 pfu is non-lethal, 10^2 pfu is sub-lethal, and 10^3 pfu is lethal (31).

Watkiss *et al.* compared 30, 300 and 3000 pfu of PVM-15 (ATCC strain) within both Balb/c and C57Bl/6 mice and detected both innate and adaptive immune response differences between the two mouse strains (21). Balb/c mice inoculated with 30 pfu expressed no significant weight loss, though mice given 300 pfu did show significant weight loss, and some succumbed to their infections. At 3000 pfu all of the mice showed drastic weight loss and started succumbing to their illnesses by day 5 p.i., none survived past day 7 p.i. C57Bl/6 mice inoculated with either 30 pfu or 300 pfu did not show significant weight loss and survived until

the end of the trial. When inoculated with 3000 pfu, these mice showed significant weight loss, and about 25% had succumbed to their illness by day 7 p.i. Therefore, the C57Bl/6 mice were more resistant to PVM infection than the Balb/c mice in this study.

According to this study, a 30 pfu inoculation of PVM-15 (non-lethal dose) within Balb/c mice induced mRNA production of IFN-α and some IFN-γ (proinflammatory cytokines), as well as CXCL8 (IL-8 – neutrophil chemokine), CXCL10 (IP-10 – effector T-cell chemokine), CCL3 (MIP-1α) and CCL2 (MCP-1) by day 5 p.i.; none of these mRNAs were induced at day 3 p.i. within the Balb/c mice. The C57Bl/6 mice had a similar increase in these cytokines and chemokines when inoculated with 3000 pfu, again at day 5 p.i. Additionally, macrophages were the most abundant cell population within the BAL fluid at day 3 p.i., but by day 5 p.i. a nominal neutrophilic influx was also detected in Balb/c mice. Similar results were found in C57Bl/6 mice inoculated with 3000 pfu. At day 5 p.i., there was an increase in chemokines CCL3, CCL2, CXCL8, and CXCL10, which also recruit NK cells (21). At day 6 p.i., a substantial population of NK cells secreting IFN-γ were detected, but neither $CD4^+$ nor $CD8^+$ T-cells were detected within the Balb/c mice. A significantly smaller number of NK cells secreting IFN-γ were found at the same time-point in C57Bl/6 mice even though both mice express the same amount of this mRNA by day 5 p.i. Watkiss *et al.* also suggests a connection between IFN-γ and the infiltration of neutrophils. A previous study showed IFN-γ-dependent neutrophilic influx using IFN-$\gamma^{-/-}$ Balb/c mice that also over-expressed CCL3 (neutrophilic chemokine). Over-expression of CCL3 did not result in neutrophilic influx until recombinant IFN-γ was administered to these mice. This study concluded that the innate response within both Balb/c and C57Bl/6 mice includes high macrophage infiltration and IFN-γ mRNA induction, which promotes a Th-1 biased adaptive immune response (21).

1.2.3 Adaptive immunity

An adaptive immune response is highly specialized and uses enhanced elimination processes that are specific for one pathogen-type (i.e. the adaptive immune cells specific towards an influenza virus will not be able to target RSV virions). Additionally, different adaptive immune responses are necessary for different types of pathogens. Therefore, the response can be either Th-1, Th-2, or Th-17 – biased or sometimes a combination of these responses, depending on the different cytokines, chemokines, and cellular populations attracted and produced by the

innate immune system within the infected tissue. Typically, Th-17 responses are neutrophil-biased and mounted towards extracellular fungal and bacterial infections, but are also implicated in immunosuppressive responses (32). Th-1 responses are considered cell-mediated and mounted to intracellular pathogens (viruses, and some bacteria). Th-2 responses are considered humoral and mounted to extracellular pathogens (some bacteria and helminths).

The Th-1 response is traditionally mounted to intracellular pathogens such as intracellular viruses and bacteria. This response is canonically defined as cell-mediated and develops due to high IL-12 concentrations produced by M1 macrophages and dendritic cells, and IFN-γ produced by NK cells during the innate response (33). Characteristics of this adaptive response include numerous IFN-γ-secreting $CD4^+$ T-cell (Th-1 $CD4^+$ T-cells) and cytotoxic $CD8^+$ T-cell populations, coupled with IgG2a production by B-cell populations. IFN-γ induces enhanced microbicidal activity within macrophages, which includes secreting TNF-α and IL-12 pro-inflammatory cytokines. IFN-γ also stimulates IgG2a class-switching in B-cells and, coupled with IL-12 from macrophages or dendritic cells, produces IFN-γ-secreting $CD4^+$ T-cells and cytotoxic $CD8^+$ T-cells. Naïve $CD4^+$ T-cells are induced to express transcription factor T-bet through both IL-12 and IFN-γ signalling. T-bet induces IFN-γ secretion and suppresses GATA3 induction. Thus the Th-2 skewed response is inhibited, and the T-cells become Th-1 biased and secrete IFN-γ. The secreted IFN-γ also stimulates macrophage microbicidal activity and IgG2a class-switching in B-cells (34). They are also important in stimulating and maturing $CD8^+$ T-cells so that their cytotoxic properties are enhanced and specific fore infectious particle. Cytotoxic T-cells are important because they can recognize infected host cells that are expressing specific pathogen targets and induce apoptosis within these cells, thus interrupting the replication cycle of an intracellular pathogen. IFN-γ is also known to suppress both the Th-2 and Th-17 immune responses.

Alternatively, the Th-2 response includes Th-2 $CD4^+$ T-cells, M2 macrophages N2 neutrophils, eosinophils, mast cells, and basophils, as well as IgE class-switching of B-cells, and secretion of cytokines such as IL-4, IL-5, IL-13, and IL-25 (34, 35). This response is typically mounted in response to extracellular pathogens and helminths that are difficult to clear with a Th-1 response. Naïve T-cells transiently express GATA3 (Th-2 $CD4^+$ T-cell transcription factor), while IL-2 (a generic cytokine transiently expressed and necessary to sustain activated $CD4^+$ T-cells) induces STAT5 activity (36). Both of these transcription factors are necessary for

Th-2 T-cell differentiation. Thus, naïve $CD4^+$ T-cells seem able to differentiate into Th-2 T-cells without extracellular cytokine stimulus (36). Th-2-cells secrete cytokines such as IL-4, IL-5, IL-9, IL-10, IL-13, and IL-25 (33). $CD4^+$ T-cell derived IL-4 induces cytotoxic $CD8^+$ T-cells that express the GATA3 transcription factor and produce IL-4 and IL-13 cytokines (37, 38). IL-4 production by Th-2 cells also induces IgE and IgG1 class switching of B-cells.

Therefore, the induction of IFN-α and IFN-γ mRNA production at day 5 p.i. coupled with the influx of macrophages and NK cells in the Watkiss *et al.* study (21) reportedly led to a Th1-biased environment. Both mouse strains were sampled at days 14 and 28 p.i. (30 pfu inoculation of Balb/c and 300 pfu of C57Bl/6) to observe the adaptive immune response through total and neutralizing antibody titers, and PVM specific IFN-γ or IL-5 secreting splenocytes. Neither strain produced PVM-specific IgE antibodies, but there was PVM-specific IgA in the lungs and PVM-specific IgG in the lungs and serum at day 14 p.i. in both Balb/c and C57Bl/6 mice. At day 28 p.i. the Balb/c mice had increased Ig titers, but the C57Bl/6 mice maintained their titers. Both strains also produced virus-neutralizing antibodies, but the C57Bl/6 mice produced a nominal, but significant, increase in the antibodies both within the serum and the lung tissue compared to the Balb/c mice.

An ELISPOT assay measuring the IFN-γ or IL-5 producing splenocytes also showed differences. Both Balb/c and C57Bl/6 mice developed IFN-γ-producing cells at day 14 p.i. and these populations significantly decreased by day 28 p.i. The Balb/c mice had a significantly lower number in comparison on day 14 p.i. however, this cell population did not decrease to the same extent and thus had a significantly larger amount by day 28 p.i. Only Balb/c mice developed IL-5-producing cells at day 28 p.i. although these cells were not detected at day 14 p.i.

Overall, Watkiss *et al.* (21) showed a sustained IFN-γ-producing cell population at day 28 p.i. in Balb/c mice, higher than the population found in C57Bl/6 mice. This constant cellular influx suggests that the response within Balb/c mice is rapid and long-lasting when compared to similar responses of the C57Bl/6 mice. Additionally, not only was there a sustained number of IFN-γ-producing lymphocytes at this time-point, but there was also a small but increasing number of IL-5 producing cells. These cells could be indicative of an eosinophilic-primed response because IL-5 is a known eosinophil chemoattractant. Therefore, both Balb/c and C57Bl/6 mice develop an initial neutrophilic and Th-1 response for viral clearance, although the Balb/c mice develop this response earlier and it decreases less after clearance of a sub-lethal

PVM-15 infection while a Th-2 and eosinophilic response also initiate at this time.

Another study by Frey *et al.* in 2008 identified a role for $CD4^+$ and $CD8^+$ T-cell - mediated immunopathology in a C57Bl/6 and PVM-15 infectious mouse model using a dose of 250 pfu (39). A sub-lethal dose of PVM-15 administered to C57Bl/6 mice resulted in weight loss around day 8 p.i.; this coincided with increasing total cell counts within the BAL fluid and a decrease in virus. Also during this time, a significant portion of the total BAL fluid cells were $CD3^+$ which is the marker for T-cells; more specifically, this group was mostly comprised of $CD8^+$ T-cells with a small population of $CD4^+$ T-cells. When comparing $TCR\beta\delta^{-/-}$ and $TCR\beta^{-/-}$ knock-out mice to wild-type mice, the virus load persisted up to day 49 p.i., but the knock-out mice no longer lost weight during infection. Thus, $\alpha\beta$ $CD3^+$ T-cells are necessary for both immunopathological symptoms and viral clearance. The transfer of $5x10^6$ splenocytes resulted in recovery and clearance of the virus by day 11 p.i. Both TCR $\beta\delta^{-/-}$ and $TCR\beta^{-/-}$ knock-out mice also showed reduced weight loss; thus confirming the previous results. CD4 T-cell deficient or CD8 T-cell deficient mice still cleared the virus at day 11 p.i., although mice without CD4 T-cells lost some weight (approximately 10% weight loss), while CD8 T-cell depleted mice lost minimal weight (approximately 5% weight loss). Depletion of both T-cell populations led to the disruption of viral clearance. A significant decrease in IFN-γ, TNF-α, MCP-1, IL-6, and IL-10, but not IL-12p70 in the BAL fluid of $TCR\beta^{-/-}$ knockout mice was also observed. Finally, histopathology results showed that despite virus persistence, the $TCR\beta^{-/-}$ knock-out mice had reduced pulmonary inflammation during a low-dose PVM infection (39).

Additionally, mice deficient in the IFN-γ receptor, perforin, or tumour necrosis factor receptor (TNFR)p55 were administered either a low or high (> 3500 pfu) dose of PVM-15. These mice still cleared the virus by day 11 p.i. and also had similar weight loss compared to the wild-type mice. Interestingly, a high dose of PVM-15 within the $TCR\beta^{-/-}$ knockout mice resulted in similar weight loss, delayed mortality and similar pulmonary inflammation as in the wild-type mice. Cytokine concentrations within the BAL fluid of these knockout mice compared to the wild-type mice still contained significantly decreased IFN-γ, MCP-1, and IL-10, and no differences in IL-12p70, but there was also a significant increase in TNF-α and no difference in IL-6 concentrations. Therefore, symptoms resulting from a low-dose PVM infection in C57Bl/6 mice are T-cell dependent and immunopathological, while a high dose of PVM will still inflict symptoms with a pathological mechanism. Additionally, T-cells are necessary for viral

clearance, but not through IFN-γ, TNFRp55, or perforin mediated mechanisms.

1.3 Indoleamine 2,3-dioxygenase (IDO)-1: An Enzyme and a Signalling Molecule

IDO is a known immunological mediator, and there are two different proteins of IDO (IDO-1 and IDO-2) that are both found in monocytes and dendritic cells (DCs). Macrophages (40) and respiratory epithelial cells (41) are also known to only produce IDO-1. IDO-2 is a more recent discovery by Metz *et al.* (42) in 2007. IDO-1 is known to have both enzymatic and signalling activity (43) and is induced by factors such as IFN-γ, cytotoxic T-lymphocyte-associated protein (CTLA)-4 and programmed cell death protein (PD)-1, (43, 44). There is, however, evidence that it can be suppressed by factors such as IL-4 and IL-13 (45, 46), although it seems these same cytokines can induce IDO enzymatic properties (47). Therefore, elucidating IDO suppressors has been controversial. There is also controversy regarding the enzymatic and signalling activity of IDO-2 (42, 43). Generally, IDO is shown to have tolerogenic functions by either depleting or suppressing the proliferation of Th-1 cells, (48, 49) thereby allowing Th-2 proliferation and biased response, (9) or by inducing T-regs (50) or regulatory DCs (51, 52). This protein was first thought to be an inducible part of the host-defence system (53). Since then, detectable levels of IDO have been found without infection, and it has been identified as a vital part of immune regulation (54). As such, it has been extensively studied within cancer and some chronic diseases (52) for its immunosuppressive properties. Only recently has it also been studied within the scope of viral infections (55) and asthma (56).

1.3.1 Activation of IDO

Many studies have been focused on the enzymatic activity of IDO; due to this, much is known about its enzymatic activation. For instance, Cheng *et al.* found that hepatic carcinoma-associated fibroblasts (hCAFs) induce tolerogenic DCs through IL-6-mediated signal transducer and activator of transcription (STAT)3 activation (51). They found that hCAF stimulation led to DCs with fewer, shorter than usual, dendrites. However, stromal cell-derived factor (SDF)-α, known to be produced by hCAFs, still allowed for DC migration. Since hCAFs were stimulating DCs in a way that showed stunted activation, though also recruited DCs, it was necessary to identify the physiological changes within DCs stimulated by hCAFs. Cheng *et al.* used

fluorescence-activating cell sorting (FACS) to observe that hCAF-stimulated DCs showed expression levels similar to iDCs except for the deficient expression of CD83 (a maturation molecule) and exceptionally high expression of tolerogenic surface molecules CD14 and CTLA-4. With this revelation made, the tolerogenic properties of these hCAF-stimulated DCs were deduced by comparing the production of pro-inflammatory or immunosuppressive cytokines within co-cultured $CD3^+$ T-cells. It was found that pro-inflammatory cytokines IL-12p70, and TNF-β decreased while immunosuppressive cytokines IL-10 and TGF-β were induced.

Additionally, overall T-cell proliferation was inhibited, while there was an increase of $CD4^+$ $CD25^+$ T-cells and $CD4^+$ $CD25^+$ $Foxp3^+$ T-cells within these cultures.

Along with this increase in phenotypical T-reg cells, there was also an increase in $CD4^+$ T-cells producing IL-10 and a decrease in $CD8^+$ T-cells producing IFN-γ within these cultures. Confirming that these DCs have tolerogenic properties, Cheng *et al.* inhibited IDO and STAT3 using 1-methyl-tryptophan (1-MT) and S31-201, respectively. Both of these inhibitors reversed the tolerogenic and pro-inflammatory effects that hCAF-DCs had on the $CD3^+$ T-cells. Since S31-201 gave the same T-cell phenotypes as IDO-inhibitor 1-MT, it was found that STAT3 is an inducer of IDO enzymatic activity within the hCAF-tolerogenic DCs. IL-6, a known STAT3 inducer, was neutralized within the hCAF-DC medium, which leads to the decreased phosphorylation of STAT3 and inhibited IDO protein production.

Additionally, exogenous IL-6 and SDF-α were able to induce STAT3 phosphorylation within mDCs together and on their own. This induction also led to increased protein production of IDO within these cells. Thus, hCAFs were able to stunt the normal maturation of DCs and induce tolerogenic DCs through the activation of IDO by the IL-6/STAT3 pathway.

Rodrigues *et al.* did a study on IDO-1 expression of iDCs co-cultured with mast cells (MCs) (44). They confirmed that co-culturing of mast cells with iDCs led to the development of $IDO\text{-}1^+$ DCs that were tolerogenic based on surface molecule phenotyping and high expression of IL-10. It was also confirmed that $CD3^+$ T-cell stimulation with these MC-DCs suppressed proliferation and differentiation was T-reg skewed. These tolerogenic properties suggested that IDO-1 may be playing a role. IDO-1 was expressed by these MC-DCs but was not found within the iDC cultures. It was confirmed MCs do not degranulate when co-cultured with iDCs. Therefore, researchers blocked the histamine receptors H1 and H2 on iDCs to see if that affected IDO-1 expression.

Interestingly blocking the H1 receptor did induce more IDO-1 mRNA expression, but this did not translate to more IDO-1 protein production. Blocking the histamine receptors did not suppress IDO-1^+ iDCs. Since neither degranulation nor MC components blocked IDO-1 expression, they looked at other surface molecules of MCs. PD-1 was expressed on MC, and it was confirmed that both programmed death-ligand (PD-L)1 and PD-L2 on iDCs increased expression after co-culturing with MCs. When the co-cultures were given anti-PD-1, anti-PD-L1, and anti-PD-L2 separately, all of them suppressed IDO-1 protein production within the DCs.

Furthermore, anti-PD-L1 also suppressed IDO-1 mRNA expression. STAT3 is a known inducer of IDO-1 expression, as previously shown by Cheng *et al.* (51). The researchers proceeded to observe the phosphorylation of STAT3 within the MC-DCs, and found a large amount of phosphorylated STAT3 (pSTAT3). Anti-PD-1 decreased phosphorylation, and the STAT3 inhibitor JSI-124 also inhibited this phosphorylation. Finally, this inhibitor ablated the IDO-1 mRNA expression and protein production within the iDCs. Rodrigues *et al.* concluded their study by looking at NFκB1, NFκB2, and suppressor of cytokine signalling (SOCS)3 mRNA expression, among other factors. They found that NFκB2 was highly expressed after culturing with MCs, and this was ablated by the addition of anti-PD-1. iDCs expressed NFκB1 without MC culturing, and this did not increase when MCs were added; anti-PD-1 did suppress some of its mRNA expression as well. Finally, SOCS3 expression was virtually ablated within the MC-DCs, but administration of anti-PD-1 recovered this expression (44).

It was also realized that inhibition of the janus kinase (JAK)1/3 pathway through tofacitinib induced IDO-1 expression within lipopolysaccharide (LPS)-stimulated monocyte-derived DCs from rheumatoid arthritis patients (57). Kubo *et al.* showed that this inhibitor also decreased expression of CD80/86, IL-1β, TNF-α, and IL-6 proteins. These DCs co-cultured with T-cells but without any previous stimulation produced IFN-γ and IL-10 secreting cells; IL-10 concentration was much lower than IFN-γ. When they were first stimulated with LPS and without tofacitinib, there was an increase in IFN-γ concentration and suppression of IL-10 secretion. When tofacitinib was added to the LPS-stimulated DCs in a dose-dependent manner, IFN-γ concentrations dropped, and IL-10 concentrations increased. Tofacitinib was also confirmed to increase both IDO-1 and IDO-2 mRNA levels within these DCs in a dose-dependent manner. This switch from IFN-γ secretion to IL-10 secretion did correlate with enhanced suppression of T-cell proliferation but did not correlate with T-reg proliferation since

these populations were stable despite the addition of tofacitinib (57). Therefore, IDO activation may be suppressed through activating the JAK1/3 signalling cascade; although suppression of this cascade seemed to induce switching of T-cell cytokine profiles from pro-inflammatory to tolerogenic without manipulating the tolerogenic T-reg cell population. Due to the contradictory results of these studies, IDO activation and suppression are shown to be complex but are still studied intensely in areas of cancer, chronic diseases, and infections because of its potential immunomodulatory and immunoregulatory aspects.

1.3.2 Enzymatic activity

IDO is the rate-limiting enzyme for tryptophan metabolism within the kynurenine pathway (40, 58). Depletion of tryptophan coupled with an increase in toxic tryptophan-intermediates, leads to a change within the mononuclear cells' environment and the extracellular environment where Tryp depletion can starve fungus, parasites and other microbes (59). This change, along with environmental chemokines and cytokines, will modulate the disease outcomes in contrasting ways. It has been shown that IDO-1 activity can lead to a Th-2 biased response through the induction of Th-1 apoptosis or attenuation of the Th-1 response (58). Both apoptosis and attenuation can be attributed to Tryp-depletion, according to Fallarino *et al.* and Munn *et al.,* respectively (48, 60).

Fallarino *et al.* first showed that 3- hydroxyantranylic acid (3-HAA), a metabolite of the tryptophan/kynurenine (tryp/kyn) metabolic pathway, administered to murine thymocytes increased apoptosis through either the condensation or the fragmentation of the cellular nucleus (48). Other kynurenines were also tested at physiologically relevant levels, and it was found that only 3-HAA and quinolinic acid (QUIN) were able to induce apoptosis at physiologically relevant levels. Then they exposed differentiated Th-1 and Th-2 cells specific for either ovalbumin (OVA) or P815AB, which is a tumour/self-antigen to 3-HAA or QUIN. When either kynurenine was administered to these cells, an increased percentages of Th-1 cells were apoptotic, while Th-2 cells were unaffected (48). Therefore, the kynurenine metabolites 3-HAA and QUIN can selectively induce apoptosis within Th-1 cells and skew a mixed Th-1/Th-2 response to become a primarily Th-2 response.

Meanwhile, Yun *et al.* identified the induction of antigen-specific T-reg cells due to IDO-1 expression within the aorta (50). Ilic *et al.* also found that kynurenine depletion due to IDO-1

within DCs led to T-reg development within an *in vitro* human cellular model (61). Cheung *et al.* were also able to induce tolerogenic DCs that stunted T-cell proliferation. Additionally, any $CD4^+$ T-cells were phenotypically T-reg and had high IL-10 production, which leads to an anti-inflammatory state with both IL-10 and TGF-β cytokines. This state also leads to the decrease of cytotoxic T-cells producing IFN-γ and the general decrease of IL-12p70 and TNF-β (51).

Both RSV (9) and PVM (unpublished data) have been shown to induce IDO-1 mRNA production during infection. Therefore, IDO-1 is a known player during infection and may play a role in the viral and immunopathology caused by both viruses.

1.3.3 Signalling activity

IDO signalling seems to be dependent on two immunoreceptor tyrosine-based inhibitory motifs (ITIM) within the protein. The binding of IL-6 or other pro-inflammatory factors on the cell's surface promotes the phosphorylation of these ITIMs, which then interact with SOCS3. This interaction results in IDO's proteasomal degradation (43). In contrast, TGF-β will lead to Fyn-mediated phosphorylation of IDO that eventually leads to noncanonical NFκB activation for an anti-inflammatory environmental induction (43). Observing the differences between the study done by Kubo *et al.* and the ones performed by both Rodrigues *et al.* and Cheng *et al.*, the development of T-reg cells by tolerogenic DCs may be dependent on IDO's enzymatic properties, while the shifting of proinflammatory T-cells towards a tolerogenic state may be due to IDO's signalling activity. However, this is just speculation because Kudo *et al.* did not measure the kynurenine or tryptophan levels within the culture medium to see if there were any differences between DCs cultured with both LPS and tofacitinib and those only cultured with LPS.

1.4 Asthma: Disease or Syndrome

1.4.1 Asthma development and epidemiology

Asthma is a commonly known chronic inflammatory disease that affects the conducting airways of an individual (62). The most common symptoms of asthma include shortness of breath, difficulty in breathing, coughing and wheezing (63, 64). This condition was traditionally caused by an exacerbated Th-2 – biased response towards common molecules (dust, smoke

particulates, chitin from insects) (62). Recently, it has been discovered that asthma is not as simple as first thought. Asthma can have an allergic phenotype, also known as atopic asthma, or an intrinsic one. The allergic phenotype is characterized by IgE production towards an allergen and is initiated through sensitization of said allergen (62), and the common symptoms in allergic asthma are caused by high mucus production, and airway narrowing and obstruction (64). Intrinsic asthma does not produce IgE towards an allergen, nor has any distinct function for the adaptive immunity (62). Its development and exacerbation have been a topic of many studies with a plethora of different mouse models and combinations of mice, viruses, and allergens (65).

1.4.2 Implications of the Immune System

Asthma can also be defined by the prominent cell type that influxes during exacerbation. Even with this definition, asthma is still considered a spectrum disorder where individuals may exhibit eosinophilic influx while others experience neutrophilic influx. Of course, other individuals develop a combination of both eosinophilic and neutrophilic influx. These can also be sub-defined based on differing cytokine and chemokine production (62). Some studies have shown an increase in eosinophilic infiltration during RSV and other respiratory infections that increases wheezing during and after severe infections (15, 17). Tang *et al.* suggest that exacerbation of asthma by RSV induces a neutrophilic influx of cells within the lungs (66). These different types of cellular influx are mirrored by the previously mentioned strains of PVM virus, where a neutrophilic or eosinophilic response has been shown depending on the virus strain and mouse strain.

B-cells produce IgE to a specific antigen and release it into the serum. Mast cells have FCεRI receptors that tightly bind the Fc portion of IgE as they are both travelling through the blood. These cells develop in the bone marrow and travel through the blood to their designated tissues (generally under the skin, and in the mucosal area such as the lungs) (67, 68). When two bound IgE molecules bind to one molecule of their specific antigen, they cross-link initiating a signalling cascade that leads to mast cell degranulation. These cells hold a multitude of cytokines, proteases, and most of the histamine found within the human body in their granules (67). Mast cells produce and secrete cytokines such as TNFα, IL-4, IL-5, IL-6, IL-1β and IL-13 (67). These mast cells are part of the early response during exacerbation of an allergic response. The cytokines and other mediators that are released are involved in bronchoconstriction of the

airways, mucus secretion of goblet cells, and the secretions of chemokines leading to the infiltration of other cell populations such as macrophages, eosinophils, neutrophils, and T-cells (69). These cells, are part of the later phase of asthma which typically leads to prolonged airway dysfunction and damage (69).

Yu and Chen established three different asthmatic models using OVA and a mixture of LPS at different time-points in order to develop an eosinophilic model, a neutrophilic model, and a mixed eosinophilic and neutrophilic model (70). When the mice from all three models were exposed to methacholine, all developed strong airway resistance; treatment of dexamethasone to reverse the resistance was only successful within the eosinophilic model. Cellular influx within the BAL fluid confirmed the establishment of the type of asthmatic model developed. The agents used in the eosinophilic model induced approximately 50% eosinophilic, less than 5% neutrophilic, and 40% macrophage influx. The agents used in the neutrophilic model induced less than 10% eosinophils, 60% neutrophils, and 20% macrophage influx, while the agents used in the mixed model induced approximately 20% eosinophils, 50% neutrophils, and 20% macrophages. Detection of lymphocytes within all three models was between 5-10% with no significant difference found between them and the negative control. The largest number of total cellular influx with about $1.5x10^7$ cells was found in the mixed model; the neutrophil model was second with about $5\text{-}10x10^6$ cells, and the eosinophilic model was third with approximately $5x10^6$ cells. In the eosinophilic model large amounts of IL-4, IL-5, and IL-13 (100, 80, and 50 pg/mL respectively), a large amount of IL-33 (50 pg/mL), and minimal IFN-γ and IL-17A (less than 20 pg/mL) was induced. In the neutrophilic model minimal IL-4, IL-5, and IL-33 (less than 20 pg/mL), and a large induction of IL-13, IL-17A, and IFN-γ (40, 300, and 75 pg/mL) were observed. Finally, in the mixed model a large amount of all proteins: 175 pg/mL of IL-4, 90 pg/mL of IL-5, 75 pg/mL of IL-13, 70 pg/mL of IL-33, 300 pg/mL of IL-17A, and approximately 85 pg/mL of IFN-γ was found. Finally, total IgE was significantly increased in all three models (at least 600 ng/mL). The eosinophilic model resulted in higher induction of OVA-specific IgE compared to the other two models, and the neutrophilic one resulted in the smallest production though it was still significantly higher than the negative control group. Therefore, the eosinophilic model established here results in high IgE production, large eosinophilic and some macrophage influx, and minimal neutrophilic influx. These cells were coupled with large Th-2 cytokines (IL-4, IL-5, and IL-13), and minimal Th-1 and Th-17 cytokines (IFN-γ and IL-17A).

Contrastingly the neutrophilic model resulted in a large neutrophilic influx with minimal eosinophilic and macrophage influx. These cells were coupled with high IL-17A, IL-13, and IFN-γ production and minimal IL-4 and IL-5 production; some IgE production was also detected within this model. In the mixed model similar cellular influx was observed as in the neutrophilic model, but high IgE induction and high concentrations of all cytokines measured were also observed.

A review in 2000 by Wardlaw *et al.* (71) confirmed typically increased eosinophilia within the airway submucosa of asthmatic patients, but not enhanced neutrophils. Bronchoscopy studies allowed for the quantification of lymphocytes and mast cells that also have a significant role in this disorder but stay within the epithelium. Eosinophils are known to both induce damage in the airways and activate portions of the adaptive immune system (69). Eosinophil secrete factors such as eosinophil peroxidase which is known to cause bronchial hyper-responsiveness directly, damage the structural cells of the lungs, and activate DC's for an adaptive immune response (62). Eosinophils also secret major basic protein which causes damage to the structural cells (62).

Contrastingly, neutrophils travel to an inflamed site and secret molecules such as granzymes and reactive oxygen species to create a hostile environment towards viral, bacterial and fungal infections (72). These molecules are also able to damage the epithelial layer in these infection sites. Typically, neutrophils can survive up to 6-8 hours when circulating; though tissue-based neutrophils may survive 3-5 days and reverse transmigrate back into the circulation (72). Th-17 cells recruit neutrophils into a site through IL-17A induction of epithelial cells to secrete IL-8, a known neutrophil chemokine. Neutrophils can express FCεRI that bind to IgE; thus modifying responses when IgE binds to their antigen (72). The neutrophil role in modifying the airways is still controversial, but the secretion of TGFβ, elastase, and matrix metalloproteinase 9 by neutrophils do confirm this possibility (72). Therefore, despite neutrophils commonly found in intrinsic asthmatic sputum, their role within the mechanisms of asthma remains unclear.

1.4.3 Effects of cockroach allergen on allergy development

Cockroach particles constitute one of the many benign macromolecules that are known allergens associated with the development of asthma (73). According to Gao, despite other

common allergens such as animal dander and house dust mites also correlating with asthmatic development, CRA seems to be the most substantial risk factor. This increased risk due to CRA was especially common within inner-city children cohorts, who had both increased severity and frequency of childhood allergies and asthma. Gao reported that approximately 50% of children who tested positive for CRA were also more likely to have high levels of CRA within their bedrooms, and this group was considerably more likely to be hospitalized, and miss more days at school due to asthma-related symptoms and exacerbations (73).

In a study performed by Whitehead *et al.*, an asthmatic mouse model was developed that utilized the sensitization of OVA alone, and when paired with known allergens correlated with increased asthmatic cases (74). They used house dust mite allergen (HDM), LPS, flagellin, *Aspergillus* (fungus) protease (asp), or papain protease (cysteine protease from papayas) (pap) as adjuvants for their OVA sensitization. This study differentiated the asthmatic responses towards OVA when sensitized with either a protease (HDM, asp, and pap) or TLR ligands (LPS and flagellin). They confirmed that OVA sensitization on its own did not induce airway inflammation when the mice were further challenged, but there were differences in cell population influxes and cytokine production when OVA was coupled with either a protease or a TLR-ligand adjuvant. Whitehead *et al.* found that, generally, TLR-ligands induced the production of TNF and IL-1β towards OVA, while the protease adjuvants did not. Additionally, the TLR-ligands induced a mixed eosinophilic/neutrophilic influx coupled with a mixed Th-2/Th-17 cytokine profile. They also showed that TNF was needed during the sensitization phase of the TLR-ligand asthma model since eosinophilic influx was decreased when the model was tested in a TNF-deficient mouse-strain. The protease adjuvants generally produced an eosinophilic influx with a primarily Th-2 cytokine profile. The HDM adjuvant seemed to show a mixture of protease and TLR-ligand response. Additionally, none of the adjuvants used induced IFN-γ production (74). Therefore, there is a difference between asthma induced by protease allergens and those induced by TLR-ligand allergens.

Kim *et al.* tested the effect of CpG oligodeoxynucleotide in a CRA-induced asthmatic model (75). Focusing on the CRA-induced model, the frequent intranasal sensitization of the Balb/c mice with CRA lead to significant airway hypersensitivity resistance and an influx of cells within the BAL fluid. Primarily, these cells consisted of neutrophil and macrophage populations, but also contained a small but significant eosinophilic population when compared to

their sham group. Additionally, total lung samples showed significantly decreased percentages of alveolar macrophages, inversely correlated with significantly increased percentages of interstitial macrophages and monocytes. Kim *et al.* showed that the CRA model induced a Th-2 (IL-5 and IL-13) biased response with increased total IgE, and CRA-specific IgE production. The CRA-specific IgG1/IgG2a ratio was also significantly increased within the CRA model. There was also nominal IFN-γ protein production. Additionally, there was an increase in IL-10 production but no change in phenotypic T-reg cell percentages (75). Therefore, this CRA model induced a mixed eosinophil/neutrophil influx coupled with a more Th-2 biased response. Coupling this with the study done by Whitehead *et al.*, CRA most-likely induces an asthmatic response based on TNF expression suggesting a TLR-ligand-like induction by CRA.

In an earlier study, Kim *et al.* focused on the protease activity of CRA (76). Here, CRA protease activity was determined to be significantly inhibited by a serine-protease inhibitor (aprotinin), and this caused slightly more inhibition than a cysteine protease inhibitor, a serine-cysteine protease inhibitor, or a trypsin inhibitor. Protease-activated receptor (Par)-2 internalization was tested with either an alveolar macrophage or a peritoneal macrophage cell line. Each cell line was administered CRA with or without aprotinin, and both showed Par-2 internalization by CRA; this was inhibited with aprotinin treatment. Both cell lines also produced TNF-α when exposed to CRA. This induction was also ablated with aprotinin treatment. Kim *et al.* then used a Par-2 antagonist (ENMD-1068) and found that CRA could neither induce internalization of Par-2 nor production of TNF-α. CRA also induced cell influx that was primarily composed of neutrophils, macrophages, and lymphocytes; there was also a small number of eosinophils. The cytokine profile of this CRA model showed a Th-2 biased response with a high concentration of IL-13 and similar, but lower, concentrations of IL-5 and IFN-γ. There was also an increase in IgE titers within the model. Blocking of TNF-α ameliorated the pulmonary inflammatory symptoms. Kim *et al.* then incubated CRA with aprotinin before sensitizing mice with the combination. This removal of serine protease activity attenuated airway inflammation and decreased alveolar macrophage influx and TNF-α expression. However, aprotinin treatment did not affect interstitial macrophage or DC influx (76). Therefore, CRA exhibits serine protease activity that leads to the induction of TNF-α and subsequent airway inflammation and asthmatic conditions.

As such, CRA is a potent immunostimulant and apparent inducer of asthmatic conditions,

although the type of asthma is dependent on how sensitization is done, and whether a viral infection is introduced before or after initial CRA exposure.

1.4.4 Clinical symptoms

According to the Asthma and Allergy Foundation of America (AAFA), asthma is a chronic inflammation of the lungs that generally manifests as difficulty breathing. Asthmatic symptoms include coughing, wheezing, shortness of breath, rapid breathing and chest tightening (63). The problem is that this set of symptoms does not account for the multiple ways that they can be manifested. Triggers for these asthmatic symptoms include allergens that the host has a corresponding allergic response against (cat dander, dust mites), or general irritants such as smoke, air pollution, and aerosolized chemicals. The AAFA even states that exercise and mood-swings are known triggers due to their systemic hormonal changes within the body that can affect lung function. Asthma is sub-divided into different categories dependent on the triggers for clinical symptoms and other biological factors. These factors are more readily available for monitoring because of the technological advances, and overall better monitoring systems, within hospitals and other care facilities.

Allergic asthma is the well-known classical trigger of asthma. Its development occurs in early-life, and exacerbation occurs due to exposure of an allergen towards which the host has a Th-2 biased response, including IgE involvement (77). Non-allergic asthma is slightly more complicated as onset is usually later in life, and exacerbation occurs without any specific trigger. Additionally, no allergen-specific IgE is found within the serum of these patients (77).

Wenzel *et al.* also describes how unbiased studies were done that had a plethora of different clinical variables such as the age of onset, gender, eosinophilia, and emergency-room visits, but also did not contain measurements of airway obstruction such as FEV1 (77). Despite these drawbacks, most of the studies discussed here found general groupings for the known sub-categories of asthma. These included early-onset being a key factor for more allergic asthma, but could not distinguish any variables that are more linked to the different severities of exacerbation seen within the observed cohorts. Late-onset asthma seemed to better cluster with other factors such as eosinophilic influx, and obesity. Primarily, this cohort was comprised of women and did not have an allergen that triggered exacerbation (77).

These subdivisions of asthma based on clinical symptoms outline how critical it is to

deduce the different pathways that can induce its development and exacerbation. These different pathways that can lead to similar symptoms show how complicated asthma is, and suggests that more than one model is necessary to determine all of the different factors of asthmatic development and exacerbation.

1.4.5 Viral induction of asthma development or exacerbation

The complexity of how respiratory viruses play a role in asthma is not only limited to its development. There are also studies showing that acute respiratory infections can either induce (78, 79) or suppress (18) asthma exacerbation.

John *et al.* used a model of CRA asthma that developed due to environmental changes within the lungs because of a previous viral infection (79). This model was initiated with viral infection occurring on day 0 and the mice were first sensitized to CRA in incomplete Freud's adjuvant (IFA), either intraperitoneally or subcutaneously on day 21. This long time-period between infection and sensitization allowed the virus to clear before the mouse immune system would respond to CRA. The mice were again sensitized to CRA intranasally two weeks after the first sensitization (day 35). Subsequently, they were challenged with an intratracheal sensitization of CRA a week later (day 42) and then sacrificed the next day (day 43). They had previously shown that RSV infection induced IL-13, which further induced the chemokine CCL5. Therefore, they tested the effects of administering anti-CCL5 within this asthmatic model. John *et al.* showed that RSV infection prior to CRA sensitization led to significantly increased eosinophilic influx. This eosinophilic influx was significant, but small, in comparison to the overall neutrophilic influx induced by CRA. Neither cellular influx was affected by RSV infection or anti-CCL5 treatment. RSV infection did induce a significantly higher lymphocyte influx when compared to the CRA group without RSV infection and the CRA/RSV group treated with anti-CCL5. Strangely, only CCL22 was inhibited by anti-CCL5 treatment, whereas neither CCL6 nor CCL11 showed any significant changes (79). John *et al.* suggest that there are long-lasting changes due to RSV infection, even after viral clearance, that are mediated by CCL5 production during the viral infection. There is a further suggestion that these changes manipulate how the lungs respond to CRA sensitization, and they seem to make the lungs permissible for asthma development.

Smit *et al.* identified $CD8^+$ T-cells and their IFN-γ production induced by RSV infection

as a necessary component for regulating asthmatic symptoms (18). *Smit et al.* initiated the study by assessing the different responses towards RSV infection, CRA sensitization, or RSV infection followed by CRA sensitization, from both C57Bl/6 and Balb/c strains. The C57Bl/6 mice had decreased airway hypersensitivity when CRA and RSV were coupled compared to CRA sensitization on its own. The RSV+CRA group of Balb/c mice showed an increased airway hypersensitivity compared to the RSV infected group, but similar resistance levels to mice sensitized to CRA. Additionally, IL-4 was only induced in the Balb/c mice. Similar levels were found after either RSV infection or CRA sensitization, but this IL-4 induction was significantly increased when CRA sensitization was coupled with RSV infection in the BALB/c mice. The C57Bl/6 strain did not show any IL-4 induction. However, it did show the induction of IL-5 within the CRA sensitized group to similar levels as Balb/c, although this was also significantly reduced when CRA was coupled with RSV; the Balb/c strain showed an increase in IL-5 secretions when RSV and CRA were coupled. This trend was mirrored when Smit *et al.* observed the IL-13 protein secretions.

Since C57Bl/6 mice had an attenuated CRA-induced Th-2 response when CRA was coupled with RSV, they investigated further by addressing whether this phenotype was only apparent when CRA was administered after RSV viral clearance. The researchers also tested whether RSV infection and viral clearance occurred after the initial CRA sensitizations and before the subsequent CRA challenges. Both models of RSV infection and CRA sensitization and challenges significantly decreased airway hypersensitivity resistance compared to the CRA models without the supplementary RSV infection. C57Bl/6 mice are resistant to viral infections due to their ability to induce a more rapid and robust Th-1 response (21). Therefore, the researchers added anti-IFN-γ to their sensitization protocol. This suppression of IFN-γ activity increases airway hypersensitivity resistance while also increasing eosinophil influx not seen without the anti-IFN-γ treatment. This time, there was an increase in IL-4 production from the group that was only sensitized to CRA, and this induction was significantly increased when anti-IFN-γ was administered. The antibodies inhibited the suppression of IL-4 production by the additional RSV infection. This trend was also seen when observing the IL-5 and IL-13 levels within these mouse groups. Finally, Smit *et al.* injected RSV-primed $CD4^+$ or $CD8^+$ T-cells within CRA sensitized mice one day before they were challenged. Airway resistance was only decreased when RSV-specific $CD8^+$ T-cells were administered, though both populations of T-

cells decreased IL-5 production and increased IFN-γ production. IL-13 had a nominally significant decrease when $CD8^+$ T-cells were administered. This decrease was not seen when $CD4^+$ T-cells were similarly administered (18).

Therefore, Smit *et al.* found that RSV infection, whether during asthma development or exacerbation, inhibited the asthmatic phenotype within C57Bl/6 mice. These results are in contrast to the study by John *et al.,* which suggested that RSV infection before sensitization would induce an asthmatic phenotype within DBA2J mice. Thus, the role that viral respiratory infections play within the development and exacerbation of asthma needs further elucidating, with multiple different models. The differing models are imperative in understanding the differences in asthma phenotypes, and what signalling pathways control their development and exacerbation.

1.4.6 Management of asthma

According to the AAFA, asthma is best managed by a combination of avoiding known triggers, especially apparent within atopic asthma, and treatment of steroids with or without beta-agonists, or leukotriene modifiers, biologicals, or theophylline (63). This list is inclusive of all long-lasting medication that may be prescribed for long-term treatment of the asthmatic condition. There is also short-lasting treatment with steroids with or without beta antagonists that are used when an exacerbation or 'asthmatic attack' occurs (63). These guidelines outlined by the AAFA stem from the original guidelines produced by the Global Initiative for Asthma (GINA), which was founded just over 25 years ago in 1993 (80). GINA was founded by a number of organizations focused on asthma and other lung diseases in order to assist in asthmatic patient care. This was done by compiling and distributing a document of guidelines which was first published in 1995 (80). Since then, the GINA guidelines have been modified and updated every year as our understanding of the intricacies of asthma has grown. As with most topics in science, new discoveries leading to better categorization of asthma and therefore treatments have also led to more questions that need to be followed up with more basic research.

A survey was done in 1999 that assessed patient's opinion on the level of controlling asthmatic symptoms and was used as an extrapolation to how the guidelines were distributed to these patients (81). Shocking results were obtained from this survey. These results included a dissonance between the GINA guidelines' definition of controlled asthma, and the patient's

perception of how controlled their asthma was. Only 4.6% of children and 7.7% of adults self-assessed their asthma as severe, despite 15.1% of children and 20.5% of adults being diagnosed with severe asthma according to the GINA guidelines. Additionally, 23% of adults have made career choices dependent on their asthma, while the GINA guidelines suggest that fully controlled asthma should not limit any life activities. Finally, the GINA guidelines recommend having a lung function test, but over half of both adults and children have never had this test (81). Conclusions pulled from this study suggested that either patients were content with defined sub-optimal control, or physicians are not as knowledgeable concerning the severity levels of asthma.

In 2007, a report was produced during the National Asthma Education and Prevention Program (NAEPP) that updated these GINA guidelines (82). The updates included better guides for assessing the severity of asthma and for assessing its control after treatment had started. Also included was a more specialized and understandable table. This table was designed to assist in the long-term management of asthma, which included modifications to treatment strategies, and new multifaceted ways of educating patients to assist in the empowerment of controlling their asthmatic condition (82).

Thus, the management of asthma is constantly being scrutinized and updated to reflect the latest studies in all aspects of asthmatic disease. These aspects include new medicine for control, and better methods for assessment of both severity and quality of control strategies. As research continues to elucidate the differences in phenotypes and asthma development, the GINA guidelines will continue to give this pertinent information to physicians so that they can make better-informed decisions to help patients control their asthma. Additionally, the GINA guidelines can be used by patients to help them better understand their conditions. Finally, the GINA guidelines stress the importance of free communication between patient and physician, so that diagnosis of severity and assessment of control measures occur without much delay.

2 HYPOTHESIS AND OBJECTIVES

There are four rationales for my hypothesis, and they are as follows:

1. Early RSV infections are linked to the development of asthma (3, 15, 17)
2. PVM-15 within the Balb/c adult mice is an established model for infant RSV infection (21, 22, 24)
3. Traditional asthma is a Th-2 exacerbated response towards a benign particulate allergen (62)
4. IDO-1 is known to either upregulate inducible T-regs (50, 61) or suppress the Th-1 response allowing the proliferation of Th-2 responses (9)

Therefore, I hypothesize: an underlying PVM infection during the first exposure towards an allergen will alter the memory response towards it, thus promoting the development of an asthmatic response.

There are three objectives to confirm this hypothesis:

1. Develop an asthmatic model using PVM-15 and 5-6 week old Balb/c mice to reproduce a severe RSV infection, and lyophilized-ground German Cockroaches as the allergen (CRA).
2. Elucidate the lung environmental response 24 hours after either CRA exposure or clearance of a PVM infection within three groups using the developed asthma model: negative control group exposed to medium followed by PBS (Medium/PBS), CRA group exposed to medium followed by CRA (Medium/CRA), and PVM group (PVM/PBS).
3. Examine the lung environment of the experimental group exposed to PVM followed by CRA (PVM/CRA) using the model based on changes within the immune response such as protein production, mRNA expression, and cellular efflux and influx.

3 MATERIALS AND METHODS

3.1 Cell line and virus propagation

Baby Hamster Kidney (BHK)-21 cell line was initially obtained from the American Type Culture Center (ATCC) to grow my PVM stock. The origin of the PVM stock is also ATCC. The BHK-21 cells were grown in BHK-21 medium. The BHK-21 medium consisted of Minimum Essential Medium (MEM) from Sigma-Aldrich supplemented with 0.1 mM non-essential amino acids, 1 mM Sodium Pyruvate, and 5 µg/mL Gentamicin, all from Thermo Fisher Scientific. It was also supplemented with 5% fetal bovine serum (FBS) from Gibco Thermo Fisher Scientific. These cells were grown to a confluence of ~80% within T-150 flasks from BD Biosciences and passaged approximately 3-4 times before being used for virus propagation and titration.

At approximately 75-80% confluency of passage 3 or 4, the medium was removed, and the cells were gently washed with PVM medium. This medium consisted of Dulbecco's Modified Eagle Medium (DMEM) base from Sigma-Aldrich supplemented with 0.1 mM non-essential amino acids, 10 mM HEPES Buffer, (21) 5 µg/mL Gentamicin (all from Thermo Fisher Scientific), and 2% FBS (Gibco Thermo Fisher Scientific). Once washed, the cells were infected with PVM at a multiplicity of infection (MOI) of 0.1 within 5 mL. The flasks were manually rotated every 15 minutes at 37 °C and 5% CO_2 for 1.5 hrs. Subsequently, an extra 11 mL of PVM medium was added, and the cells were incubated in the same conditions, without rotation, for 3 days. On that third day, the virus was harvested by scraping the cells from the flask using a 39 cm handle/3.0 cm blade cell scraper from Corning Inc. The cells were further disrupted by pipetting them up and down multiple times within the spent medium. Once thoroughly mixed, the solution was aliquoted, and immediately frozen using liquid nitrogen. The frozen aliquots were stored in the minus 80 °C freezer for long-term use including more propagation of this virus as a stock for the mouse trials.

3.2 Cockroach allergen preparation

Lyophilized German Cockroach Antigen (*Blattella germanica*) from Stallergenes Greer was resuspended at a concentration of 5 µg/µL in PBS from Gibco Thermo Fisher Scientific. It was aliquoted and stored at -20 °C for long-term use.

3.3 Sample preservations

3.3.1 Lung tissue

All lung tissues were collected from the mice and aliquoted as described below. After collection, the smallest section of the multi-lobe was collected into a 2 mL screwcap tube containing 2.99-3.01 g of 2.4 mm zirconia beads from BioSpec Products Inc and 1 mL of TRIzol® reagent from Thermo Fisher Scientific. It was then homogenized in a mini bead-beater from BioSpec Products Inc for 10 seconds at 4,800 rpm, centrifuged in 4 °C at 10,000 rpm for 1 min, frozen in liquid nitrogen, and stored at -80 °C for future mRNA extraction and qPCR analysis.

The middle section of the multi-lobe was also removed into a 2 mL screwcap tube with 2.4 mm zirconia beads, and 1 mL of sample medium consisting of DMEM supplemented with 0.1 mM non-essential amino acids, 10 mM HEPES Buffer, 5 µg/mL gentamicin, and 1X antibiotic/antimycotic from Thermo Fisher Scientific. These samples were also homogenized and centrifuged in the same way, and then aliquoted into new 2 mL screwcap tubes, frozen in liquid nitrogen and stored at -80 °C for either virus titration assays or multiplex ELISAs.

The largest section of the multi-lobe was inserted into a sterile 15 mL Falcon centrifuge tube from Thermo Fisher Scientific containing 2 mL of lung fragment culture (LFC) medium. This medium consisted of RPMI 1640 (1X) from Gibco Thermo Fisher Scientific, with 10% FBS, 10 mM HEPES, 0.1 M non-essential amino acids, 1 M Sodium Pyruvate, 2 mM L-glutamine, 1X antibiotic/antimycotic, and 5 µg/mL gentamicin. They were transported on ice from the sampling room to a biosafety cabinet (BSC) where they were chopped into two pieces; each piece was deposited into 2 wells pre-prepared (the same day) with 500 µL of LFC medium and incubated at 37 °C and 5% CO_2 until needed. Once the two pieces were distributed, they were minced with scissors from Thermo Fisher Scientific and left to incubate for 5 days at 37 °C

and 5% CO_2. On day 5, 2 wells/mouse were pooled into a Fisherbrand 1.5 mL MCT Graduated Natural tube from VWR and centrifuged for 1 minute at 10,000 x g. They were then aliquoted into three 2 mL screwcap tubes and frozen/stored at -80 °C for total IgE analysis.

The single-lobe was pooled per mouse group into a gentle MACS C tube from Miltenyi Biotech with 5 mL of Hans Balanced Salt Solution (HBSS) from Gibco Thermo Fisher Scientific supplemented with 5% FBS. The tissue was then mechanically disrupted using a gentle MACS dissociator from Miltenyi Biotech, according to the manufacturer's instructions. Then, 0.5 mg/mL of Collagenase type IA and 20 µg/mL of type IV Bovine Pancreatic DNase (both from Sigma-Aldrich) were added to the homogenate, and the tubes were incubated in a 37 °C hot water bath for 20 min. The homogenate was then further dissociated into a suspension using the same gentle MACS dissociator and transferred to a 50 mL Falcon centrifuge tube. The suspensions were centrifuged, and the supernatant was decanted. Any red blood cells were lysed using 2 mL of ACK lysis buffer from Thermo Fisher at room temperature for 30 seconds. The buffer was neutralized with approximately 13 mL of lung tissue wash buffer. This buffer consisted of PBS with 0.5% bovine serum albumin (BSA) from Thermo Fisher Scientific. Once the buffer was neutralized, the samples were centrifuged. They were subsequently washed with the same wash buffer and passed through a 40 µM nylon cell strainer from Thermo Fisher Scientific. A Beckman Coulter Counter from Beckman Coulter Inc was used to determine the total cell count, and the cells were centrifuged and resuspended in the corresponding volume at $4x10^7$ cells/mL, to be used for FLOW cytometry analysis of different cell populations.

3.3.2 Bronchoalveolar lavage (BAL) fluid

The lungs were rinsed with 700 µL of PBS with 2% FBS and 3 mM EDTA (7.5% disodium ethylenediaminetetraacetic acid.$2H_2O$). The rinse was pooled per group in a 15 mL Falcon centrifuge tube or collected individually for some experiments in a 2 mL screwcap tube and set on ice for processing after sampling had completed. The samples were spun and the supernatants aliquoted for IgE and Multiplex ELISA analysis, frozen and stored as described above. The cells were resuspended in Facola (0.03% sodium azide and 0.2% gelatin in PBS pH 7.3) and processed for FLOW cytometry.

3.3.3 Blood samples

The mice were euthanized with an overdose of isoflurane and then subjected to cardiac puncture. Blood was collected in a BD Microtainer Serum Separator Tube and spun at 10,000 xg for 3 min, then frozen and stored at -20 °C for later use.

3.4 Virus titration assay

96-well plates were seeded with 15,000 BHK-21 cells per well. Approximately, 15-20 hours later, the lung homogenate samples and PVM virus stock, as a positive control, were defrosted and diluted, in PVM medium, 1/10 in the top row of a 96-well dilution plate. Each sample was plated twice for accuracy and serially diluted 1/10 down the plate. The medium from the BHK-21 plate was pipetted off and replaced by the samples in the dilution plate. The plates were then incubated at 37 °C and 5% CO_2 for 3 days.

On the third day, 100 µL of 25% acetic acid 75% ethanol was added to each well on top of the medium, and the plates were incubated at room temperature for 20 min to fix the cells. The supernatant was decanted, and plates were washed with 1X-PBS 4 times and tapped dry. Then, 100 µL of a permeabilizing and blocking solution consisting of PBS with 20% FBS and 0.2% Triton X-100 was added to the fixed cells, and the plates were incubated at 37 °C for 30 min. The primary antibody solution (1X PBS with 5% heat-inactivated (HI)-FBS, 1% HI-goat serum, and 1:500 rabbit anti-PVM antibody) was added, and the plates were incubated under the same temperature for 2 hrs. The plates were rewashed 4 times with 1X-PBS and 0.5% Tween and then tapped dry. Then 100 µL of the secondary antibody (1X PBS with 5% HI-FBS, 1% HI-goat serum, 1:1000 alkaline phosphatase-conjugated goat anti-rabbit IgG) was applied, and the plates were again incubated for 1 hr. After this incubation, the plates were rewashed with 1X-PBS, and BIORAD AP Conjugate Substrate was added to each well. The plates were incubated at room temperature for approximately 20 min. The reaction was stopped by washing the plates with dH_2O. The wells were filled with dH_2O and read using an inverted microscope. Virus plaques were counted, and dilutions were accounted for when reporting the titers of viable virions.

3.5 qPCR RNA procedure for analysis of mRNA expression

3.5.1 Isolation of mRNA from homogenate lung tissue

TRIzol samples were defrosted in an RNase/DNase-free fume hood and left at room temperature for another 5 min. 500 µL were collected into a 1.5 mL DNase and RNase Free Graduated Microtube from FroggaBio, and 100 µL of chloroform was added to this aliquot. They were shaken for 15 seconds and left at room temperature for 2-3 minutes. The tubes were centrifuged using the Centrifuge 5415 R machine set at 4 °C for 15 min at 12,000 xg. The clear chloroform layered at the top of the sample solution was carefully removed and collected in another microtube. Then, 250 µL of isopropanol was used to precipitate the RNA from the separated chloroform solution by letting it sit for 10 min after multiple slow inverts. The samples were centrifuged at the same temperature and speed for an additional 10 min. After this centrifugation, the supernatant was pipetted off, and 500 µL of ethanol was added for washing. The samples were again centrifuged at 4 °C for 5 min at a speed of 7,600 xg. The ethanol was pipetted off again, and the tubes were left to dry for approximately 20-30 min. This drying was to let any remaining ethanol dissipate. The dried samples were then dissolved in RNase and DNase-free dH_2O and frozen/stored at -80 °C overnight. Once all RNA had been extracted from all of the samples, they were defrosted on ice. Their 260/280 ratio, 260/230 ratio, and concentrations in ng/µL of each sample were then determined by using the ND-1000 Spectrophotometer and corresponding ND-1000 V3.8.1 software. An aliquot of each sample was diluted to 100 ng/µL and used for preparing cDNA.

3.5.2 Transcription to cDNA for qPCR

Using the QuantiTect Reverse Transcription kit from Qiagen, a 500 ng aliquot of each sample was prepared in 60 µL of RNase and DNase-free dH_2O as instructed by the manual. These cDNA samples were used for qPCR analysis.

3.5.3 qPCR and data analysis

The qPCR was run as per the instruction manual for PowerUP SYBR Green from Thermo Fisher Scientific. All of the primers were ordered from Thermo Fisher, and their annealing temperatures were identified in-house using gradient PCR. **Table 3.1** lists the primer

sequences and corresponding annealing temperatures. The qPCR reaction was performed in the following way: 1st step at 50 °C for 2 min and then 95 °C for another 2 min. The 2nd step was repeated 40X starting with 15 sec at 95 °C, 30 sec at the annealing temperature, and another 30 sec at 72 °C with a reading taken at the end of this 30 sec. The 3rd step was to analyze the melting curve of the products. Therefore, the temperature increased from 65 °C up to 95 °C in 1 °C increments. This increase occurred every 10 sec, and a reading was taken before each subsequent increase. All results were normalized based on average GAPDH levels of the Medium/PBS group within each trial.

Table 3.1 qPCR primer list

List of qPCR primers used in this project. All sequences were made at Thermofisher, and PCR gradient was performed to check the sequences that were not already used within the lab. These sequences were Muc5A and Gob5. All other sequences were already optimized by previous lab members.

Target Gene	Direction	Sequence	Amplicon Size	Annealing Temperature (°C)
GAPDH	Forward	5’ AACTTTGGCATTGTGGAAGG 3’	223 bp	57.5
	Reverse	5’ ACACATTGGGGGTAGGAACA 3’		
β-actin	Forward	5’ ACTGGGACGACATGGAG 3’	266 bp	57.5
	Reverse	5’ GTAGATGGGCACAGTGTGGG 3’		
IDO-1	Forward	5' ATGTGGGCTTTGCTCTACCA 3'	228 bp	57.5
	Reverse	5' CCCCTCGGTTCCACACATAC 3'		
Muc5AC	Forward	5' TGTCCTGAGGGTATGGTGCT 3'	99 bp	55.4
	Reverse	5' ACCCGGTGCATAAAGTGTCC 3'		
Gob5	Forward	5' GAGCAGCACCTCCGAAGAACA 3'	150 bp	61.4
	Reverse	5' CCACAAACGATCCCCCTGAAGA 3'		
IL-4	Forward	5' GGAGATGGATGTGCCAAACG 3'	78 bp	61.4
	Reverse	5' ACCTTGGAAGCCCTACAGAC 3'		
IFN-γ	Forward	5' TCAAGTGGCATAGATGTGGAAGAA 3'	92 bp	57.5
	Reverse	5' TGGCTCTGCAGGATTTTCATG 3'		

3.6 FLOW cytometry procedure

The BAL fluid cells were resuspended in cold Facola or PBS to aliquot a triplicate for each group, and to be pooled with other groups for the control wells. The lung tissue samples were resuspended in the same solutions at a concentration of 4 x10^7 cells/mL. 50 µL of these samples were dispensed into plates. The lung homogenates were separated into two plates based on if they were stained for neutrophils and eosinophils or stained for macrophages and DCs with subsequent internal staining for IDO-1. The BAL fluid cells were plated on a separate plate from the lung homogenates and only stained for neutrophils or eosinophils. The surface-staining procedure was the same for all plates, although PBS was used for the macrophages and DCs with the internal IDO-1 staining.

All of the stained samples and controls (but not the un-stained controls) were blocked with TruStain fcX^{TM} (anti-mouse CD16/32) Clone 93 from Biolegend, and incubated in the dark on ice for 5 min. Then 48 µL of the staining solution consisting of either Facola or PBS and designated conjugated antibodies (FITC, PE, APC, or eFluor 660) for each particular cell population (listed in **Table 3.2**) were added for staining. The un-stained controls received 50 µL of Facola or PBS to their wells. These plates were incubated under the same conditions for 30 min and then centrifuged at 500 xg for 10 min. The supernatant was decanted from each well, and the cells were resuspended with 100 µL of their corresponding solution (the first wash). They were centrifuged at 500 xg for 5 min and resuspended in the same way a further 2 times as washes. After the third, and final wash, the wells with Facola were decanted, and the cells were resuspended in a fixing solution of Facola and 2% formaldehyde. The samples were shielded from light and stored at 4 °C to be analyzed within a week of processing.

The plate with PBS was decanted, and the Cytofix/Cytomer Plus from BD Biosciences was used for internal staining of IDO-1 as instructed by the manual. The cells were resuspended in PBS at the end of the staining protocol and stored at 4 °C for reading.

The samples were read with a BD FACSCalibur, and both gating and analysis were done using the Kaluza software. Initially, eosinophils were gated as CD11c$^-$ F4/80$^+$, although there is evidence of subset macrophage populations that can also be identified this way. Besides, anti-Gr-1 antibodies bind to both Ly6C and Ly6G. While Ly6G is only expressed on neutrophils, Ly6C is expressed on multiple immune cell types, including eosinophils. Therefore, to mitigate the

masking effect that neutrophils incur onto eosinophils seen within the data, the gating technique employed by Zaynagetdinov *et al.* (83) was used since the expression of Gr-1, and their side scattering (SSC), are distinct differences between these two cell populations. Thus, the neutrophils were gated as Gr-1^{high} SSC^{int} and the eosinophils as Gr-$1^{int/low}$ SSC^{high}.

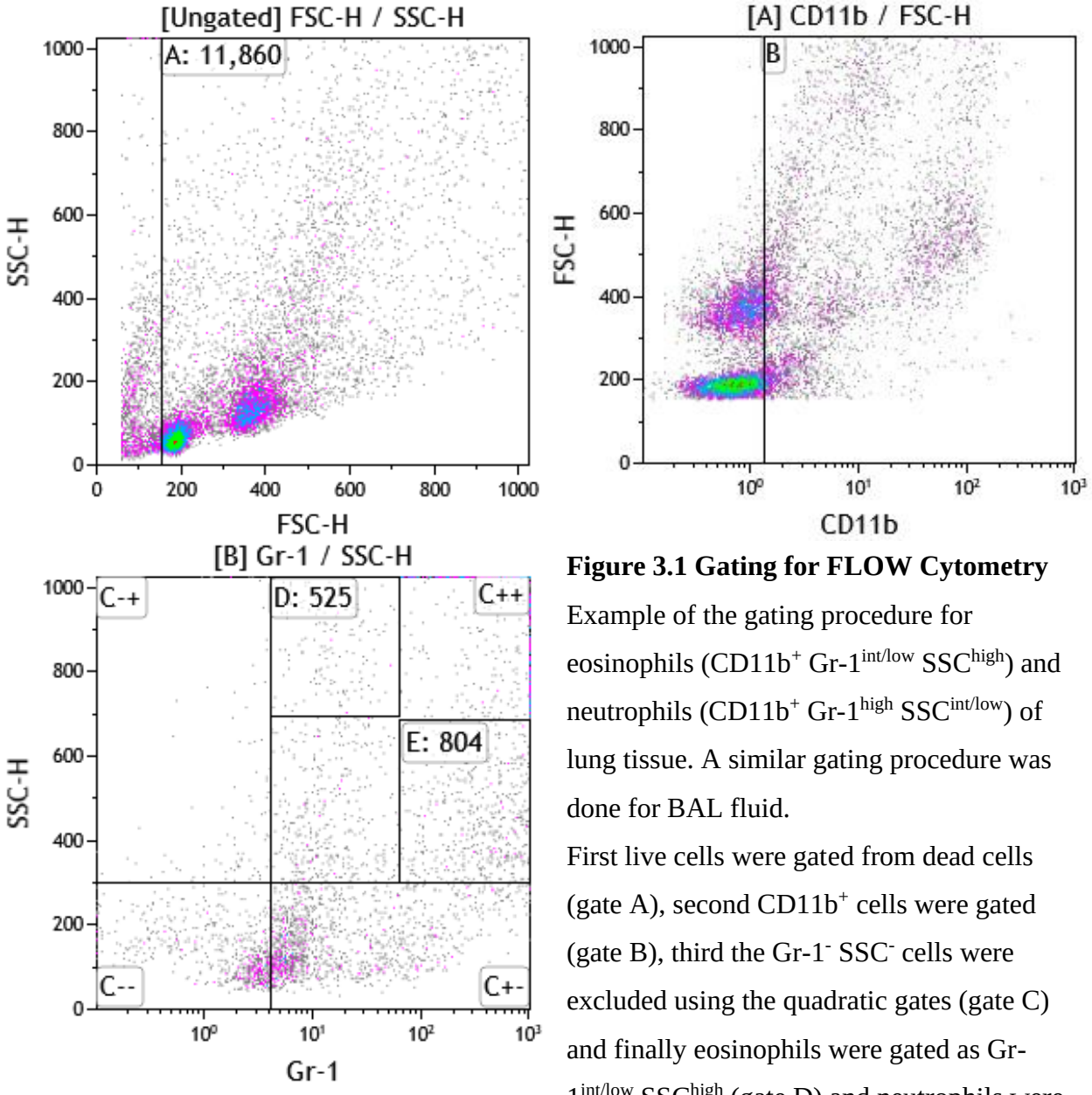

Figure 3.1 Gating for FLOW Cytometry

Example of the gating procedure for eosinophils ($CD11b^{+}$ Gr-$1^{int/low}$ SSC^{high}) and neutrophils ($CD11b^{+}$ Gr-1^{high} $SSC^{int/low}$) of lung tissue. A similar gating procedure was done for BAL fluid.

First live cells were gated from dead cells (gate A), second $CD11b^{+}$ cells were gated (gate B), third the Gr-1^{-} SSC^{-} cells were excluded using the quadratic gates (gate C) and finally eosinophils were gated as Gr-$1^{int/low}$ SSC^{high} (gate D) and neutrophils were gated as Gr-1^{high} $SSC^{int/low}$ (gate E) and their percentages relative to total living cells was recorded.

Table 3.2 FLOW Cytometry cell marker list

List of fluorescence-conjugated antibodies grouped by cell-type used within this project.

Cell Type	Cell Marker	Isotype	Clone	Supplier
Neutrophils/ Eosinophils	FITC anti-mouse/humanCD11b	Rat IgG2b, k	M1/70	Biolegend
	APC anti-mouse Ly-6G/Ly-6C (Gr-1)	Rat IgG2b, k	RB6-8C5	
Macrophage	FITC anti-mouse CD11b	Armenian Hamster IgG	N418	Biolegend
	PE anti-mouse F4/80	Rat IgG2a, k	BM8	
	eFluor® 660 IDO	Rat IgG2b, k	mIDO-48	Invitrogen
Dendritic Cell	FITC anti-mouse CD11c	Armenian Hamster IgG	N418	Biolegend
	PE anti-mouse I-A/I-E (MHCII)	Rat IgG2b, k	M5/114.1 5.2	
	eFluor® 660 IDO	Rat IgG2b, k	mIDO-48	Invitrogen

3.7 Multiplex ELISA procedure for analysis of cytokine and chemokine profiles

The lung homogenate and BAL fluid samples for Multiplex ELISA were defrosted, and the procedure within the instructor's manual from Meso Scale Discovery was followed. The U-Plex Custom Biomarker (ms) Assay and U-Plex T-Cell Combo kits were used for cytokine and chemokine detection. The Meso Scale Discovery software was used to measure the concentration of each protein.

3.8 Total IgE titration

The total IgE titration was done using the BD OptEIA Mouse IgE ELISA Set as per the instruction manual for blood, BAL fluid, and lung fragment cultures. A dilution of 1:2 was determined to provide the most accurate results, though both 1:2 and 1:5 dilutions were done in duplicate for each trial. The plates were read using the SPECTRA max 340PC and matching SOFTmaxPRO4.3.1 software. The software was used to calculate the standard curve, and Excel for the subsequent IgE titers for each of the samples.

3.9 Statistical analysis

GraphPad Prism 7 was used for statistical analysis of all results. One-way ANOVAs and Newman-Keuls methods were used to compare differences between multiple groups. Student t-tests were used to compare individual groups if significance was found among the groups. Differences were considered significant if $P < 0.05$. As stated in **Figure 3.1**, all graphs are representative of three separate trials. All trials consisted of either 5 or 6 mice in each group. The dot plots represent individual mice within each group, and the error bars show median with 95% CI. The bar graphs are representative of pooled data within each group, and these error bars show the mean with SD.

4 RESULTS

4.1 Developing an asthma model

An asthma model was developed to determine how an underlying infection affects the response within the lung environment towards the CRA allergen. This model went through multiple iterations and improvements before obtaining adequate results. These iterations included a shift from the model based on a Kaiko *et al.* study to combining a model used by Whitehead *et al.* with one used by Lukas *et al*. This model provided an overall shorter timeline that revealed significant differences when compared to a negative group of mice, a second one that was only exposed to CRA and a third group that only had a PVM viral infection.

4.1.1 The first model

First, a model that was based on a Kaiko *et al.* study in 2013 (84) was previously initiated, and then improved on by myself. The model (**Figure 4.1**) was lengthy at 30 days long; 30 pfu of PVM and 1 µg of CRA were used per mouse (combination group). Additionally, lung tissue mRNA (**Figure 4.2**) did not show any significant differences in the cytokines measured except for IFN-γ (**Figure 4.2 A**) when comparing the combination group with the CRA group and the negative control group. IL-4 mRNA did show a very small trending increase but was quite variable, and therefore no significance was identified (**Figure 4.2 B**). IDO-1 mRNA levels were also not different between the three groups (**Figure 4.2 C**).

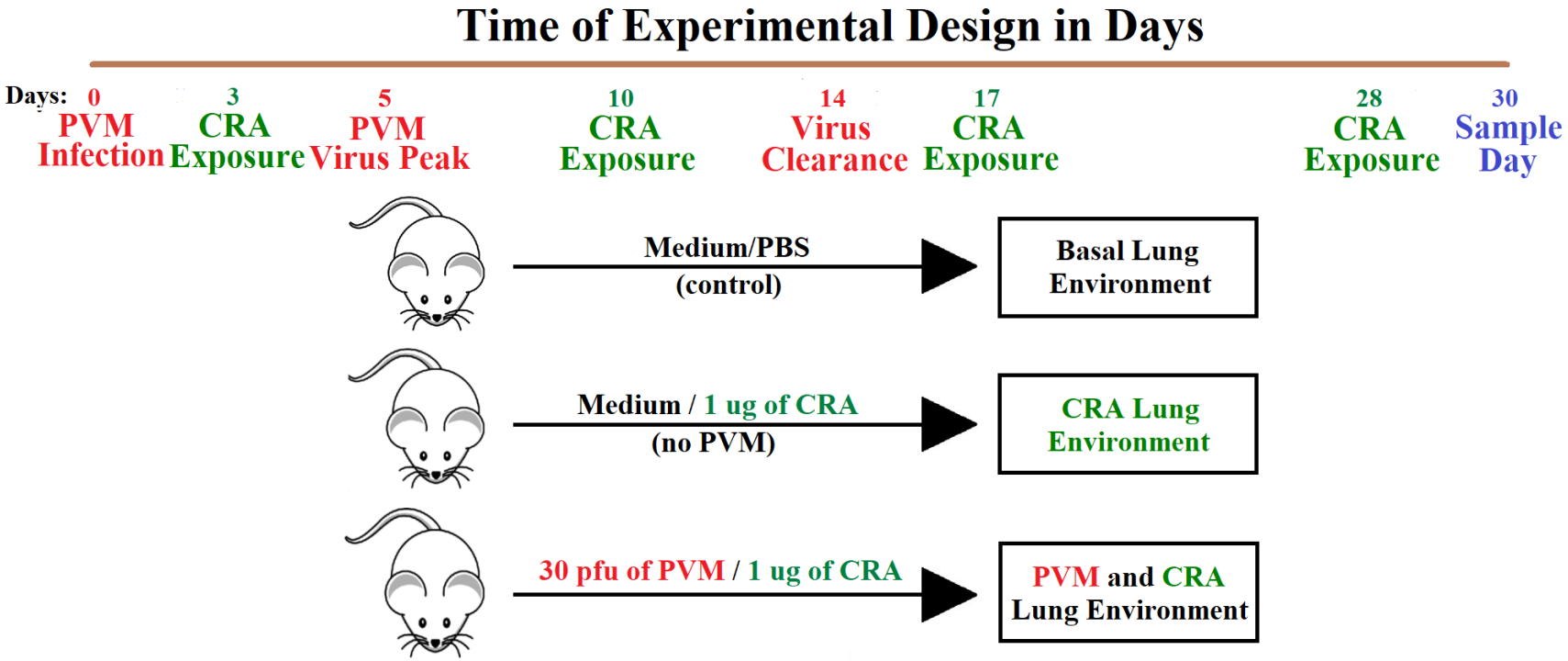

Figure 4.1: First asthmatic model

Schematic representation of the mouse model from a Kaiko *et al.* study (83). In the experiment there were three different groups of BALB/c mice aged 4-5 weeks: a negative control group (Medium/PBS), a CRA group (Medium/CRA), and a PVM/CRA group (combination). Mice were infected with 30 pfu of PVM in 50 µL of medium or 50 µL of medium without virus. Virus or medium was always administered intranasally on day 0. This was followed by intranasal inhalation of 1 µg of CRA allergen in 20 µL of PBS or 20 µL of PBS on day 3 p.i. A second and third inhalation of the same type was administered on day 10 and 17 p.i.; one week after the first and second exposure respectively. A fourth inhalation was administered on day 28 p.i. The first inhalation occurred two days before the viral infection had peaked, on day 5 p.i. (21). The lung environments were measured for changes in mRNA production of cytokines and IDO-1; Each finding shown is a representation of 1 trial, with 5 mice/group.

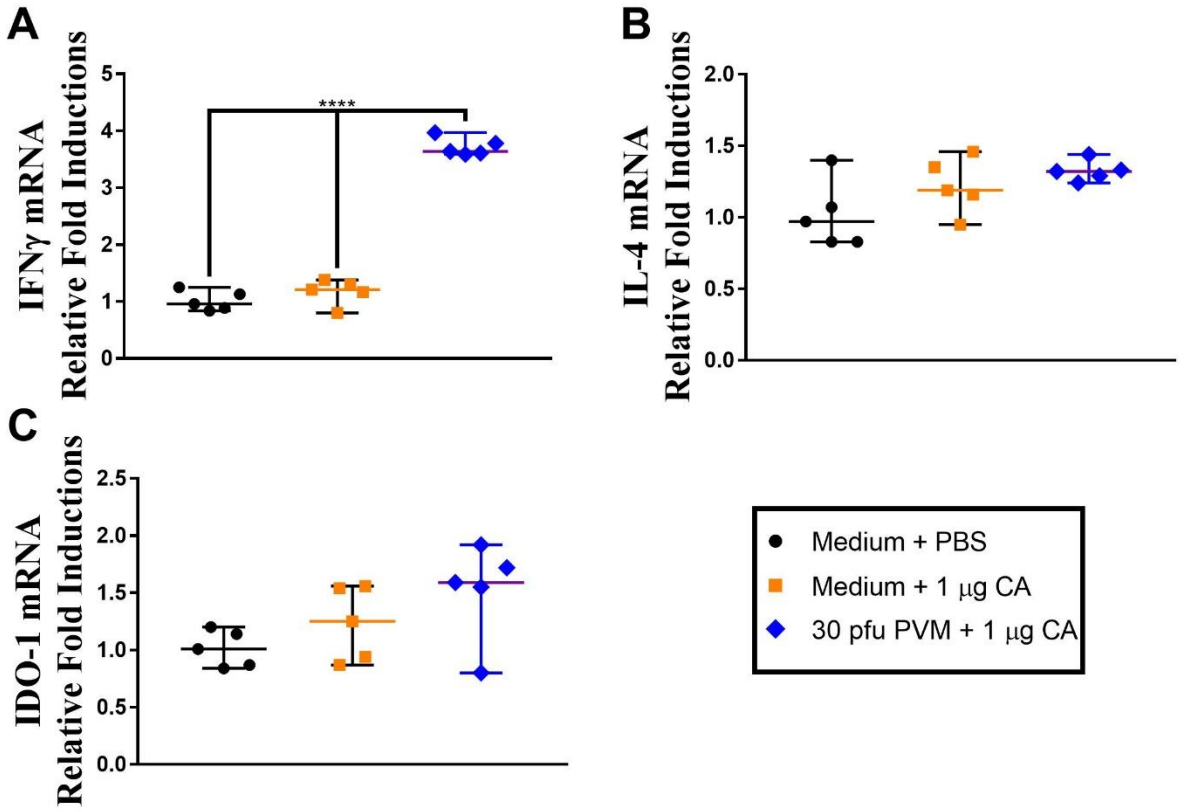

Figure 4.2 Cytokine and IDO-1 mRNA

The mice were either inoculated with Medium or 30 pfu PVM and PBS or 1 μg of CRA. At day 30 p.i. lung tissue mRNA expression levels of select cytokines, and IDO-1 were observed. The lung tissue was flash-frozen in liquid nitrogen and stored at -80 °C for mRNA extraction. cDNA was produced and qPCR was performed. Both GAPDH and β-actin were used as housekeeping genes, but GAPDH has more stable mRNA basal levels. In each group, all 5 mice are shown as individuals. Each datum point corresponds to individual mice and the horizontal line represents the median with 95% CI.

**** = $P < 0.0001$

4.1.2 Modification of this model

Asthmatic symptoms are categorized as either early reactions or late reactions (85). Therefore, observations of symptoms 6 hours and 2 days after the last exposure would capture changes in the lung environment using the same combination group as used in the previous model (**Figure 4.3**). As can be seen in **Figure 4.4 A** IFN-γ mRNA is only significantly induced in the combination group on day 26 + 6 hrs p.i. There is too much variability within the day 28 p.i. data to determine any significance. **Figure 4.4 B** shows the IL-4 mRNA expression, which did not show any significant differences between any of the three groups at either time-point. There is a trending increase in IDO-1 mRNA on Day 26 + 6 hrs p.i. that is also not significant at this time-point but became significant by day 28 p.i. (**Figure 4.4 C**). We also observed the mRNA production of mucosal proteins Muc5AC and Gob5. **Figures 4.4 D & E** show that neither of the mucous mRNAs was significantly induced in either the CRA group or the combination group. Finally, BAL fluid and lung tissue samples also did not show significant differences between the groups, although there were some trending differences within the BAL fluid at day 28 p.i. (**Figure 4.4 F & G** respectively).

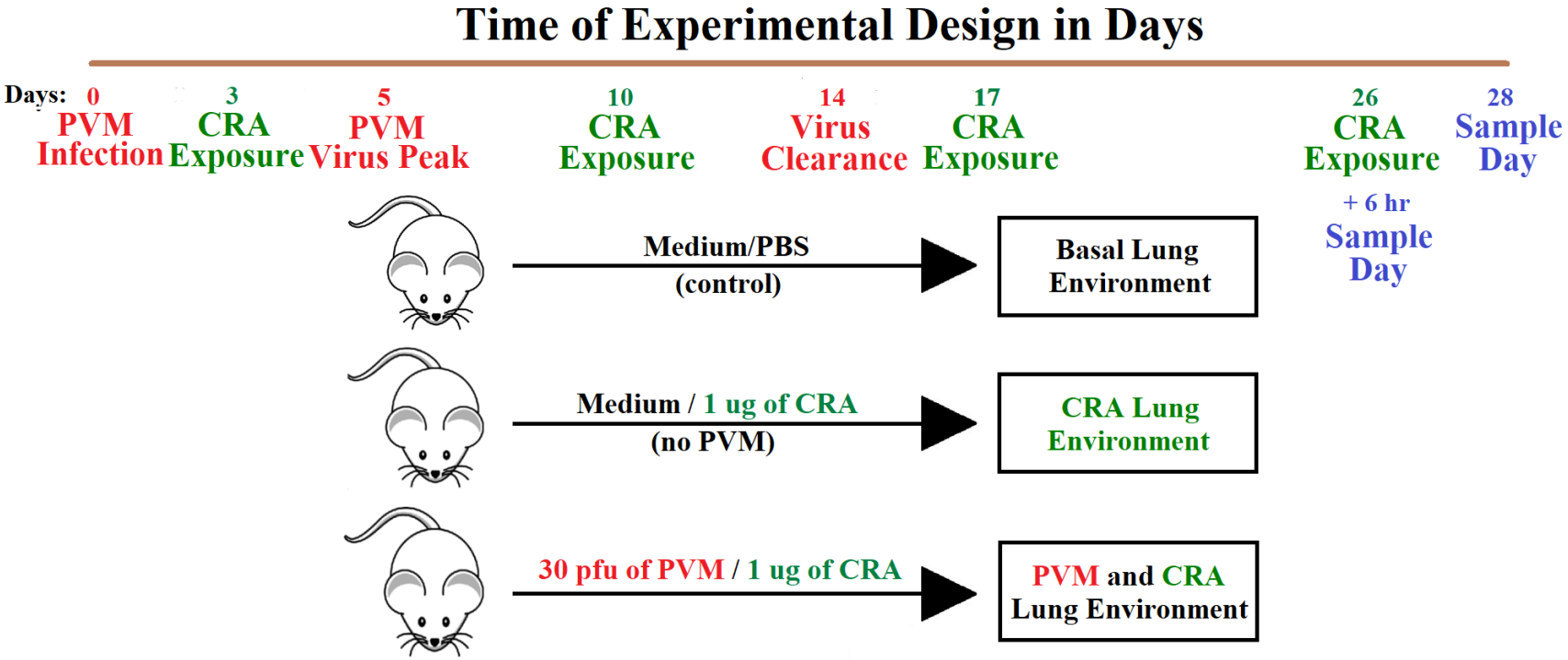

Figure 4.3: Modified asthmatic model

Schematic representation of a modified mouse model from a Kaiko *et al.* study (83). In the experiment there were three different groups of BALB/c mice aged 4-5 weeks: a negative control group (Medium/PBS), a CRA group (Medium/CRA), and a PVM/CRA group (combination). Mice were infected with 30 pfu of PVM in 50 µL of medium or 50 µL of medium without virus. Virus or medium was always administered intranasally on day 0. This was followed by intranasal inhalation of 1 µg of CRA allergen in 20 µL of PBS or 20 µL of PBS on day 3 p.i. A second and third inhalation of the same type was administered on day 10 and 17 p.i.; one week after the first and second exposure respectively. A fourth inhalation was administered on day 26. The first inhalation occurred two days before the viral infection had peaked, on day 5 p.i. (21). The lung environments were measured for changes in mRNA production of cytokines and IDO-1; Each finding shown is a representation of 1 trial, with 5 mice/group.

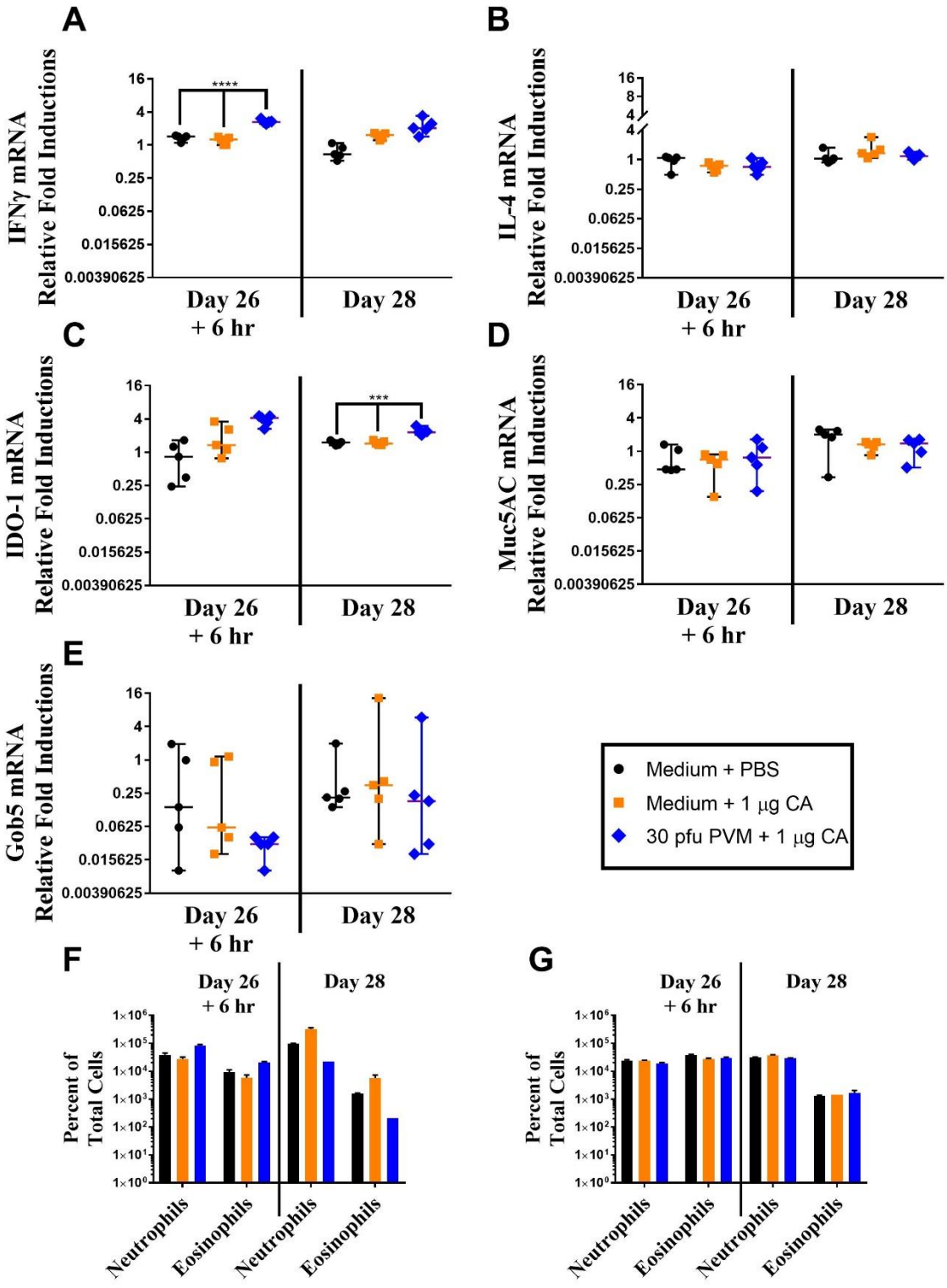
A
IFNγ mRNA
Relative Fold Inductions
16
4
1
0.25
0.0625
0.015625
0.00390625
****
Day 26
+ 6 hr
Day 28
B
IL-4 mRNA
Relative Fold Inductions
16
8
4
4
1
0.25
0.0625
0.015625
0.00390625
Day 26
+ 6 hr
Day 28
C
IDO-1 mRNA
Relative Fold Inductions
16
4
1
0.25
0.0625
0.015625
0.00390625
***
Day 26
+ 6 hr
Day 28
D
Muc5AC mRNA
Relative Fold Inductions
16
4
1
0.25
0.0625
0.015625
0.00390625
Day 26
+ 6 hr
Day 28
E
Gob5 mRNA
Relative Fold Inductions
16
4
1
0.25
0.0625
0.015625
0.00390625
Day 26
+ 6 hr
Day 28
Medium + PBS
Medium + 1 μg CA
30 pfu PVM + 1 μg CA
F
Day 26
+ 6 hr
Day 28
Percent of
Total Cells
1×10^6
1×10^5
1×10^4
1×10^3
1×10^2
1×10^1
1×10^0
Neutrophils
Eosinophils
Neutrophils
Eosinophils
G
Day 26
+ 6 hr
Day 28
Percent of
Total Cells
1×10^6
1×10^5
1×10^4
1×10^3
1×10^2
1×10^1
1×10^0
Neutrophils
Eosinophils
Neutrophils
Eosinophils

Figure 4.4 Cytokine and IDO-1 mRNA, and cellular influx in BAL fluid and lung tissue
The mice were either inoculated with Medium or 30 pfu PVM and PBS or 1 µg of CRA. (A – E) At day 28 p.i. lung tissue mRNA expression levels of select cytokines, and IDO-1 was observed. The lung tissue was flash-frozen in liquid nitrogen and stored at -80 °C for mRNA extraction. cDNA was produced and qPCR was performed. Both GAPDH and β-actin were used as housekeeping genes, but GAPDH has more stable mRNA basal levels. In each group, all 5 mice are shown as individuals. Each datum point corresponds to individual mice and the horizontal line represents the median with 95% CI. (F & G) BAL fluid and lung tissue cells were isolated on day 28 p.i. for the presence of eosinophils and neutrophils. Living cells were gated, and eosinophils were further gated as $CD11b^{+}$ $Gr\text{-}1^{int/low}$ SSC^{high}; neutrophils were gated as $CD11b^{+}$ $Gr\text{-}1^{high}$ $SSC^{int/low}$. The percentage of eosinophils and neutrophils in the BAL fluid (F) and lung tissue (G) are shown. Each group consisted of 5 mice that were pooled and analyzed in triplicates. Each bar represents the group as mean and the line represents the SD.

4.1.3 Final model

Due to the lack of changes seen in the previous two models a combination of the Whitehead *et al.* and Lukacs *et al.* (74, 86, 87) models were altered to obtain a new infection/exposure protocol as shown in **Figure 4.5**. This protocol is much shorter in length and able to identify changes within the lung environment between a negative control group, a model with two CRA sensitizations (CRA group), and the same model with two CRA sensitizations and an underlying PVM infection during the first sensitization (combination group).

In **Figure 4.6 A** the IFN-γ mRNA expression is increased in the combination group when compared to both the negative control and the CRA group. This result was similar to the same measurement in the last model, but the increased relative fold induction of this model was promising. IL-4 mRNA induction was also significantly increased in the CRA group (**Figure 4.6 B**). Additionally, the combination group produced significantly more IL-4 mRNA when compared to the CRA group. **Figure 4.6 C** shows induction of IDO-1 mRNA within the combination group, but not in either of the other two groups. Finally, the mRNA induction of mucosal proteins Muc5AC (**Figure 4.6D**) and Gob5 (**Figure 4.6 E**) showed significant or trending increases within the CRA group compared to the negative control group, and significant increases in the combination group when compared to the CRA group.

Additionally, there was a significant decrease of eosinophils within the BAL fluid of the combination group. The neutrophil population that increased within the BAL fluid of the CRA group was suppressed within the BAL fluid of the combination group (**Figure 4.6 F**). The lung tissue eosinophil and neutrophil populations were also significantly increased in the CRA group compared to the negative control group; the combination group showed enhanced significant increases of these populations compared to the CRA group (**Figure 4.6 G**). Finally, previous work establishing the virulence of the PVM strain defined that infection peaks at day 5 p.i. and is resolved by day 14 p.i. at a 30 pfu dose within Balb/c mice (**Figure 4.7**). Therefore, any differences in the lung environment of the combination group are towards CRA and not due to the remnants of the underlying PVM infection that ultimately effected how the lungs respond to CRA.

Time of Experimental Design in Days

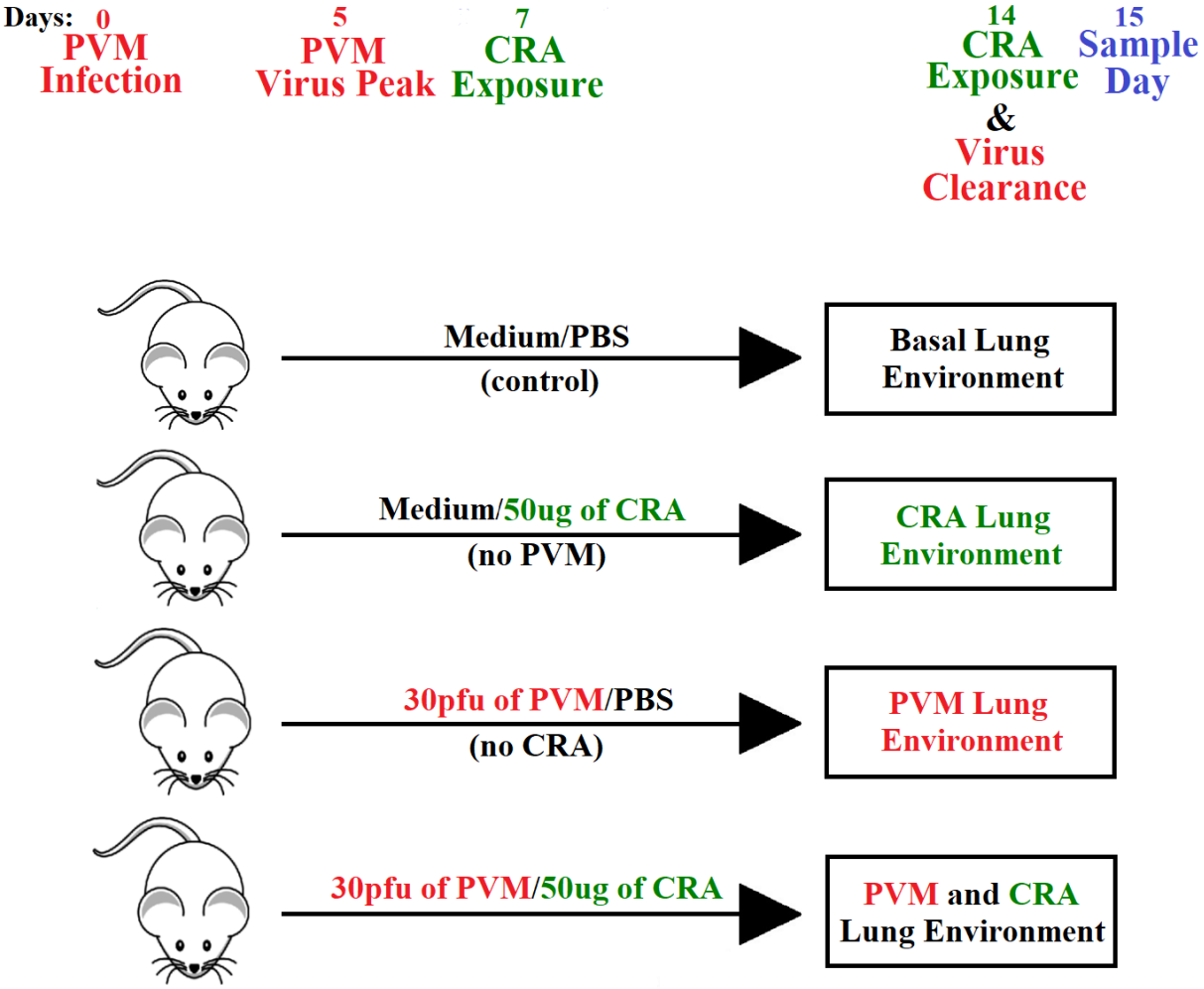

Figure 4.5 Schematic Representation of Mouse Model

Schematic representation of the mouse model developed by combining a model used by Lukas (62) and one used by Whitehead (51). In each experiment there were three different groups of BALB/c mice aged 4-5 weeks: a negative control group (Medium/PBS), a CRA group (Medium/CRA), and either a PVM group (PVM/PBS) or a PVM/CRA group (combination). Mice were infected with 30 pfu of PVM in 50 µL of medium or 50 µL of medium without virus. Virus or medium was always administered intranasally on day 0. This was followed by intranasal inhalation of 50 µg of CRA allergen in 20 µL of PBS or 20 µL of PBS one week after infection on day 7 p.i. A second inhalation of the same type was administered on day 14 p.i.; one week after the first exposure. The first inhalation occurred two days after the viral infection had peaked, on day 5 p.i. (21), and the second inhalation was given on the day of viral clearance and one day before the mice were sacrificed. The lung environments were measured for changes in mRNA production of mucus proteins, cytokines and IDO-1; cellular influx of eosinophils, neutrophils, macrophages, and dendritic cells; and protein concentrations of cytokines. Each finding shown is a representation of 1 of 3 trials, with 6 mice/group.

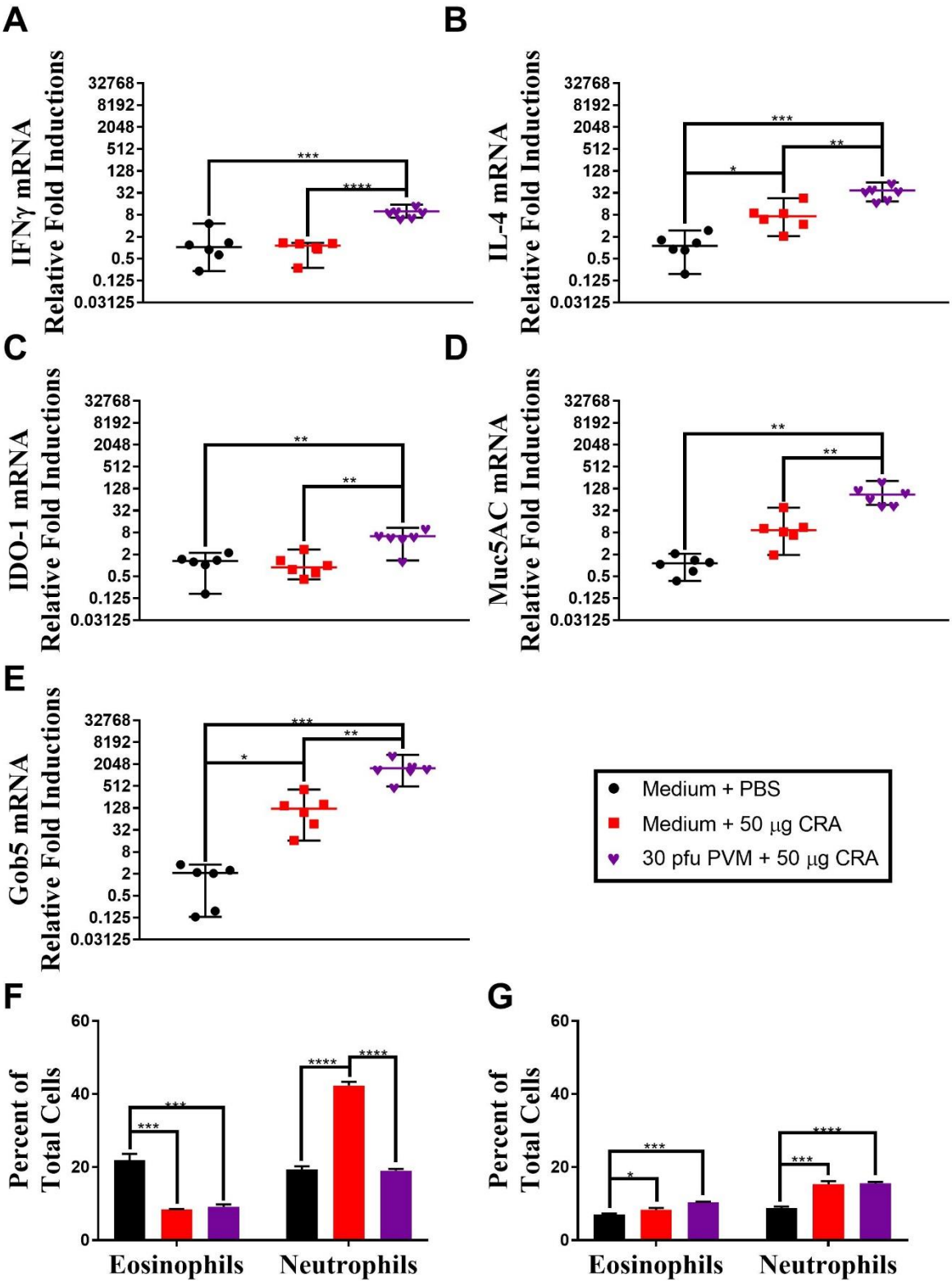
A
IFNγ mRNA
Relative Fold Inductions
B
IL-4 mRNA
Relative Fold Inductions
C
IDO-1 mRNA
Relative Fold Inductions
D
Muc5AC mRNA
Relative Fold Inductions
E
Gob5 mRNA
Relative Fold Inductions
32768
8192
2048
512
128
32
8
2
0.5
0.125
0.03125
Medium + PBS
Medium + 50 μg CRA
30 pfu PVM + 50 μg CRA
F
G
Percent of Total Cells
60
40
20
0
Eosinophils
Neutrophils

Figure 4.6 Lung tissue mRNA, and cellular influx in BAL fluid and lung tissue

The mice were either inoculated with Medium or 30 pfu PVM and PBS or 50 µg of CRA. (A – E) At day 15 p.i. lung tissue mRNA expression levels of select cytokines, mucin, and IDO-1 was observed. The lung tissue was flash-frozen in liquid nitrogen and stored at -80 °C for mRNA extraction. cDNA was produced and qPCR was performed. Both GAPDH and β-actin were used as housekeeping genes, but GAPDH has more stable mRNA basal levels. In each group, all 6 mice are shown as individuals. Each datum point corresponds to individual mice and the horizontal line represents the median with 95% CI. (F & G) BAL fluid and lung tissue cells were isolated on day 15 p.i. for the presence of eosinophils and neutrophils. Living cells were gated; while eosinophils were as $CD11b^{+}$ $Gr\text{-}1^{int/low}$ SSC^{high}, neutrophils were gated as $CD11b^{+}$ $Gr\text{-}1^{high}$ $SSC^{int/low}$. The percentage of eosinophils and neutrophils in the BAL fluid (F) and lung tissue (G). Each group consisted of 5 mice that were pooled and analyzed in triplicates. Each bar represents the group as mean and the line represents the SD.

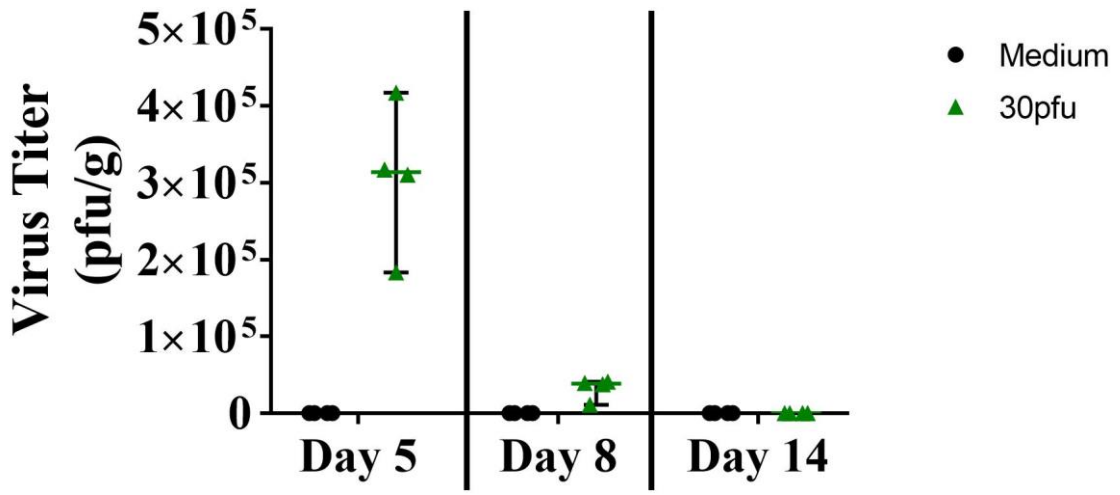

Figure 4.7 PVM-15 virus titration peak and clearance

Balb/c mice were inoculated with 30 pfu of PVM-15 and sacrificed at days 5, 8, or 14 p.i. for viral titration assays. Individual lungs were weighed, homogenized, aliquoted, and flash frozen at minus 80°C. Samples were plated on pre-grown BHK-21 cells and incubated for 3 days. Anti-PVM rabbit antibodies were applied to the wells after fixation and permeabilization; followed by alkaline phosphatase-conjugated goat anti-rabbit IgG; BIORAD substrate was used to identify virions. The plaques were numerated and titers as pfu/g were calculated.

4.2 Cockroach allergen and PVM infection inflict different long-lasting alterations to the lung environment

In order to examine the lung environmental changes from either two CRA exposures or any long-lasting effects of a sub-lethal PVM viral infection, the mice were either infected with PVM or exposed to CRA. Three groups of mice were compared: the Medium/PBS group (control), CRA group (Medium/CRA), and PVM group (PVM/PBS). The changes in cytokine mRNA expression and protein production, as well as cell influx into the BAL fluid and lung tissue, were determined between the three groups.

4.2.1 Gene expression within the lung tissue

The lung tissue was homogenized within TRIZol solution to extract the mRNA produced and observe any differences between the three groups. As shown in **Figure 4.8 A & B**, the amounts of Gob5 and Muc5AC mRNA production of the CRA and PVM groups were equivalent at day 15 p.i. Gob5 only achieved a trending increase within the CRA group and the PVM group when compared to the Media/PBS group. While Muc5AC mRNA induction was significantly increased in both the CRA group and the PVM group as compared to the Media/PBS group, there was no difference found between the CRA group and the PVM group. The similarity in expression between the two groups indicated that CRA induced these two mRNAs to be produced, but the viral infection also induced mucosal mRNA production to occur even after viral clearance. Thus, the viral infection still affected mucus production even after it was cleared, and CRA induced mucosal mRNA production. This could be a possible memory response that lasted 24 hours after the encounter occurred.

In addition, CRA did not induce an increase in IL-4 mRNA production with the exception of one mouse (**Figure 4.8 C**). None of the mice within the PVM group developed IL-4 mRNA production. According to the research, there were no differences in IL-4 mRNA expression between the three groups. The lack of IL-4 mRNA production in response to the PVM infection was expected since PVM induces a Th-1 response rather than a Th-2 response (21, 22, 24). In contrast, the lack of IL-4 mRNA expression induced by the CRA was not expected since CRA is known to induce a Th-2 response (75).

The expected increase in IFN-γ mRNA production (**Figure 4.8 D**) was observed in response to the residual PVM infection, but it did not occur after CRA inhalation.

IDO-1 mRNA was also measured as shown in **Figure 4.8 E.** It was found that CRA does not induce IDO-1 mRNA production 24 hours after stimulation, but it was still present after clearance of the viral infection. We have previously established that PVM does induce IDO-1 mRNA during infection, and this mRNA seems to still be present after clearance. The induction of IDO-1mRNA within the PVM group suggests that it may be playing a role in resolving this viral infection.

Within the overall results from the mRNA expression, it seems that CRA exposure may induce a similar mucosal response as PVM, but this would not be in a Th-2 mediated way, nor a Th-1 mediated way as the PVM infection had induced.

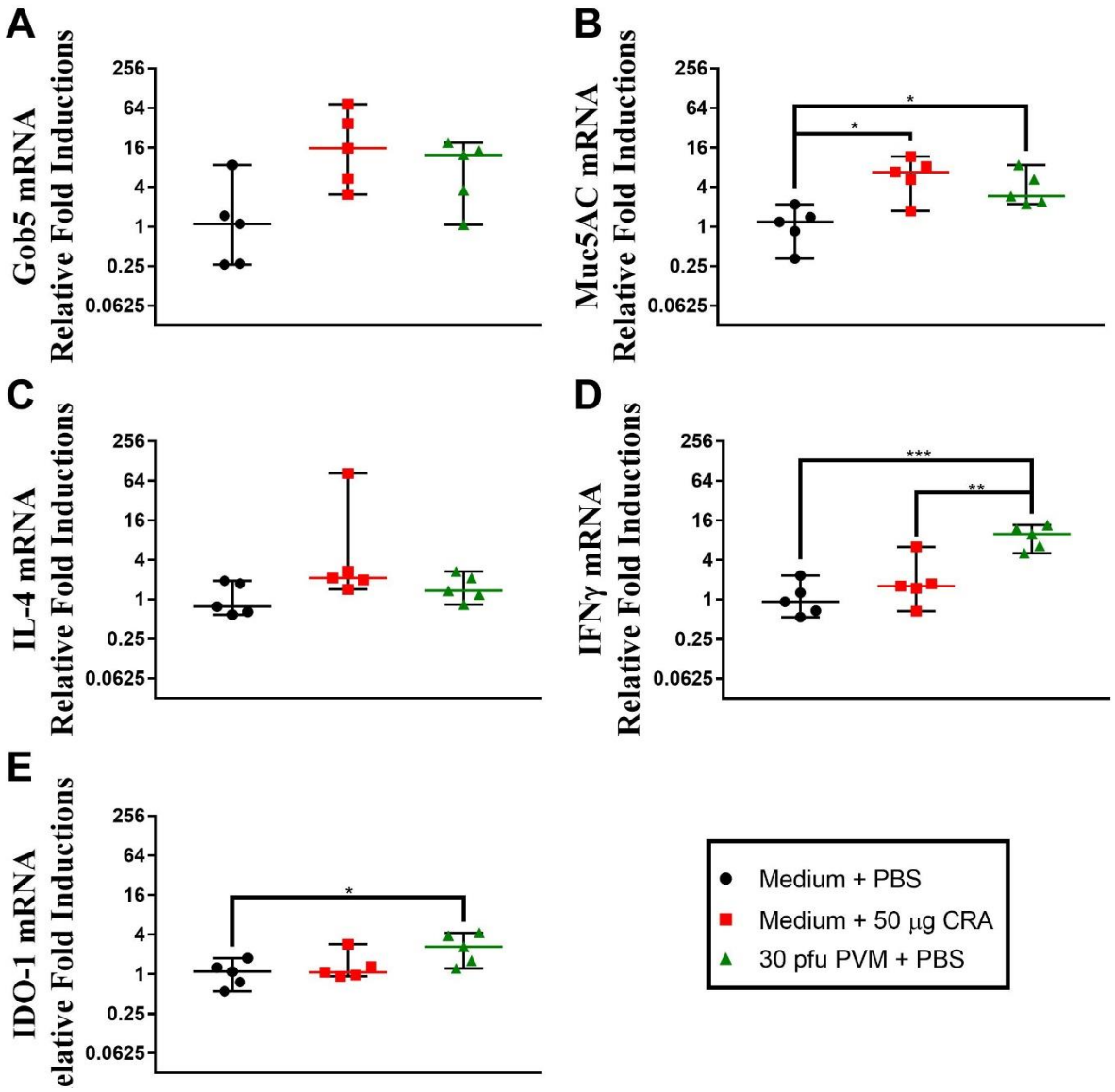

Figure 4.8 mRNA expression of cytokines and IDO-1 in the lung tissue

The mice were either inoculated with Medium or 30 pfu PVM and PBS or 50 μg of CRA. At day 15 p.i. lung tissue mRNA expression levels of mucus proteins, select cytokines, and IDO-1 was observed. The lung tissue was flash-frozen in liquid nitrogen and stored at -80 °C for mRNA extraction. cDNA was produced and qPCR was performed. Both GAPDH and β-actin were used as housekeeping genes, but GAPDH had more stable mRNA basal levels. In each group, all 5 mice are shown as individuals. Each datum point corresponds to individual mice and the horizontal line represents the median with 95% CI.

* = $P < 0.05$ ** = $P < 0.01$ *** = $P < 0.001$

4.2.2 Cytokine and chemokine protein analysis

Multiplex ELISA (Enzyme-Linked Immunosorbent Assay) was used to determine protein concentrations for a select number of cytokines and chemokines (**Figure 4.9**) within the BAL fluid of these three groups. We confirmed that IL-4 protein (**Figure 4.9 A**) was indeed present in the BAL fluid 24 hours after CRA exposure, but not seen after PVM clearance or within the Medium/PBS group. Significant amounts of IFN-γ protein (**Figure 4.9 B**) were also found in the BAL fluid of both the CRA and PVM groups compared to the Medium/PBS group. We did expect the PVM group to have residual IFN-γ proteins based on the mRNA data; thus, this continued presence after clearance is not too surprising. Unexpectedly, a similarly significant amount of IFN-γ protein was present within the BAL fluid after CRA inhalation. The relatively low amount of IFN-γ compared to IL-4 supports the conclusion that CRA induces a mixed, but dominantly Th-2, type of response.

Interestingly, there was a small but significant increase of IL-10 protein (**Figure 4.9 C**) within the BAL fluid of the CRA group that was not observed in either the Medium/PBS group or the PVM group. This IL-10 is classically known to be secreted by T-reg cells, but there is also evidence of both Th-1 and Th-2 $CD4^+$ T-cells secreting this cytokine after repeated exposure to an antigen (88, 89).

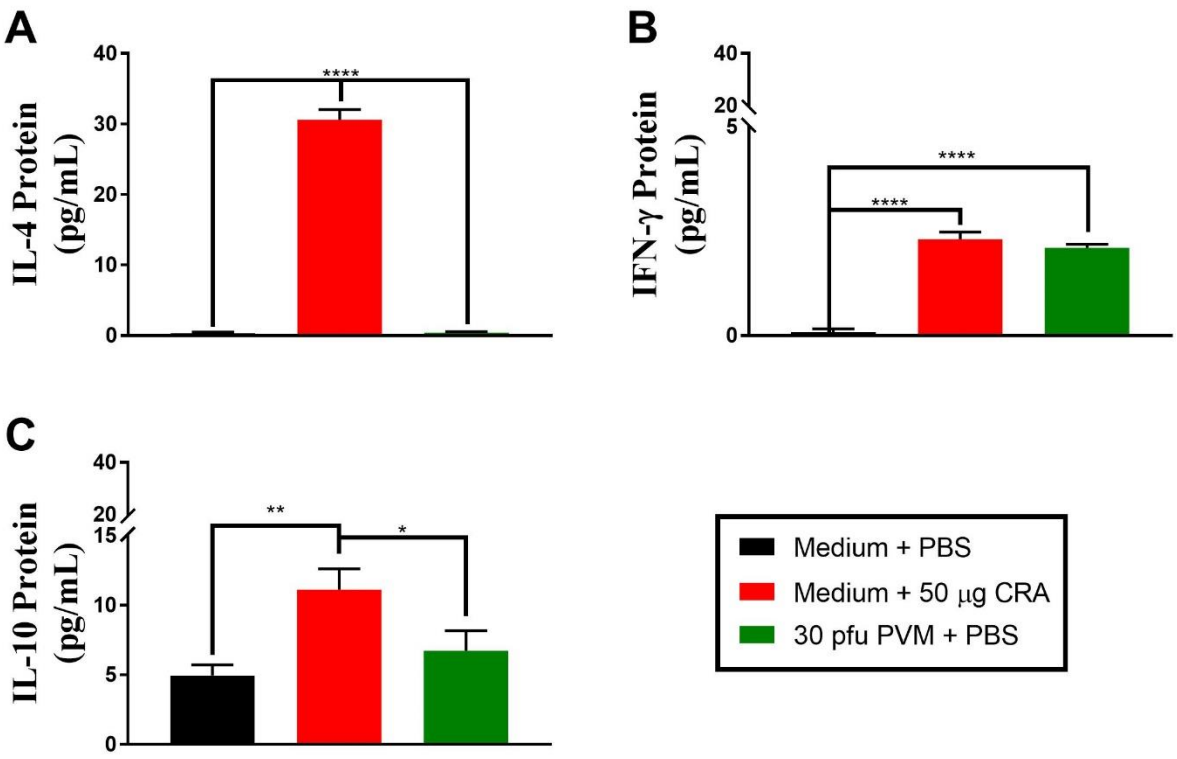

Figure 4.9 Protein profile of the BAL fluid

The mice were either inoculated with Medium or 30 pfu PVM and PBS or 50 µg of CRA. Protein leve1s within the BAL fluid of each group at day 15 p.i. for select cytokines of Th-1 (IFN-γ and sometimes IL-10) and Th-2 (IL-4 and sometimes IL-10) origin were measured with multiplex ELISA using the MSD kit and protocols. Each group consists of 5 mice and all are pooled and analyzed in triplicate. The data plots are shown as mean with SD.

* = P < 0.05 ** = P < 0.01 **** = P < 0.0001

4.2.3 Lung tissue and BAL fluid cell efflux and influx

After clearance of the virus and 24 hours after exposure to CRA, we investigated the BAL fluid and lungs for eosinophil and neutrophil presence. The BAL fluid within the PVM group contained a higher percentage of eosinophils (approximately 10% increase) and a lower percentage of neutrophils (~2%) compared to the CRA group and the Medium/PBS group (**Figure 4.10 A**). Conversely, CRA induced an opposite effect within the BAL fluid compared to the PVM group and the Medium/PBS group. Neutrophils increased by about 35%, while eosinophils decreased by about 4-5% compared to the Medium/PBS group. Therefore, the suppression of eosinophil or neutrophil influx within the BAL fluid at the end of these trials shows that the lungs react to a CRA exposure differently than towards a PVM infection. The lung tissue cell influx (**Figure 4.10 B**) was also drastically different, but in other ways. The eosinophilic influx was reasonably stable between all three compared groups, but the neutrophils reacted differently between the CRA and PVM groups when compared to the Medium/PBS group. CRA induced a significant increase of about 5%, while the PVM infection suppressed neutrophilic influx by about 5%, below levels found in the Medium/PBS group.

Therefore, the effects of PVM after viral clearance increased the eosinophilic influx within the BAL fluid while maintaining the regular proportion within the tissue. This eosinophilic increase is in conjunction with the suppression of neutrophils within both the BAL fluid and the lung tissue. In contrast, the CRA induction resulted in lower than average eosinophil, and higher than average neutrophil populations within the BAL fluid. Similarly, to the BAL fluid, the lung tissue contained an increased neutrophil population, while the eosinophilic population was maintained. Therefore, PVM promotes a high eosinophilic and low neutrophilic BAL, and low neutrophilic tissue environment. In contrast, CRA promotes a high neutrophilic, low eosinophilic BAL, and high neutrophilic tissue environment. These environmental differences within the lung tissue are indicative of the different immune responses induced by PVM (Th-1) and CRA (Th-2).

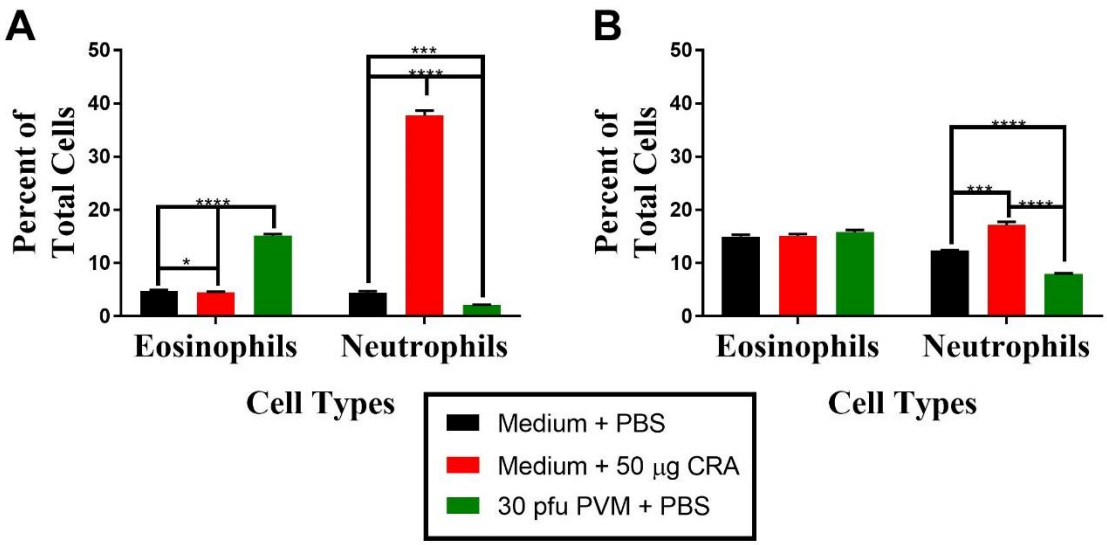

Figure 4.10 Cellular influx and efflux of neutrophils and eosinophils

The mice were either inoculated with Medium or 30 pfu PVM and PBS or 50 µg of CRA. Lung tissue and BAL fluid cells were isolated on day 15 p.i. to detect the presence of eosinophils and neutrophils. Living cells were gated; while eosinophils were as $CD11b^{+}$ $Gr\text{-}1^{int/low}$ SSC^{high}, neutrophils were gated as $CD11b^{+}$ $Gr\text{-}1^{high}$ $SSC^{int/low}$. The percentage of eosinophils and neutrophils in the BAL fluid (A) and lung tissue (B). Each group consisted of 5 mice that were pooled and analyzed in triplicates. Each bar represents the group as mean and the line represents the SD.

* = $P < 0.05$ *** = $P < 0.001$ **** = $P < 0.0001$

4.3 The lung environment is altered when an allergen is introduced during an acute viral infection

The previous set of experiments showed the different responses that the lungs mounted towards either a set of CRA exposures or a sub-lethal PVM infection. The next step was to observe how the lungs would respond to a second CRA exposure when the first one occurred during the acute phase of a sub-lethal PVM infection. For this set of experiments, the Medium/PBS group (control), the CRA group (Medium/CRA), and the PVM/CRA group were tested to elucidate the type of response that would occur under these circumstances.

4.3.1 Gene Expression Within the Lung Tissue

The lung mRNA environment was extracted from the lung tissue 24 hours after CRA exposure with or without an underlying viral infection during the first exposure. As shown in **Figure 4.11 A & B**, while both of the CRA and PVM groups induced mRNA production of Gob5 and Muc5AC, the PVM/CRA group produced more Gob5 and Muc5AC mRNA than either of the CRA group or the Medium/PBS group. This increase could be a slight additive effect on the lung environment. Little to no IL-4 mRNA was produced by the CRA and PVM groups in **Figure 4.8 C**, though there was a trend of increase within the CRA group compared to the Media/PBS group. In these trials, both the PVM/CRA group and the CRA group (**Figure 4.11 C**) did show a significant increase in IL-4 mRNA production. This significant increase was in comparison to the Medium/PBS group, while the PVM/CRA group was additionally increased compared to the CRA group. The IFN-γ mRNA production (**Figure 4.11 D**) also was significantly increased within the PVM/CRA group compared to both the Medium/PBS group and the CRA group. Expectedly, there was no IFN-γ mRNA expression in the CRA group compared to the Medium/PBS group. Finally, the induction of IDO-1 mRNA (**Figure 4.11 E**) was only increased when there was a previous underlying PVM infection when compared to both the PVM/CRA group and the Medium/PBS group. The CRA group did not induce any differences in IDO-1 mRNA expression when compared to the Medium/PBS group.

Therefore, the underlying previous PVM infection, and it is effects on the environment after clearance, leads to a different mRNA production profile towards CRA, and these differences are part of asthmatic development.

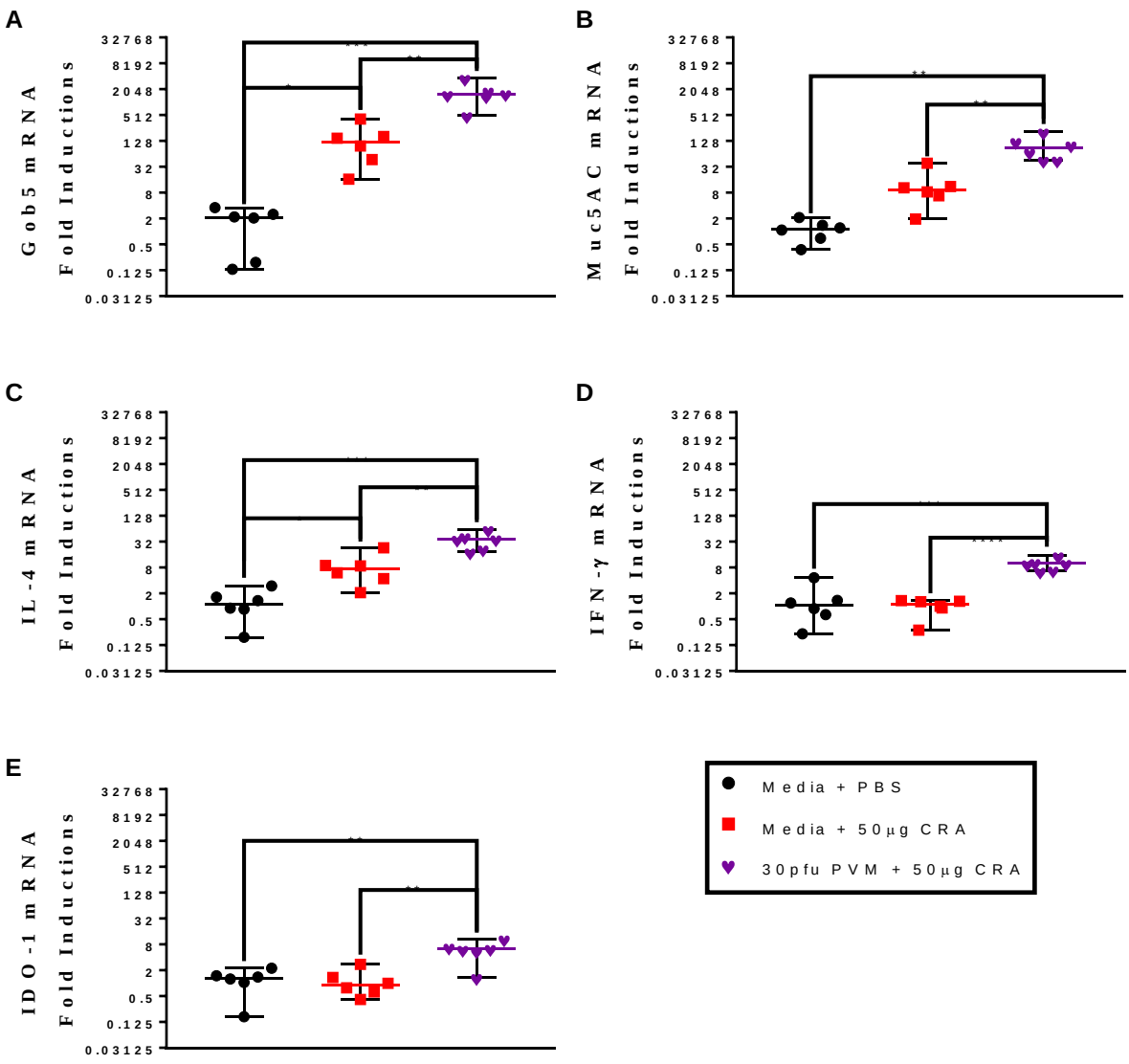

Figure 4.11 mRNA profile of the lung tissue within the thee groups

The mice were either inoculated with Medium or 30 pfu PVM and PBS or 50 µg of CRA. At day 15 p.i. lung tissue mRNA expression levels of mucus proteins, select cytokines, and IDO-1 was observed. The lung tissue was flash-frozen in liquid nitrogen and stored at -80 °C for mRNA extraction. cDNA was produced and qPCR was performed. Both GAPDH and β-actin were used as housekeeping genes, but GAPDH has more stable mRNA basal levels. In each group, all 5 mice are shown as individuals. Each datum point corresponds to individual mice and the horizontal line represents the median with 95% CI.

* = $P < 0.05$ ** = $P < 0.01$ *** = $P < 0.001$ **** = $P < 0.0001$

4.3.2 Cytokine and chemokine protein analysis

The lung tissue was also homogenized and stored for cytokine analysis using a Multiplex ELISA kit from Meso Scale Delivery. Despite the PVM infection not inducing IL-4 protein production within the BAL fluid (**Figure 4.9 A**), there was a significant increase in this protein's production in the PVM/CRA group. (**Figure 4.12 A & B**) This increase was significant in comparison to both the Medium/PBS group and the CRA group within the BAL fluid. This increase was seen in both BAL fluid and lung tissue of the PVM/CRA group compared to the Medium/PBS group. However, there was only a trending increase of IL-4 within the tissue of the PVM/CRA group compared to the CRA group. Therefore, the underlying PVM infection led to an increase in IL-4 production towards CRA.

IFN-γ protein production within the BAL fluid was significantly increased towards CRA, and even more so when there was an underlying PVM infection (**Figure 4.12 C & D**). IFN-γ was increased within the PVM/CRA group despite PVM not inducing much IFN-γ on its own during the same time point (**Figure 4.9 B**). Even so, the lung tissue only determined an increase within IFN-γ proteins in the PVM/CRA group as compared to both the CRA group and the Medium/PBS group. There was no IFN-γ protein found within the CRA group or the Medium/PBS group.

There was also a significant increase in IL-10 protein (**Figure 4.12 E & F**) in both BAL fluid and lung tissue when there was the underlying PVM infection as compared to the Medium/PBS group. This IL-10 was only seen within the PVM/CRA group compared to the CRA group. IL-10 protein was not found within the BAL fluid of the CRA group, although there was an increase in this protein found in the lung tissue compared to the Medium/PBS group. This increase was not significantly more induced in the PVM/CRA group's lung tissue.

IL-13 (**Figure 4.12 G**) was produced within the BAL fluid of the CRA group and was increased compared to the Medium/PBS group. The IL-13 within the BAL fluid of the PVM/CRA group was significantly increased compared to the Medium/PBS group, but it only showed a trending increase when compared to the CRA group. This IL-13 production further indicated that CRA induced a Th-2 response. Additionally, the Th-2 response became more balanced when the first CRA exposure occurred during a PVM infection.

Therefore, based on the protein analysis, it can be concluded that the response towards CRA is altered from an overall high IL-4 induction to a mixed IL-4 and IFN-γ production, while

also producing IL-10 and IL-13. Except for IL-13, this combination of proteins was seen in both tissue and BAL fluid samples, but the BAL fluid supported a Th-1 induction while the lung tissue produced a Th-2 response.

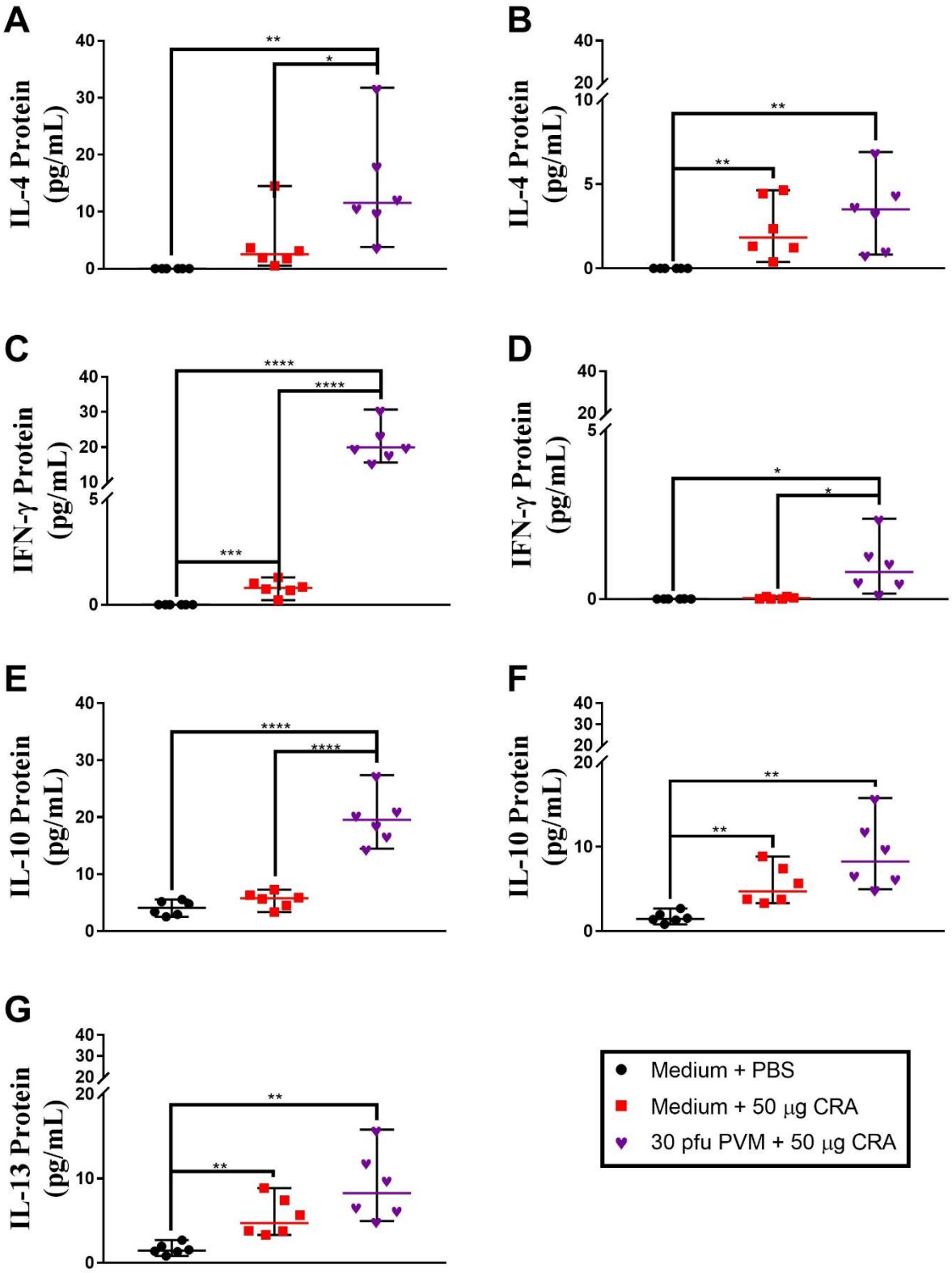
BAL fluid
Lung tissue
A
IL-4 Protein (pg/mL)
B
IL-4 Protein (pg/mL)
C
IFN-γ Protein (pg/mL)
D
IFN-γ Protein (pg/mL)
E
IL-10 Protein (pg/mL)
F
IL-10 Protein (pg/mL)
G
IL-13 Protein (pg/mL)
Medium + PBS
Medium + 50 μg CRA
30 pfu PVM + 50 μg CRA

Figure 4.12 Protein profile of the BAL fluid and the lung tissue of the groups

The mice were either inoculated with Medium or 30 pfu PVM and PBS or 50 µg of CRA. Protein leve1s for select cytokines of Th-1 and Th-2 origin within both the BAL fluid (A, C, E, and G) and the lung homogenate samples (B, D, and F) from day 15 p.i. All samples were measured with multiplex ELISA using the MSD kit and protocols. Each group (Medium/PBS, CRA group, and PVM/CRA group) consisted of 6 mice. Each datum point correspond to individual mice and the horizontal line represents the median with 95% CI.

* = $P < 0.05$ ** = $P < 0.01$ *** = $P < 0.001$ **** = $P < 0.0001$

4.3.3 Total IgE concentrations

Both BAL fluid and LFC supernatants were stored and analyzed with an IgE ELISA kit to observe whether there were any changes in the IgE titers between the three groups. IgE was not induced by CRA exposure alone within the BAL fluid and the lung tissue. Thus, an underlying PVM infection was necessary for this induction (**Figure 4.13 A & B**). IgE titers increased within both BAL fluid and the lung tissue samples of the PVM/CRA group when compared to both the Medium/PBS group and the CRA group. This lack of increase in IgE titer within the CRA group was unexpected since CRA has been reported to increase both total and CRA-specific IgE titers (75). Therefore, there was a change in how IgE induction occurs when the mice are exposed to CRA during an underlying PVM infection. The exacerbated Th-2 response shown through the mRNA expression and protein production suggests that there could be a necessary threshold to induce IgE production.

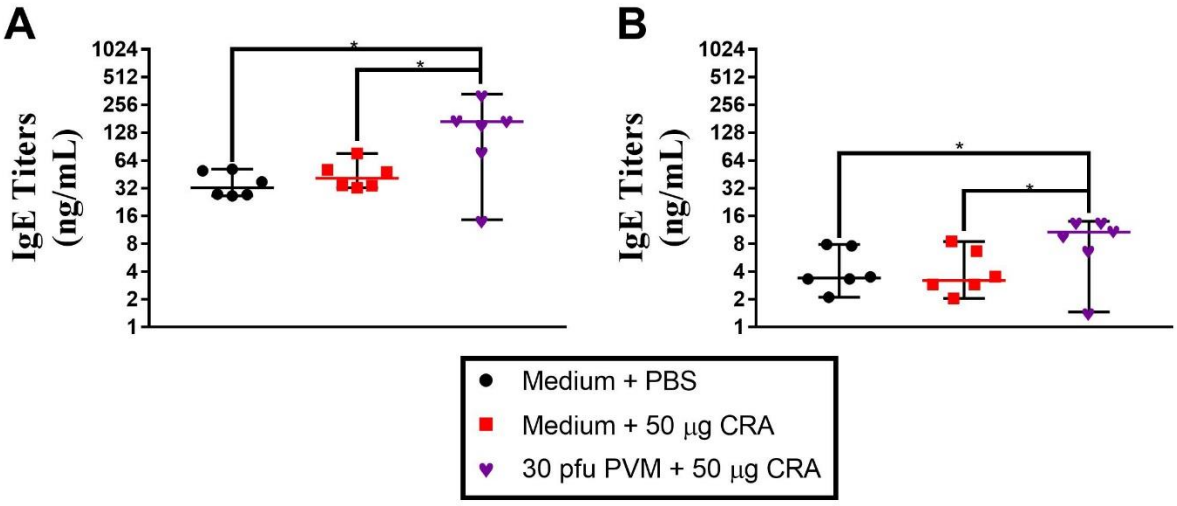

Figure 4.13 Total IgE titers in LFC and BAL fluid samples

The mice were either inoculated with Medium or 30 pfu PVM and PBS or 50 μg of CRA. IgE titers in BAL fluid (A) and lung fragment cultures (B) collected at day 15 p.i. measured by a sandwich-ELSA from BD Biosciences. Each group (Medium/PBS, CRA group, and PVM/CRA group) consisted of 6 mice. Each datum point corresponds to an individual mouse and the horizontal line represents the median with 95% CI.

* = $P < 0.05$

4.3.4 Lung tissue and BAL fluid cell efflux and influx

The presence of eosinophils and neutrophils was observed within the lung tissue and the BAL fluid using FLOW Cytometry. Additionally, macrophages and DCs and their expression of IDO-1 protein were also measured using this method. The cellular influx within the lungs of the PVM/CRA group was also different from the response towards each treatment on its own. In the BAL fluid (**Figure 4.14 A**), the eosinophils were similarly suppressed in the CRA group and the PVM/CRA group, in contrast to the massive eosinophil influx found within the PVM group (**Figure 4.10 A**). In spite of this similar eosinophil proportion, the high neutrophil influx to the BAL fluid in the CRA group was also reduced back to almost normal levels in the PVM/CRA group. Therefore, the high neutrophilic and low eosinophilic levels within the BAL fluid towards CRA has been altered to be low eosinophilic with no changes in neutrophilic influx when there was an underlying PVM infection. This cellular influx combination was also different from the high eosinophilic low neutrophilic BAL fluid found within the PVM group (**Figure 4.10 A**).

The lung tissues (**Figure 4.14 B**) showed a small, but significant, increase in eosinophil and neutrophil influx within the CRA group and the PVM/CRA group compared to the Medium/CRA group. However, there was no difference in either the eosinophil or neutrophil influx between the PVM/CRA group and the CRA group.

Correspondingly, there was an overall increase in total macrophage and DC populations within the PVM/CRA group's lung tissue compared to the Medium/PBS group (**Figure 4.14 C & D**). Although there was no difference in the macrophage populations between the PVM/CRA group and the CRA group, the number of DCs were different between these groups. Additionally, there was an increase of IDO-1^+ macrophages and DCs within the PVM/CRA group compared to both the Medium/PBS group and the CRA group. Increased IDO-1^+ macrophage and DC populations within the CRA group were also found when compared to the Medium/PBS group. The IDO-1 mean fluorescent index (MFI) within the macrophage populations was significantly increased in the PVM/CRA group and the CRA group when compared to the Medium/PBS group (**Figure 4.14 E**). However, there was no difference in the macrophage population between the CRA group and the PVM/CRA group. The IDO-1 MFI was also significantly increased within the DCs when comparing the PVM/CRA group to the CRA and Medium/PBS groups. The CRA group also had a significant increase of IDO-1^+ DCs compared to the Medium/PBS group, but the PVM/CRA group was further increased. Therefore,

the underlying PVM infection within the PVM/CRA group did significantly change the lung environment and cellular influx when compared to the Medium/PBS and CRA groups.

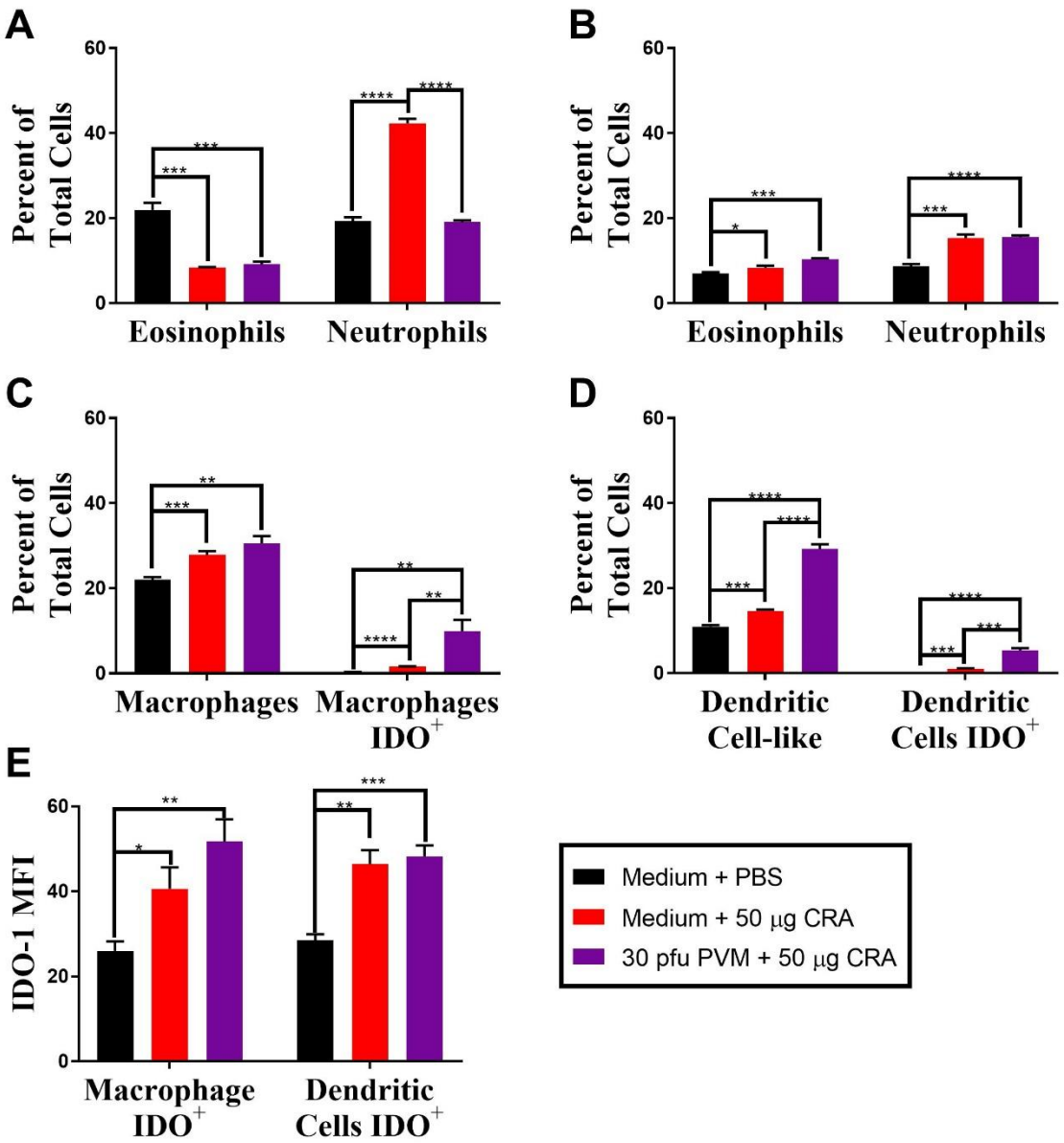
A
Percent of Total Cells
60
40
20
0
Eosinophils
Neutrophils
B
Percent of Total Cells
Eosinophils
Neutrophils
C
Percent of Total Cells
Macrophages
Macrophages IDO+
D
Percent of Total Cells
Dendritic Cell-like
Dendritic Cells IDO+
E
IDO-1 MFI
Macrophage IDO+
Dendritic Cells IDO+
Medium + PBS
Medium + 50 μg CRA
30 pfu PVM + 50 μg CRA

Figure 4.14 BAL fluid and lung tissue cellular influx and efflux

The mice were either inoculated with Medium or 30 pfu PVM and PBS or 50 µg of CRA and their lung tissue and BAL fluid sampled at day 15 p.i. Percentage of cell populations in the BAL fluid (A) and lung tissue (B – E). FLOW cytometry was performed and gating was as follows: living cells were gated based on FSC and SSC. Eosinophils are $CD11b^{+}$ $Gr\text{-}1^{low/int}$ SSC^{high}, neutrophils are $CD11b^{+}$ $Gr\text{-}1^{high}$ $SSC^{low/int}$, macrophages are gated as $CD11b^{+}$ $F4/80^{+}$, finally DCs are gated as $CD11c^{+}$ $MHCII^{+}$. Additionally, macrophages and DCs were gated as either being IDO-1^{+} or IDO-1^{-} and the MFI was measured using the geometric mean of the IDO-1 axis. Each group consisted of 6 mice that were pooled and tested in triplicate. The data is represented as mean with SD.

* = $P < 0.05$ ** = $P < 0.01$ *** = $P < 0.001$ **** = $P < 0.0001$

5 DISCUSSION AND CONCLUSION

5.1 RSV infection and allergen exposure

Both RSV and PVM are known to be associated with eosinophil influx during infection (90). This association has always been shown as a negative function of the immune response, but it could be assisting in viral clearance (90, 91). The data has shown that after viral clearance within the PVM group, there is still a high eosinophil influx within the lungs of these mice. This influx can be indicative of viral clearance since the virus is cleared by day 14 p.i. Also, the cellular response of the CRA group is neutrophilic with eosinophilic efflux suggesting the eosinophils are not necessary for CRA clearance. The dampening of the eosinophil influx from the viral response after two CRA introductions is primarily a response induced by CRA since this suppression was also seen in the CRA group when compared to the Medium/PBS group. Therefore, it is a product of how the response is shifting from antiviral to anti-CRA. I have confirmed that viral clearance still occurs by day 15 p.i. and therefore is not delayed due to CRA introduction. In addition, the level of cell influx is reasonably equivalent between the PVM/CRA and the CRA group. Therefore, this suggests that suppression or dampening of eosinophil influx is due to the introduction of CRA within the lungs, and not modified by the viral infection that has been cleared by day 15 p.i.

The mRNA expression of mucus glycoproteins, Muc5AC and Gob5, seems to have a synergistic induction. The high level of mucus mRNA still found at day 15 p.i. was similar within the PVM and CRA groups. When CRA was introduced into an environment where mucus production was still quite high, it induced even more mRNA production. RSV is also able to induce mucus production, (92) and mucus production seems to be governed by many factors, including IL-13. It is well known that CRA induces IL-13 secretion, so it is not surprising to find mucosal mRNA induction. PVM also induces IL-13 within the BAL fluid as seen in the Kaiko *et al.* paper (84).

Many researchers have shown that CRA induces IL-4 protein production, but only one of them has also looked at IFN-γ production (75). Within this model, CRA did induce low levels of IFN-γ protein production within the BAL fluid, although it was at similar levels to those induced by the PVM group after viral clearance. IFN-γ protein significantly increased within the BAL fluid and the lung tissue when CRA was administered to mice with an underlying PVM infection, but there was not as much of an increase within the tissue samples. The lung environment induced by PVM lead to a significantly higher IFN-γ production than that promoted by the CRA group and the Medium/PBS group. This amount was overall lower within the BAL fluid. Therefore, the cells producing IFN-γ were re-stimulated when CRA was introduced; alternatively, the stimulation could be an enhancement of the continued sequela from the viral response. Since the first CRA exposure in the model used here was during acute viral infection, and not before infection or after it has been cleared, the immune system may have had some additional responses towards CRA that are not usually seen.

Neither IDO-1 enzymatic activity nor induction of IDO-1 protein has been investigated within CRA asthma models. One study evaluated IDO-1 activity within human DCs sensitized to HDM allergen (93). In this study, the IDO-1 activity and its metabolites (3HAA and KYN) seem to give previously sensitized DCs a Th-2 skewed response with little to no IFN-γ production. The Th-2 skewed response was prominent in the lung tissue while the BAL fluid showed a more mixed Th-1/Th-2 response. These differences are more than likely due to the fact that HDM probably elicits a different outcome than CRA when it enters the lung environment.

In contrast, CRA did not induce IDO-1 mRNA production. However, there was an overall increase in IDO-1^{+} macrophages and DCs and amount of IDO-1 within each cell of these populations. The PVM infection did significantly induce this mRNA, and also showed increased IFN-γ mRNA expression. Therefore, the increased IDO-1 mRNA could have been due to the IFN-γ mRNA expression. The increase in IDO-1 protein found within the macrophages and the DCs could be due to the significant IFN-γ protein found within the CRA group even though there was no IFN-γ mRNA being expressed by this point. Alternatively, the macrophages and DCs within the lung tissue were being restimulated by CRA regardless of a previous underlying PVM infection, and that stimulation had induced more overall IDO-1 mRNA that was already degraded by day 15 p.i. Alternatively, because more IDO-1 protein was found within each cell, the increased protein amount could also be due to a lack of IDO-1 degradation within these cells.

Therefore, IDO-1 activity is a new function of PVM/CRA induced asthma. The introduction of CRA during a viral infection, where IDO-1 production is already induced, promotes a response that includes more IDO-1 mRNA expression and protein production instead of just a sustained increase of IDO-1 protein production.

5.2 Understanding the implications of allergen exposure during early-childhood

While there was a study done by the Lukacs lab (18) that suggests CRA induces an eosinophilic response, this model is different compared to my model. This model consisted of daily intranasal exposures to 1 µg of CRA for 7 days (days 0-6), after an RSV infection, instead of PVM. The mice were infected either 21 days before (day -21), on the day of (day 0), or 21 days after the first CRA exposure (day 21). This continual introduction of CRA would have stimulated a different response due to the much smaller amount of CRA used, and the constant restimulation of the lungs. Also, 35 days after the first CRA exposure, the mice were re-exposed to 1 µg of CRA intranasally and then exposed to 4 µg of CRA intratracheally on days 40 and 42. Although this model also replicates how the exposure timeline may occur within a child that could develop asthmatic responses, this is not the only timeline of exposure a child could go through. These different observations within different models can emulate the variation in asthma development and manifestation.

A second study was done by the same group that did show a polymorphonuclear cellular influx (commonly known as neutrophils) due to CRA introduction (79). These two studies differed in their CRA exposure timeline, the number of exposures, and the exposure method. This neutrophilic influx does not change whether RSV was administered beforehand. CRA did induce quite a large influx of neutrophils within the BAL. This study also confirmed that more neutrophils influx to the BAL than do eosinophils. My model's neutrophilic influx was slightly dampened when PVM was first administered; the timing of viral and CRA administration could account for the difference in neutrophil response.

Similarly, a model with only CRA induction also showed a high neutrophilic influx, with the induction of IL-5, IL-13, and IL-10 (75). Their model was somewhat intense with intranasal exposures of 120 µg of CRA twice a week, one day apart, for three weeks (days 3, 5, 10, 12, 17, and 19 p.i.). The mice were sacrificed 4 days after the last CRA treatment. Therefore, their

results represented the late or chronic response towards CRA, while mine represented more of the early responses induced by CRA. Hence, a more chronic response towards significant CRA exposure coincides with the constant neutrophilic influx and a gradual increase of IFN-γ protein secretion along with Th-2 cytokine secretions. This cellular influx is difficult to explain in context with the cytokine profile, since neutrophils are considered part of the Th-17 response, (20) while eosinophils are considered part of the Th-2 response. Even so, neutrophils are known to have a protective phenotype as well, which is a potential reason for this seemingly inappropriate combination of responses. Again, this model showed nominal eosinophilic influx, whereas mine showed suppression, but that could be either the intensity of the exposures or the delayed time between the last exposure and the sampling day. Since neutrophilic influx is maintained for 24 hrs and up to 4 days after CRA induction, this is a noteworthy part of why CRA on its own seems to be such an essential factor in asthma induction.

There are still some commonalities between the previously reported models and the one used here. Those include a higher induction of IL-4 and some induction of IL-13. CRA can induce an eosinophilic influx after multiple closely spaced exposures, though it promotes a more neutrophilic influx after a few introductions spaced over a more extended period. There is still high IL-4, and IL-13 induction regardless of how the mice are exposed to the CRA allergen. Therefore, CRA does seem to induce a traditional Th-2 cytokine environment. The implication of a viral infection is still quite complex; I feel it is based on the timing of compounding factors as much as it is based on the type of viral infection or allergen combination used.

5.3 General conclusion and future directions

A future direction would be to perform an extended trial where this second CRA exposure, or even a third one, occurs after viral clearance and when the environment has returned to normal levels. This way, the CRA exposure would be based on memory response and not also on the lasting effects of viral infection after clearance. Also, another sacrificial time-point at day 8 would be beneficial to observe the initial immune response towards the antigen during infection, while also confirming that there are still viable virions within the lungs after this exposure. Another future direction would be to elucidate the effects of IDO-1 enzymatic activity on this model. The signalling activity would be vital to elucidate as well, though that could be

compensated through IDO-2 signalling function. Therefore, an IDO-2KO and IDO-1 enzymatic mutation (or adding 1-MT to the drinking water) would be ideal variables to investigate. Although increasing the amount of CRA and PVM given to the mice could be modified in the future, a combination of 50 pfu PVM-15 and 100 µg CRA was attempted. This combination could not be replicated due to the unhealthy condition of mice during this trial.

Another thought is differentiating the types of neutrophils that are entering the BAL fluid because it is known that neutrophils are either protective or pathological depending on the cytokine environment (94). IL-33 secretion within the liver environment produced immunosuppressive neutrophils during an LCMV infection. According to Liang *et al.*, this was due to ILC2 cells that are potently stimulated by IL-33 and start producing IL-13 (94). This IL-13 then induced neutrophils to produce arginase (Arg)-1, which is an enzyme that breaks down arginine. This break-down of arginine led to the stunted proliferation of $CD8^+$ T-cells. Therefore, more studies need to be done on the asthmatic neutrophil influx and how it may be an 'over-protective' response, which may lead to different aspects of tissue injury.

In conclusion, the mouse model used here is indicative of another way asthma development may occur. This model also showed how exposure after the acute respiratory infection was able to modify the natural CRA response that showed a dampening of the long-lasting neutrophilic response, while promoting a more traditional Th-2 response, without the addition of eosinophil influx. This response was stronger than what was induced in the CRA group.

More work needs to be done in the early stages of response development, such as on day 8 of this model. The changes in memory response towards CRA seen on day 15 p.i. within the PVM/CRA group compared to the CRA group suggests that there is an alteration of the cytokine profile and cell populations within the lungs. This alteration would happen as a result of CRA being administered on day 7 post PVM infection. Therefore, sampling on day 8 of the PVM infection (24 hours after the first CRA exposure) could ideally show whether the initial response towards CRA is altered due to the underlying PVM infection. In this way, it may be possible to determine how the mixing of signals could develop different combinations of memory responses towards what should be a benign particle.

REFERENCES

1. Ueno, F., R. Tamaki, M. Saito, M. Okamoto, M. Saito-Obata, T. Kamigaki, A. Suzuki, E. Segubre-Mercado, H. D. Aloyon, V. Tallo, S. P. Lupisan, H. Oshitani, and R. S. V. W. G. i. t. Philippines. 2019. Age-specific incidence rates and risk factors for respiratory syncytial virus-associated lower respiratory tract illness in cohort children under 5 years old in the Philippines. *Influenza and Other Respiratory Viruses* 0.
2. Graham, B. S. 2019. Immunological goals for respiratory syncytial virus vaccine development. *Current Opinion in Immunology* 59: 57-64.
3. Homaira, N., N. Briggs, C. Pardy, M. Hanly, J.-L. Oei, L. Hilder, B. Bajuk, K. Lui, W. Rawlinson, T. Snelling, and A. Jaffe. 2017. Association between respiratory syncytial viral disease and the subsequent risk of the first episode of severe asthma in different subgroups of high-risk Australian children: a whole-of-population-based cohort study. *BMJ open* 7: e017936-e017936.
4. Falsey, A. R., and E. E. Walsh. 2000. Respiratory syncytial virus infection in adults. *Clinical Microbiology Reviews* 13: 371-384.
5. World Health, O. 2019. WHO meeting of mid-term review of the RSV surveillance pilot based on the global influenza surveillance and response system: 18–20 December 2017 PAHO, Washington DC, USA. World Health Organization.
6. Bem, R. A., J. B. Domachowske, and H. F. Rosenberg. 2011. Animal models of human respiratory syncytial virus disease. *American Journal of Physiology-Lung Cellular and Molecular Physiology* 301: L148-L156.
7. Mandelberg, A., G. Tal, L. Naugolny, K. Cesar, A. Oron, S. Houri, E. Gilad, and E. Somekh. 2006. Lipopolysaccharide hyporesponsiveness as a risk factor for intensive care unit hospitalization in infants with respiratory syncitial virus bronchiolitis. *Clinical & Experimental Immunology* 144: 48-52.
8. Sun, L., T. T. Cornell, A. LeVine, A. A. Berlin, V. Hinkovska-Galcheva, A. J. Fleszar, N.

W. Lukacs, and T. P. Shanley. 2013. Dual role of interleukin-10 in the regulation of respiratory syncitial virus (RSV)-induced lung inflammation. *Clinical & Experimental Immunology* 172: 263-279.

9. Ajamian, F., Y. Wu, C. Ebeling, R. Ilarraza, S. O. Odemuyiwa, R. Moqbel, and D. J. Adamko. 2015. Respiratory syncytial virus induces indoleamine 2,3-dioxygenase activity: a potential novel role in the development of allergic disease. *Clinical & Experimental Allergy* 45: 644-659.
10. Altamirano-Lagos, M. J., F. E. Díaz, M. A. Mansilla, D. Rivera-Pérez, D. Soto, J. L. McGill, A. E. Vasquez, and A. M. Kalergis. 2019. Current Animal Models for Understanding the Pathology Caused by the Respiratory Syncytial Virus. *Frontiers in Microbiology* 10.
11. Saturni, S., M. Contoli, A. Spanevello, and A. Papi. 2015. Models of Respiratory Infections: Virus-Induced Asthma Exacerbations and Beyond. *Allergy, Asthma & Immunology Research* 7: 525-533.
12. Gershwin, L. J. 2007. Bovine respiratory syncytial virus infection: immunopathogenic mechanisms. *Animal Health Research Reviews* 8: 207-213.
13. Christiaansen, A. F., C. J. Knudson, K. A. Weiss, and S. M. Varga. 2014. The CD4 T cell response to respiratory syncytial virus infection. *Immunologic Research* 59: 109-117.
14. Brown, P. M., D. L. Schneeberger, and G. Piedimonte. 2015. Biomarkers of respiratory syncytial virus (RSV) infection: Specific neutrophil and cytokine levels provide increased accuracy in predicting disease severity. *Paediatric Respiratory Reviews* 16: 232-240.
15. Shinohara, M., H. Wakiguchi, H. Saito, and K. Matsumoto. 2008. Presence of eosinophils in nasal secretion during acute respiratory tract infection in young children predicts subsequent wheezing within two months. *Allergology International* 57: 359-365.
16. Moreno-Solis, G., J. Torres-Borrego, M. J. de la Torre-Aguilar, F. Fernandez-Gutierrez, F. J. Llorente-Cantarero, and J. L. Perez-Navero. 2015. Analysis of the local and systemic inflammatory response in hospitalized infants with respiratory syncitial virus bronchiolitis. *Allergologia et Immunopathologia* 43: 264-271.
17. Okamoto, N., M. Ikeda, M. Okuda, T. Sakamoto, M. Takasugi, N. Takahashi, T. Araki, T. Morishima, and K. Yasui. 2011. Increased eosinophilic cationic protein in nasal fluid in hospitalized wheezy infants with RSV infection. *Allergology International* 60: 467-

472.

18. Smit, J. J., L. Boon, and N. W. Lukacs. 2007. Respiratory Virus-Induced Regulation of Asthma-Like Responses in Mice Depends upon CD8 T Cells and Interferon-γ Production. *American Journal of Pathology* 171: 1944-1951.
19. Bertrand, P., M. K. Lay, G. Piedimonte, P. E. Brockmann, C. E. Palavecino, J. Hernández, M. A. León, A. M. Kalergis, and S. M. Bueno. 2015. Elevated IL-3 and IL-12p40 levels in the lower airway of infants with RSV-induced bronchiolitis correlate with recurrent wheezing. *Cytokine* 76: 417-423.
20. Mukherjee, S., D. M. Lindell, A. A. Berlin, S. B. Morris, T. P. Shanley, M. B. Hershenson, and N. W. Lukacs. 2011. IL-17–Induced Pulmonary Pathogenesis during Respiratory Viral Infection and Exacerbation of Allergic Disease. *American Journal of Pathology* 179: 248-258.
21. Watkiss, E. R. T., P. Shrivastava, N. Arsic, S. Gomis, and d. H. van Drunen Littel-van. 2013. Innate and Adaptive Immune Response to Pneumonia Virus of Mice in a Resistant and a Susceptible Mouse Strain. *Viruses* 5: 295-320.
22. Martinez, E. C., R. Garg, P. Shrivastava, S. Gomis, and S. van Drunen Littel-van den Hurk. 2016. Intranasal treatment with a novel immunomodulator mediates innate immune protection against lethal pneumonia virus of mice. *Antiviral Research* 135: 108-119.
23. Krempl, C. D., and P. L. Collins. 2004. Reevaluation of the Virulence of Prototypic Strain 15 of Pneumonia Virus of Mice. *Journal of Virology* 78: 13362.
24. Shrivastava, P., I. Sarkar, E. Atanley, S. Gomis, and S. van Drunen Littel-van den Hurk. 2016. IL-12p40 gene-deficient BALB/c mice exhibit lower weight loss, reduced lung pathology and decreased sensitization to allergen in response to infection with pneumonia virus of mice. *Virology* 497: 1-10.
25. Dyer, K., K. Garcia-Crespo, S. Glineur, J. Domachowske, and H. Rosenberg. 2012. The pneumonia virus of mice (PVM) model of acute respiratory infection. *Viruses* 4: 3494-3510.
26. Domachowske, J. B., C. A. Bonville, A. J. Easton, and H. F. Rosenberg. 2002. Differential Expression of Proinflammatory Cytokine Genes In Vivo in Response to Pathogenic and Nonpathogenic Pneumovirus Infections. *Journal of Infectious Diseases* 186: 8-14.

27. Domachowske, J. B., C. A. Bonville, K. D. Dyer, A. J. Easton, and H. F. Rosenberg. 2000. Pulmonary Eosinophilia and Production of MIP-1α Are Prominent Responses to Infection with Pneumonia Virus of Mice. *Cellular Immunology* 200: 98-104.
28. Randhawa, J. S., P. Chambers, C. R. Pringle, and A. J. Easton. 1995. Nucleotide Sequences of the Genes Encoding the Putative Attachment Glycoprotein (G) of Mouse and Tissue Culture-Passaged Strains of Pneumonia Virus of Mice. *Virology* 207: 240-245.
29. Harter, D. H., and P. W. Choppin. 1967. STUDIES ON PNEUMONIA VIRUS OF MICE (PVM) IN CELL CULTURE: I. REPLICATION IN BABY HAMSTER KIDNEY CELLS AND PROPERTIES OF THE VIRUS. *Journal of Experimental Medicine* 126: 251-266.
30. Horsfall, F. L., and R. G. Hahn. 1940. A LATENT VIRUS IN NORMAL MICE CAPABLE OF PRODUCING PNEUMONIA IN ITS NATURAL HOST. *Journal of Experimental Medicine* 71: 391.
31. Krempl, C. D., A. Wnekowicz, E. W. Lamirande, G. Nayebagha, P. L. Collins, and U. J. Buchholz. 2007. Identification of a Novel Virulence Factor in Recombinant Pneumonia Virus of Mice. *Journal of Virology* 81: 9490.
32. Sandquist, I., and J. Kolls. 2018. Update on regulation and effector functions of Th17 cells. *F1000Research* 7.
33. Zhu, J., and W. E. Paul. 2008. CD4 T cells: fates, functions, and faults. *Blood* 112: 1557.
34. Randolph, D. A., C. J. L. Carruthers, S. J. Szabo, K. M. Murphy, and D. D. Chaplin. 1999. Modulation of airway inflammation by passive transfer of allergen- specific Th1 and Th2 cells in a mouse model of asthma. American Association of Immunologists (9650 Rockville Pike, Bethesda MD 20814, United States), United States. 2375-2383.
35. Wynn, T. A. 2015. Type 2 cytokines: mechanisms and therapeutic strategies. *Nature Reviews Immunology* 15: 271.
36. Zhu, J. 2015. T helper 2 (Th2) cell differentiation, type 2 innate lymphoid cell (ILC2) development and regulation of interleukin-4 (IL-4) and IL-13 production. *Cytokine* 75: 14-24.
37. Mousset, C. M., W. Hobo, R. Woestenenk, F. Preijers, H. Dolstra, and A. B. van der Waart. 2019. Comprehensive Phenotyping of T Cells Using Flow Cytometry. *Cytometry*

Part A 95: 647-654.

38. Gelfand, E. W., A. Joetham, M. Wang, K. Takeda, and M. Schedel. 2017. Spectrum of T-lymphocyte activities regulating allergic lung inflammation. *Immunological Reviews* 278: 63-86.
39. Frey, S., C. D. Krempl, A. Schmitt-Gräff, and S. Ehl. 2008. Role of T cells in virus control and disease after infection with pneumonia virus of mice. *Journal of Virology* 82: 11619-11627.
40. Schulz, S., A. Landi, R. Garg, J. A. Wilson, and d. H. van Drunen Littel-van. 2015. Indolamine 2,3-dioxygenase expression by monocytes and dendritic cell populations in hepatitis C patients. *Clinical and Experimental Immunology* 180: 484-498.
41. Fox, J. M., J. M. Crabtree, L. K. Sage, S. M. Tompkins, and R. A. Tripp. 2015. Interferon Lambda Upregulates IDO1 Expression in Respiratory Epithelial Cells After Influenza Virus Infection. *Journal of Interferon & Cytokine Research* 35: 554-562.
42. Metz, R., J. B. DuHadaway, U. Kamasani, L. Laury-Kleintop, A. J. Muller, and G. C. Prendergast. 2007. Novel Tryptophan Catabolic Enzyme IDO2 Is the Preferred Biochemical Target of the Antitumor Indoleamine 2,3-Dioxygenase Inhibitory Compound 1-Methyl-Tryptophan. *Cancer Research* 67: 7082.
43. Fallarino, F., U. Grohmann, and P. Puccetti. 2012. Indoleamine 2,3-dioxygenase: From catalyst to signaling function. *European Journal of Immunology* 42: 1932-1937.
44. Rodrigues, C. P., A. C. F. Ferreira, M. P. Pinho, M. C. De, P. C. Bergami-Santos, and J. A. M. Barbuto. 2016. Tolerogenic IDO+ dendritic cells are induced by pd-1-expressing mast cells. Frontiers Research Foundation, Switzerland.
45. Musso, T., G. L. Gusella, A. Brooks, D. L. Longo, and L. Varesio. 1994. Interleukin-4 inhibits indoleamine 2, 3-dioxygenase expression in human monocytes. *Blood* 83: 1408-1411.
46. Chaves, A. C. L., I. P. Cerávolo, J. A. S. Gomes, C. L. Zani, A. J. Romanha, and R. T. Gazzinelli. 2001. IL‐4 and IL‐13 regulate the induction of indoleamine 2, 3‐dioxygenase activity and the control of Toxoplasma gondii replication in human fibroblasts activated with IFN‐γ. *European Journal of Immunology* 31: 333-344.
47. Yadav, M. C., E. M. E. Burudi, M. Alirezaei, C. C. Flynn, D. D. Watry, C. M. Lanigan, and H. S. Fox. 2007. IFN‐γ‐induced IDO and WRS expression in microglia is

differentially regulated by IL‐4. *Glia* 55: 1385-1396.

48. Fallarino, F., U. Grohmann, C. Vacca, R. Bianchi, C. Orabona, A. Spreca, M. C. Fioretti, and P. Puccetti. 2002. T cell apoptosis by tryptophan catabolism. *Cell Death and Differentiation* 9: 1069-1077.
49. Odemuyiwa, S. O., A. Ghahary, Y. Li, L. Puttagunta, J. E. Lee, S. Musat-Marcu, A. Ghahary, and R. Moqbel. 2004. Cutting edge: human eosinophils regulate T cell subset selection through indoleamine 2, 3-dioxygenase. *Journal of Immunology* 173: 5909-5913.
50. Yun, Tae J., Jun S. Lee, K. Machmach, D. Shim, J. Choi, Young J. Wi, Hyung S. Jang, I.-H. Jung, K. Kim, Won K. Yoon, Mohammad A. Miah, B. Li, J. Chang, Mariana G. Bego, Tram N. Q. Pham, J. Loschko, Jörg H. Fritz, Anne B. Krug, S.-P. Lee, T. Keler, Jean V. Guimond, E. Haddad, Eric A. Cohen, Martin G. Sirois, I. El-Hamamsy, M. Colonna, Goo T. Oh, J.-H. Choi, and C. Cheong. 2016. Indoleamine 2,3-Dioxygenase-Expressing Aortic Plasmacytoid Dendritic Cells Protect against Atherosclerosis by Induction of Regulatory T Cells. *Cell Metabolism* 23: 852-866.
51. Cheng, J. t., Y. n. Deng, H. m. Yi, G. y. Wang, B. s. Fu, W. j. Chen, W. Liu, Y. Tai, Y. w. Peng, and Q. Zhang. 2016. Hepatic carcinoma-associated fibroblasts induce IDO-producing regulatory dendritic cells through IL-6-mediated STAT3 activation. *Oncogenesis* 5: e198.
52. Popov, A., and J. L. Schultze. 2008. IDO-expressing regulatory dendritic cells in cancer and chronic infection. *Journal of Molecular Medicine* 86: 145-160.
53. Mellor, A. L., P. Chandler, G. K. Lee, T. Johnson, D. B. Keskin, J. Lee, and D. H. Munn. 2002. Indoleamine 2,3-dioxygenase, immunosuppression and pregnancy. *Journal of Reproductive Immunology* 57: 143-150.
54. Kudo, Y., C. A. Boyd, I. L. Sargent, and C. W. Redman. 2001. Tryptophan degradation by human placental indoleamine 2,3-dioxygenase regulates lymphocyte proliferation. *Journal of Physiology* 535: 207-215.
55. Pett, S. L., K. M. Kunisaki, T. J. Griffin, I. Kalomenidis, R. Nahra, R. M. Sanchez, S. W. Hodgson, C. H. Wendt, J. Lundgren, P. Jansson, M. Pearson, F. Hudson, R. Bennet, F. Pacciarini, N. Paton, Y. Collaco Moraes, D. Cooper, S. Emery, D. Courtney-Rogers, R. Robson, F. Gordin, A. Sanchez, B. Standridge, M. Vjecha, A. Moricz, M. Delfino, W. Belloso, K. Tillmann, G. Touloumi, V. Gioukari, O. Anagnostou, A. La Rosa, M. J.

Saenz, P. Lopez, P. Herrero, B. Portas, P. Kaewon, S. Ubolyam, K. Brekke, M. Campbell, E. Denning, A. DuChene, N. Engen, M. George, M. Harrison, J. D. Neaton, R. Nelson, S. F. Quan, T. Schultz, D. Wentworth, S. Brown, M. Hoover, J. Beigel, R. T. Davey, R. Dewar, E. Gover, R. McConnell, J. Metcalf, V. Natarajan, T. Rehman, J. Voell, D. E. Dwyer, J. Kok, T. Uyeki, D. Munroe, M. Bertrand, Z. Temesgen, S. Rizza, C. Wolfe, J. Carbonneau, R. Novak, M. Schwarber, H. Polenakovik, L. Clark, N. Patil, P. Riska, J. Omotosho, L. Faber, N. Markowitz, M. Glesby, K. Ham, D. Parenti, G. Simon, J. Baxter, P. Coburn, M. Freiberg, G. Koerbel, N. Dharan, M. Paez-Quinde, J. Gunter, M. Beilke, Z. Lu, E. Gunderson, J. Baker, S. Koletar, H. Harber, C. Hurt, C. Marcus, M. Allen, S. Cummins, D. Uslan, T. Bonam, A. Paez, F. Santiago, D. States, E. Gardner, J. DeHovitz, S. Holman, V. Watson, D. Nixon, D. Dwyer, M. Kabir, S. Pett, F. Kilkenny, J. Elliott, J. Garlick, J. McBride, S. Richmond, L. Barcan, M. Sanchez, G. Lopardo, L. Barcelona, P. Bonvehi, E. R. Temporiti, M. Losso, L. Macias, H. Laplume, L. Daciuk, E. Warley, S. Tavella, E. Fernandez Cruz, J. Pano, V. Estrada, P. Lopetegui, T. Gimenez Julvez, P. Ryan, J. Sanz Moreno, H. Knobel, V. Soriano, D. Dalmau, D. Dockrell, B. Angus, D. Price, M. Newport, D. Chadwick, L. Ostergaard, Y. Yehdego, C. Pedersen, L. Hergens, Z. Joensen, B. Aagaard, G. Kronborg, P. Collins, H. Nielsen, J. Gerstoft, B. Baadegaard, N. Koulouris, A. Antoniadou, K. Protopappas, V. Polixronopoulos, F. Diamantea, H. Sambatakou, I. Mariolis, N. Vassilopoulos, A. Gerogiannis, Y. Pinedo Ramirez, E. Cornelio Mauricio, J. Vega Bazalar, R. Castillo Cordova, G. Fatkenhuerer, F. Bergmann, U. Follmer, J. Rockstroh, A. Englehardt, C. Stephan, E. Thomas, J. Bogner, N. Brockmeyer, H. Klinker, P. Chetchotisakd, T. Jumpimai, A. Avihingsanon, K. Ruxrungtham, N. Clumeck, K. Kameya, M. Y. Chu, T. C. Wu, A. Horban, E. Bakowska, H. Burgmann, S. Tobudic, A. Maagaard, M. Wolff, and G. Allendes. 2018. Increased indoleamine-2,3-dioxygenase activity is associated with poor clinical outcome in adults hospitalized with influenza in the INSIGHT FLU003Plus study. *Open Forum Infectious Diseases* 5 (1)

56. Hu, Y., Z. Chen, L. Jin, M. Wang, and W. Liao. 2017. Decreased expression of indolamine 2,3-dioxygenase in childhood allergic asthma and its inverse correlation with fractional concentration of exhaled nitric oxide. *Annals of Allergy, Asthma & Immunology* 119: 429-434.

57. Kubo, S., K. Yamaoka, M. Kondo, K. Yamagata, J. Zhao, S. Iwata, and Y. Tanaka. 2014. The JAK inhibitor, tofacitinib, reduces the T cell stimulatory capacity of human monocyte-derived dendritic cells. *Annals of the Rheumatic Diseases* 73: 2192-2198.
58. Hayashi, T., L. Beck, C. Rossetto, X. Gong, O. Takikawa, K. Takabayashi, D. H. Broide, D. A. Carson, and E. Raz. 2004. Inhibition of experimental asthma by indoleamine 2,3-dioxygenase. *Journal of Clinical Investigation* 114: 270-279.
59. Kwidzinski, E., J. Bunse, O. Aktas, D. Richter, L. Mutlu, F. Zipp, R. Nitsch, and I. Bechmann. 2005. Indolamine 2,3-dioxygenase is expressed in the CNS and down-regulates autoimmune inflammation. *FASEB Journal* 19: 1347-1349.
60. Munn, D. H., M. Zhou, J. T. Attwood, I. Bondarev, S. J. Conway, B. Marshall, C. Brown, and A. L. Mellor. 1998. Prevention of allogeneic fetal rejection by tryptophan catabolism. *Science* 281: 1191-1193.
61. Ilic, N., A. Gruden-Movsesijan, J. Cvetkovic, S. Tomic, D. B. Vucevic, C. Aranzamendi, M. Colic, E. Pinelli, and L. Sofronic-Milosavljevic. 2018. Trichinella spiralis Excretory-Secretory Products Induce Tolerogenic Properties in Human Dendritic Cells via Toll-Like Receptors 2 and 4. *Frontiers in Immunology* 9: 11-11.
62. Lambrecht, B. N., and H. Hammad. 2015. The immunology of asthma. *Nature Immunology* 16: 45-56.
63. America, A. a. A. F. o. 2019. Your Guid to Managing Asthma. A. a. A. F. o. America, ed.
64. Al-Sawalha, N., I. Pokkunuri, O. Omoluabi, H. Kim, V. J. Thanawala, A. Hernandez, R. A. Bond, and B. J. Knoll. 2015. Epinephrine Activation of the β2-Adrenoceptor Is Required for IL-13-Induced Mucin Production in Human Bronchial Epithelial Cells. *PloS One* 10: e0132559-e0132559.
65. Grayson, M. H., S. Feldman, B. T. Prince, P. J. Patel, E. C. Matsui, and A. J. Apter. 2018. Advances in asthma in 2017: mechanisms, biologics, and genetics. *Journal of Allergy and Clinical Immunology* 142: 1423-1436.
66. Tang, F. S. M., D. Van Ly, K. Spann, P. C. Reading, J. K. Burgess, D. Hartl, K. J. Baines, and B. G. Oliver. 2016. Differential neutrophil activation in viral infections: Enhanced TLR-7/8-mediated CXCL8 release in asthma. *Respirology* 21: 172-179.
67. Amin, K. 2012. The role of mast cells in allergic inflammation. *Respiratory Medicine* 106: 9-14.

68. Lukacs, N. W. 2001. Role of chemokines in the pathogenesis of asthma. *Nature Reviews Immunology* 1: 108-116.

69. Lukacs, N. W., R. M. Strieter, S. W. Chensue, and S. L. Kunkel. 1996. Activation and regulation of chemokines in allergic airway inflammation. *Journal of Leukocyte Biology* 59: 13-17.

70. Yu, Q. L., and Z. Chen. 2018. Establishment of different experimental asthma models in mice. *Experimental and Therapeutic Medicine* 15: 2492-2498.

71. Wardlaw, A. J., C. Brightling, R. Green, G. Woltmann, and I. Pavord. 2000. Eosinophils in asthma and other allergic diseases. *British Medical Bulletin* 56: 985-1003.

72. Panettieri, R. A. 2018. The Role of Neutrophils in Asthma. *Immunology and Allergy Clinics of North America* 38: 629-638.

73. Gao, P. 2012. Sensitization to Cockroach allergen: Immune regulation and genetic determinants. *Clinical and Developmental Immunology* 2012: Arte Number: 563760. ate of Pubaton: 562012.

74. Whitehead, G. S., S. Y. Thomas, K. H. Shalaby, K. Nakano, T. P. Moran, J. M. Ward, G. P. Flake, H. Nakano, and D. N. Cook. 2017. TNF is required for TLR ligand–mediated but not protease-mediated allergic airway inflammation. *Journal of Clinical Investigation* 127: 3313-3326.

75. Kim, D.-H., J.-H. Sohn, H.-J. Park, J.-H. Lee, J.-W. Park, and J.-M. Choi. 2016. CpG Oligodeoxynucleotide Inhibits Cockroach-Induced Asthma via Induction of IFN-γ+ Th1 Cells or Foxp3+ Regulatory T Cells in the Lung. *Allergy Asthma Immunol Res* 8: 264-275.

76. Kim, J. Y., J. H. Sohn, J. M. Choi, J. H. Lee, C. S. Hong, J. S. Lee, and J. W. Park. 2012. Alveolar Macrophages Play a Key Role in Cockroach-Induced Allergic Inflammation via TNF-alpha Pathway. *PLoS ONE* 7: Arte Number: e47971.

77. Wenzel, S. E. 2012. Asthma phenotypes: the evolution from clinical to molecular approaches. *Nature Medicine* 18: 716.

78. Mahmutovic, P. I., H. Akbarshahi, M. Menzel, A. Brandelius, and L. Uller. 2016. Increased expression of upstream TH2-cytokines in a mouse model of viral-induced asthma exacerbation. BioMed Central Ltd., United Kingdom.

79. John, A. E., A. A. Berlin, and N. W. Lukacs. 2003. Respiratory syncytial virus-induced

CCL5/RANTES contributes to exacerbation of allergic airway inflammation. *European Journal of Immunology* 33: 1677-1685.

80. Kroegel, C. 2009. Global Initiative for Asthma (GINA) guidelines: 15 years of application. *Expert Review of Clinical Immunology* 5: 239-249.
81. Rabe, K. F., P. A. Vermeire, J. B. Soriano, and W. C. Maier. 2000. Clinical management of asthma in 1999: the Asthma Insights and Reality in Europe (AIRE) study. *European Respiratory Journal* 16: 802-807.
82. National, A. E., and P. Prevention. 2007. Expert Panel Report 3 (EPR-3): guidelines for the diagnosis and management of asthma-summary report 2007. *The Journal of Allergy and Clinical Immunology* 120: S94.
83. Zaynagetdinov, R., T. P. Sherrill, P. L. Kendall, B. H. Segal, K. P. Weller, R. M. Tighe, and T. S. Blackwell. 2013. Identification of myeloid cell subsets in murine lungs using flow cytometry. *American Journal of Respiratory Cell and Molecular Biology* 49: 180-189.
84. Kaiko, G. E., Z. Loh, K. Spann, J. P. Lynch, A. Lalwani, Z. Zheng, S. Davidson, S. Uematsu, S. Akira, J. Hayball, K. R. Diener, K. J. Baines, J. L. Simpson, P. S. Foster, and S. Phipps. 2013. Toll-like receptor 7 gene deficiency and early-life Pneumovirus infection interact to predispose toward the development of asthma-like pathology in mice. *Journal of Allergy and Clinical Immunology* 131: 1331-1339e1310.
85. Smit, J. J., and N. W. Lukacs. 2006. A closer look at chemokines and their role in asthmatic responses. *European Journal of Pharmacology; The Pharmacology of the Respiratory Tract* 533: 277-288.
86. Lukacs, N. W., K. K. Tekkanat, A. Berlin, C. M. Hogaboam, A. Miller, H. Evanoff, P. Lincoln, and H. Maassab. 2001. Respiratory Syncytial Virus Predisposes Mice to Augmented Allergic Airway Responses Via IL-13-Mediated Mechanisms. *Journal of Immunology* 167: 1060.
87. Campbell, E. M., S. L. Kunkel, R. M. Strieter, and N. W. Lukacs. 1998. Temporal Role of Chemokines in a Murine Model of Cockroach Allergen-Induced Airway Hyperreactivity and Eosinophilia. *Journal of Immunology* 161: 7047.
88. Wang, J., L. Ma, S. Yang, S. Wang, X. Wei, and S. Song. 2016. IL-10-Expressing Th2 Cells Contribute to the Elevated Antibody Production in Rheumatoid Arthritis.

Inflammation 39: 1017-1024.

89. Mitchell, R. E., M. Hassan, B. R. Burton, G. Britton, E. V. Hill, J. Verhagen, and D. C. Wraith. 2017. IL-4 enhances IL-10 production in Th1 cells: implications for Th1 and Th2 regulation. *Scientific Reports* 7: 11315.
90. Percopo, C. M., K. D. Dyer, S. I. Ochkur, J. L. Luo, E. R. Fischer, J. J. Lee, N. A. Lee, J. B. Domachowske, and H. F. Rosenberg. 2013. Activated mouse eosinophils protect against lethal respiratory virus infection. *Blood* 123: 743-752.
91. Rosenberg, H. F., K. D. Dyer, and J. B. Domachowske. 2009. Respiratory viruses and eosinophils: exploring the connections. *Antiviral Research* 83: 1-9.
92. Lukacs, N. W., M. L. Moore, B. D. Rudd, A. A. Berlin, R. D. Collins, S. J. Olson, S. B. Ho, and R. S. Peebles Jr. 2006. Differential Immune Responses and Pulmonary Pathophysiology Are Induced by Two Different Strains of Respiratory Syncytial Virus. *The American Journal of Pathology* 169: 977-986.
93. Royer, P.-J., M. Emara, C. Yang, A. Al-Ghouleh, P. Tighe, N. Jones, H. F. Sewell, F. Shakib, L. Martinez-Pomares, and A. M. Ghaemmaghami. 2010. The Mannose Receptor Mediates the Uptake of Diverse Native Allergens by Dendritic Cells and Determines Allergen-Induced T Cell Polarization through Modulation of IDO Activity. *Journal of Immunology* 185: 1522.
94. Liang, Y., P. Yi, D. M. K. Yuan, Z. Jie, Z. Kwota, L. Soong, Y. Cong, and J. Sun. 2019. IL-33 induces immunosuppressive neutrophils via a type 2 innate lymphoid cell/IL-13/STAT6 axis and protects the liver against injury in LCMV infection-induced viral hepatitis. *Cellular & Molecular Immunology* 16: 126-137.